AD-A062 981 DEUTSCHE FORSCHUNGS- UND VERSUCHSANSTALT FUER LUFT- U--ETC F/G 11/6
DEVELOPMENT OF IMPROVED HIGH STRENGTH ALUMINUM POWDER METALLURG--ETC(U)
MAY 78 D P VOSS AFOSR-77-3440
UNCLASSIFIED DFVLR-IB-354-77/14 EOARD-TR-78-3 NL

1 OF 2
AD
A062981

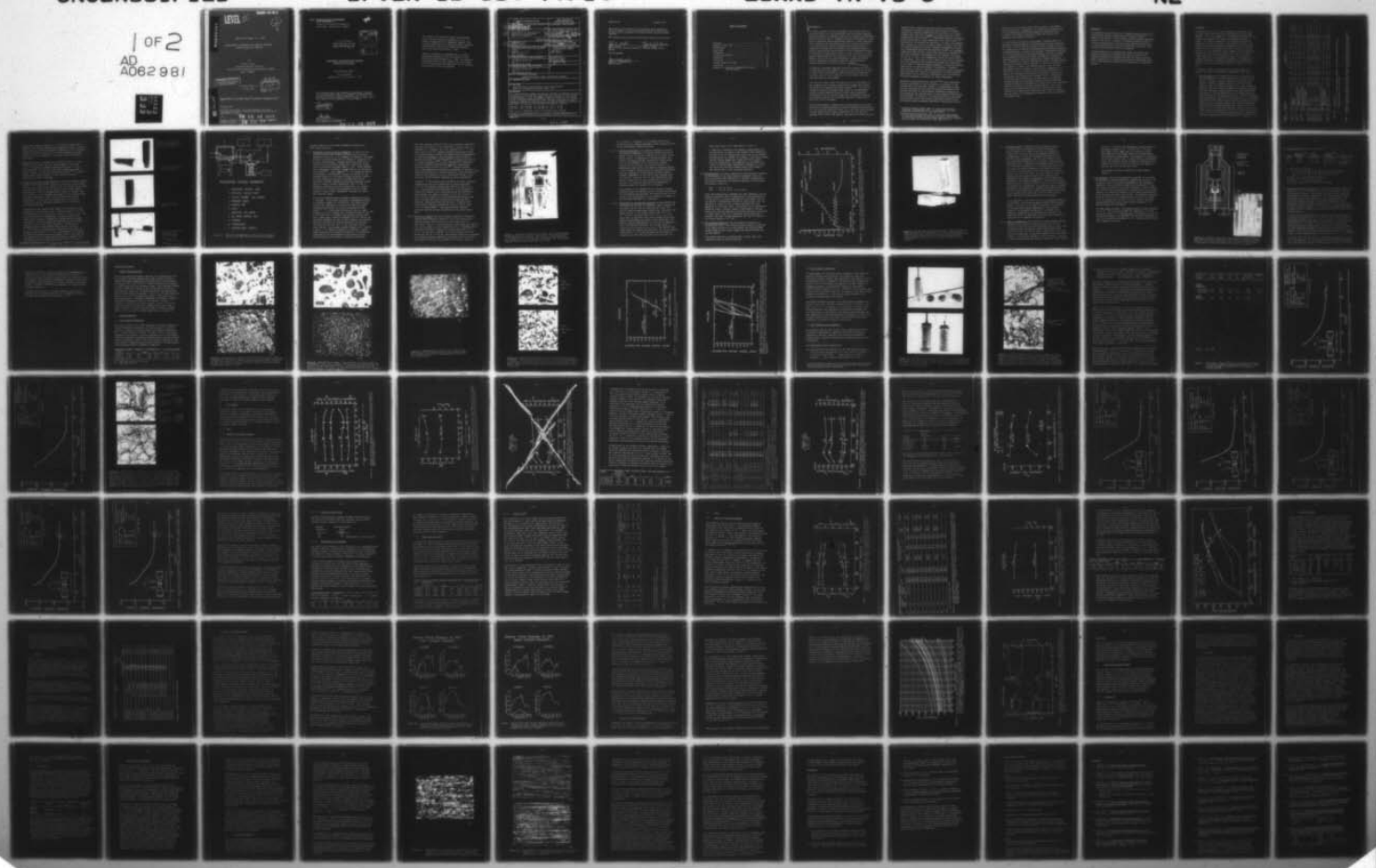

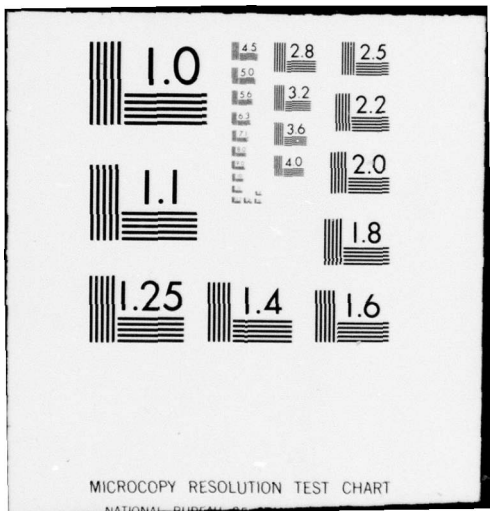
1.0
1.1
1.25
1.4
1.6
1.8
2.0
2.2
2.5
2.8
3.2
3.6
4.0
4.5
5.0
5.6
6.3
MICROCOPY RESOLUTION TEST CHART

AD A062981

EOARD-TR-78-3

LEVEL II

2

AFOSR Grant Number: 77 - 3440

DEVELOPMENT OF IMPROVED HIGH STRENGTH ALUMINUM POWDER METALLURGY PRODUCTS

by

David P. Voss

Materials Research Institute

German Aerospace Research Establishment (DFVLR)

Köln, Germany

DISTRIBUTION STATEMENT A
Approved for public release;
Distribution Unlimited

DDC
RECEIVED
8 JAN 1979
E

Progress Report # 1

31 May 1978

This report is intended only for internal management use.

Prepared for

Deutsche Forschungs- und Versuchsanstalt für Luft- und Raumfahrt (DFVLR), Institut für Werkstoff-Forschung, 5000 Köln, Germany

and

European Office of Aerospace Research and Development, London, England

78 12 14 037

78 12 14 037

DDC FILE COPY

DFVLR **Deutsche Forschungs- und Versuchsanstalt für Luft- und Raumfahrt e.V.**

-Institut für Werkstoff-Forschung-
Linder Höhe, 5000 Köln 90, Germany

ACCESSION for
NTIS White Section
DDC Buff Section
UNANNOUNCED
JUSTIFICATION
BY
DISTRIBUTION/AVAILABILITY CODES
AVAIL. and/or SPECIAL
A

U.S. Air Force
AFOSR Grant No. 77-3440
~~EOARD P.R. No. G77-0004~~

Development of Improved High Strength Aluminum P/M Products

(9)

First Progress Report No 1,

for the period
September 30, 1977 to May 31, 1978

This progress report was prepared for management purposes. It is a preliminary report of information generated during the initial phase of this investigation, and as such, the data and conclusions reported may be subject to major change. This report will be replaced by a Final Report.

David P. Voss
DAVID P. VOSS
Project Engineer

Dr. G. Wirth
Chief, Materials Technology and
High Temperature Strengths

78 12 14 037

Foreword

The research work reported within this progress report has been partially funded by the U.S. Air Force, European Office of Aerospace Research, and has been conducted at the German Aerospace Research Establishment, Institute for Material Research under the direction of David P. Voss.

Special recognition is warranted for Dr. Scharf and Herren Bauerfeind, Pütz, and Schmitz of the Vereinigte Aluminium-Werke A.G. (VAW), Leichtmetall-Forschungsinstitut, Bonn, Germany for their support of this investigation and help with the hot pressing and extrusion of the P/M products.

REPORT DOCUMENTATION PAGE		READ INSTRUCTIONS BEFORE COMPLETING FORM
1. Report Number EOARD-TR-78-3	2. Govt Accession No.	3. Recipient's Catalog Number
4. Title (and Subtitle) DEVELOPMENT OF IMPROVED HIGH STRENGTH ALUMINUM POWDER METALLURGY PRODUCTS.		5. Type of Report & Period Covered Progress Report. # 1 no. 1 Sept. 30, 1977 - May 31, 1978
		6. Performing Org. Report Number DFVLR — IB-354 — 77/14
7. Author(s) DAVID P. VOSS (USAF)		8. Contract or Grant Number AFOSR [redacted] — 77 — 3440
9. Performing Organization Name and Address Institute for Materials Research DFVLR Postfach 90 60 58 5000 Cologne 90 West Germany		10. Program Element, Project, Task Area & Work Unit Numbers 2307/A1
11. Controlling Office Name and Address European Office of Aerospace Research and Development/LNM Box 14 FPO New York 09510		12. Report Date 31 May 1978 13. Number of Pages 105
14. Monitoring Agency Name and Address European Office of Aerospace Research and Development/LNM Box 14 FPO New York 09510		15.

16. & 17. Distribution Statement

Approved for public release; distribution unlimited.

18. Supplementary Notes

19. Key Words

Powder Metallurgy, Aluminum Powder Alloys, Vacuum Degassing
Extrusion, P/M Mechanical Properties, 2024, 7075

20. Abstract

This report summarizes findings involving the influence of processing variables on the production of 2024 and 7075 aluminum P/M alloy products. The study includes vacuum degassing at 10^{-4}Pa (vac. chamber) pressure and evaluation of outgassed products by partial pressure measurements. Extrusion from 90 % to 98 % reduction in area at temperatures from 613 K to 753 K have been investigated by tensile, compression, NTS/YS, and notched fatigue (K_t=3) testing. Mechanical properties for 2024 from 82 µm powder and for 7075 from 88 µm powder are reported.

2024-T351: UTS = 603 MPa, YS = 474 MPa, %e = 15,7 % (in 4D)
7075-T651: UTS = 679 MPa, YS = 627 MPa, %e = 12,6 % (in 4D)

with a an 33 % improvement in K_t=3 notch fatigue life of 2024-T351

The aim of this continuing effort is to develop a thorough understanding of the processing-structure-property interrelationship for these aluminum P/M alloys.

FORM 1473

409 451

EOARD-TR-78-3

1 December 1978

This report has been reviewed by the Information Office (EOARD/CMI) and is releasable to the National Technical Information Service (NTIS). At NTIS it will be releasable to the general public, including foreign nationals.

This technical report has been reviewed and is approved for publication.

John T. Milton

JOHN T. MILTON
Scientific and Technical Information Officer

Charles J. LaBlonde

FOR GORDON L. HERMAN
Materials Liaison Officer

FOR THE COMMANDER

Michael A. Greenfield

MICHAEL A. GREENFIELD, Ph.D.
Deputy Director

Table of Contents

	Page
Foreword	ii
Abstract (Form 1473)	iii
Introduction	1
Objectives	4
Procedures	5
Progress and Results	22
Discussion	72
Conclusion	83
Further Research Program	85
References	86
Appendix A (Diagrams of Mechanical Property Test Specimens)	97

Introduction

The powder approach to alloy development has distinct metallurgical advantages over the conventional cast and wrought approach. Processes employed for powder production can generate solidification rates sufficiently fast to suppress nucleation and growth of intermetallic compounds and/or low-melting eutectics. Powder metallurgy (P/M) processing also provides the ability to add large amounts of the commonly used primary hardening constituents without segregation problems and to introduce fine dispersed phases of normally hard-to-alloy constituents in a well distributed fashion. The quenched microstructure of such an alloy is primarily a homogeneous supersaturated solid solution with a very fine dendritic spacing. This allows for the development of improved combinations of mechanical properties along with improved ease of wrought fabrication of the P/M product.

In addition, the powder approach affords the opportunity for a low-cost manufacturing method. Direct near net shape hot pressing or powder forging combines the superior mechanical properties discussed above with the reduction of final product machining costs and material requirements.

Since the late 1950's there has been activity in development of heat-treatable high strength aluminum base alloys and products fabricated by the powder metallurgy process[1-66]. Distinction is made at this point between these recent alloy development efforts of heat-treatable alloys for near room temperature applications, and the earlier dispersion strengthened aluminum and aluminum alloy work for elevated temperature applications which will not be discussed.

Results from several of these recent investigations, which were conducted by research personnel at Kaiser Aluminum and Chemical Co., CA or at the Alcoa Technical Center, PA., show that heat-treatable aluminum powder alloys having combinations of high strength (greater than 7075-T6) and superior resistance to stress corrosion

cracking can be produced. The early Kaiser P/M program[1] investigated evacuation technology and aluminum P/M alloys intended for elevated temperature service wherein the alloying elements were relatively insoluble in solid aluminum at high temperatures. Later studies[2-5] investigated greatly increasing, by P/M technology,the ingot metallurgy (I/M) alloy limits, or alloyability, of aluminum for service at, or near, room temperature. Similar to the early research effort at Kaiser, the early P/M research programs at Alcoa concerned development of dispersion strengthened aluminum* and aluminum alloys** for elevated temperature applications. Later Alcoa aluminum P/M programs[6-31] have been directed at development of high strength P/M alloys for use at, or near, room temperature, where the oxide content is incidental - less than 0.5 w/o. These (latter Alcoa) programs have been centered around composition studies and examination of the effect of some processing variables on achieving definite combinations of improved mechanical properties - strength, ductility,K_{Ic} fracture toughness, and stress corrosion threshold; these programs were basically intended as a P/M alloy development effort with an associate investigation of the processing variables necessary to produce full scale components.

Additional investigations and reviews[32-66] have contrasted strength properties of various aluminum P/M products to the conventional I/M properties. However, no comprehensive study has been published for air atomized prealloyed powders which details the effect of metallurgical processing parameters on the properties and microstructure of high strength aluminum P/M alloy products. In addition, no concerted effort has been made and thus very little work has been published concerning the relationship among processing parameters, metallurgical micro-

* Sintered aluminum powder (SAP) is a non-heat-treatable dispersion strengthened alloy of aluminum and its oxide developed in Switzerland in the late 1940's.

**Aluminum powder metallurgy (APM) is the Alcoa designation for non-heat-treatable alloys with alloying elements added to form finely dispersed, insoluable components with aluminum, oxide contents are incidental - less than 0.5 w/o.

structure, and the fatigue crack growth behavior of aluminum alloy P/M products. Consequently, an insufficient understanding of the processing-microstructure-property interrelationship of these high strength aluminum P/M materials exists today, especially with regard to fatigue.

It is therefore the intent of the present research effort to develop an understanding of the metallurgical factors governing the types of microstructure obtained in high strength aluminum P/M products and to define the processing-microstructure-property interrelationship. In pursuit of this goal the complete potential of the P/M technology is not being employed. That is, alloying with elements which are not added to commercial wrought high strength aluminum alloys by conventional casting techniques, due to deleterious, brittle intermediate phase or nonequilibrium, low-melting eutectic phase formation, is not being pursued in this program. In short, the present program is not an alloy development effort. Instead, it was chosen to investigate the same alloy content in both the P/M and standard I/M condition to permit the correlation of mechanical properties, fabrication parameters, and microstructure between P/M and I/M materials of the same basic composition. In particular, this approach involves determining the metallurgical features controlling structure-property relationships in powder alloys with particular emphasis directed at the crack growth behavior. The two most widely used aerospace aluminum alloys, 2024 and 7075, were selected for investigation because of their current relevancy and the wealth of I/M background information that is available for these alloys.

Objective

The objective of this effort is to determine the processing and metallurgical factors controlling the structure-fatigue behavior relationship in high strength aluminum powder metallurgy products. The aim is to develop a processing schedule based on a desired microstructure that will yield improved combinations of crack growth behavior and other mechanical properties, while maintaining good stress corrosion resistance.

A second objective is to combine the optimum microstructure-property relationship described above with an economic hot compaction process. Hot pressing and near net shape forging of powder compacts are two viable manufacturing technologies which offer a high potential pay-off for an economical hot compaction process.

Procedures

The compositions of the alloys investigated are based on the two most widely used high strength aluminum I/M alloys 2024 (AlCuMg2) and 7075 (AlZnMgCu1,5). The chemical analysis for the P/M and corresponding I/M alloys investigated are given in Table 1. The various prealloyed, air atomized powders were commercially produced by Alcoa (Alcoa Technical Center). The oxygen content was determined by standard wet-filter analysis methods for the uncompacted powder and by photon activation analysis for the compacted/extruded samples. After compaction and extrusion the particles oxide surface layer has been so finely broken up that the oxide particles flow through the filter paper used for standard wet analysis. Consequently, the standard filtration analysis of compacted and extruded P/M products yields oxygen contents which are a factor of 10^2 to low.

The improved compaction/fabrication procedures employed to produce high quality P/M products consists of seven steps.

(1) Cold Compaction: Room temperature isostatic compaction at 240 MPa employing a wet bag technique in a National Forge hydraulic machine is used to produce an 80 % dense green compact. Isostatic pressing results in somewhat higher densities than conventional pressing for a given compacting pressure. However, isostatic pressures significantly higher than 240 MPa produce green compacts with densities greater than 85-90 %. This higher density level hinders evacuation and seals much of the gaseous product so it cannot be removed during evacuation. Both of the P/M alloys have a 45 % apparent "as poured" density which can be vibratory compacted or hand tamped to 58% tap density before cold isostatic pressing. The isostatic pressing operation has no effect on the P/M product's final mechanical properties. However, because an upper bound on the end mass of the final P/M product results from the size of the extrusion press container, production efficiency and capacity are maximized by hot pressing an 80 %

alloy designation	fabrication condition	composition weight percent (w/o)										
		Cu	Mg	Zn	Mn	Cr	Ti	Ni	Fe	Si	O[1.]	Al
2024 - A	I/M - Commercial Extrusion	4.80	1.58	N.D.	0.81	N.D.	N.D.	N.D.	0.34	0.27	N.D.	balance
2024 - B	I/M - high purity base 99.99% Commercial Extrusion	4.10	1.50	N.D.	0.89	N.D.	N.D.	N.D.	0.25	0.20	N.D.	"
2024 - C	I/M - Specially Cast Laboratory Ingot (Fe&Si content levels similar to powder)	4.42	1.50	<0.01	0.66	N.D.	0.01	N.D.	0.15	0.07	N.D.	"
2024 - D	P/M APD 117 µm	4.45	1.37	0.01	0.64	-	<0.01	-	0.12	0.05	0.134	"
2024 - E	P/M " 82 µm	4.45	1.37	0.01	0.64	-	<0.01	-	0.12	0.05	0.195*	"
2024 - F	P/M " 44 µm	4.46	1.51	0.02	0.73	-	0.03	0.01	0.27	0.10	N.D.	"
2024 - G	P/M " 36 µm	4.45	1.37	0.01	0.64	-	<0.01	-	0.12	0.05	0.012	"
7075 - H	I/M - Specially Cast Laboratory Ingot (Fe&Si content levels similar to powders)	1.72	2.68	5.67	0.02	0.19	0.01	N.D.	0.16	0.07	N.D.	"
7075 - L	P/M APD 88 µm	1.66	2.67	5.83	-	0.20	0.04	-	0.12	0.07	0.054	"

Notes: N.D. - not determined

* - 0.54 w/o in the as isostatic compacted condition, determined by standard wet analysis

1. - determined by photon activation analysis

Table 1. Chemical Analysis of powder and ingot materials as determined from wrought products.
(I/M - ingot metallurgically produced, P/M - powder metallurgically produced)

dense green compact instead of 45 % or 55-60 % dense green compacts. The average experimental compression ratio for both alloys from the vibratory compacted condition to the isostatic pressed condition is C_{Vol}*= 0.715. Green compacts have been produced in 44 mm diameter by 55 mm and 76 mm dia. by 205 mm long forms.

(2) Canning: The green compacts can be easily turned on a lathe, center rest necessary for the longer compacts, and thereafter fit snugly into AlMg-3 aluminum alloy cans of 3 mm wall thickness. The cans must be double welded to prevent vacuum leakage, as has been reported by Cebulak[24e]. Figure 1 shows typical green compacts in the isostatic pressed, machined and canned conditions.

(3) Preheating and Evacuation: Because the aluminum powder's surface oxide is very reactive with respect to moisture at room temperature, it is necessary to remove a high percentage of the water and hydrogen content from the surface oxide before complete densification. This is accomplished in order to prevent high gas pressures in the finished P/M product at the solution heat treatment temperature (SHT). High gas pressures at this temperature in the near 100 % dense product can cause additional internal porosity, delamination, or blistering of the metal surface.

Evacuation of the canned green compact is initiated at room temperature and continues until a vacuum pressure of 10^{-4} Pa is reached in the vacuum chamber, figure 2. At this point the cans are checked for leakage and, if sound, placed in an electrically heated air furnace for preheating and further evacuation. A flexible steel hose connects the can's AlMg-3 evacuation tube to the vacuum chamber. The furnace is automatically switched-off when the pressure increases to 10^{-2} Pa and is automatically switched-on again when the pressure falls below $3 \cdot 10^{-3}$ Pa. This procedure is followed to prevent contamination of the compact since a cold trap is not employed on the vacuum system and also to expedite the evacuation process by reducing the likelihood of an over-

* modified compression ratio = ρ_{green}/ρ_{tap} instead of $\rho_{green}/\rho_{apparent}$

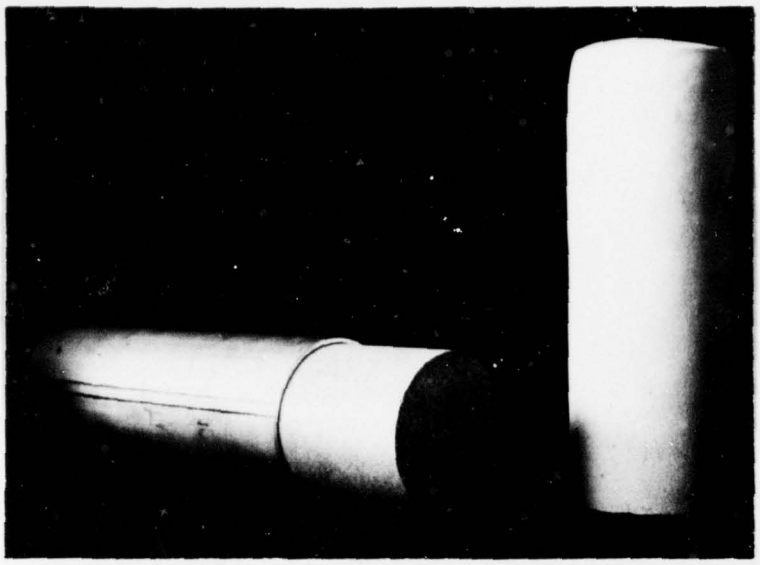

Figure 1: Pictures of typical cold isostatic pressed and canned green compacts 80 % dense.

1a) as cold isostatically pressed (right) and after machining

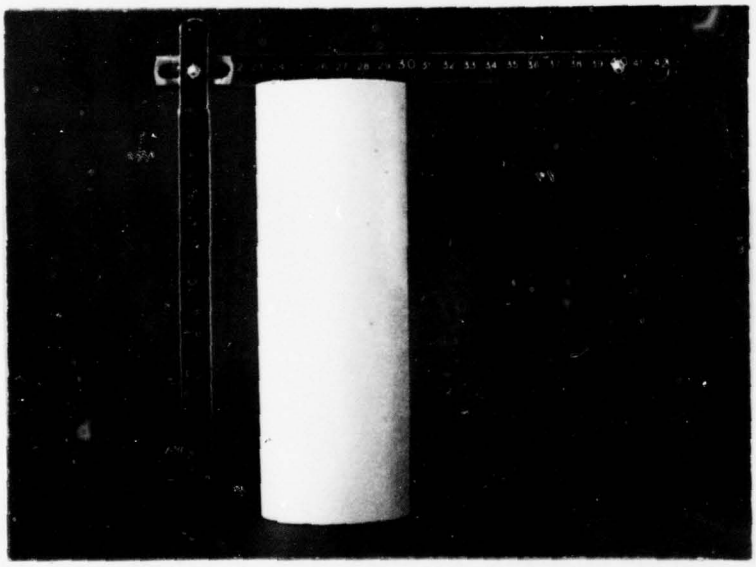

1b) after machining (lathe) 76 mm Ø x 200 mm

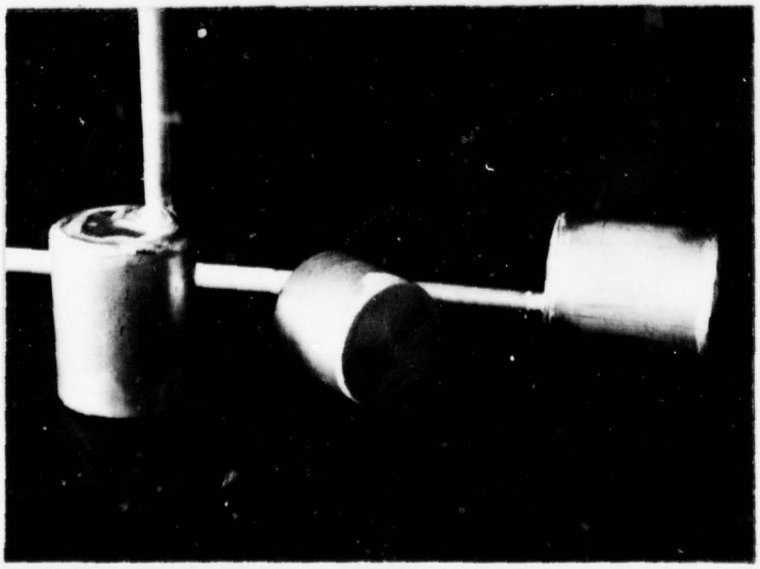

1c) as machined (middle) and canned with evacuation tube (double welded)

green compact:
44 mm Ø x 52 mm

canned:
50 mm Ø x 60 mm

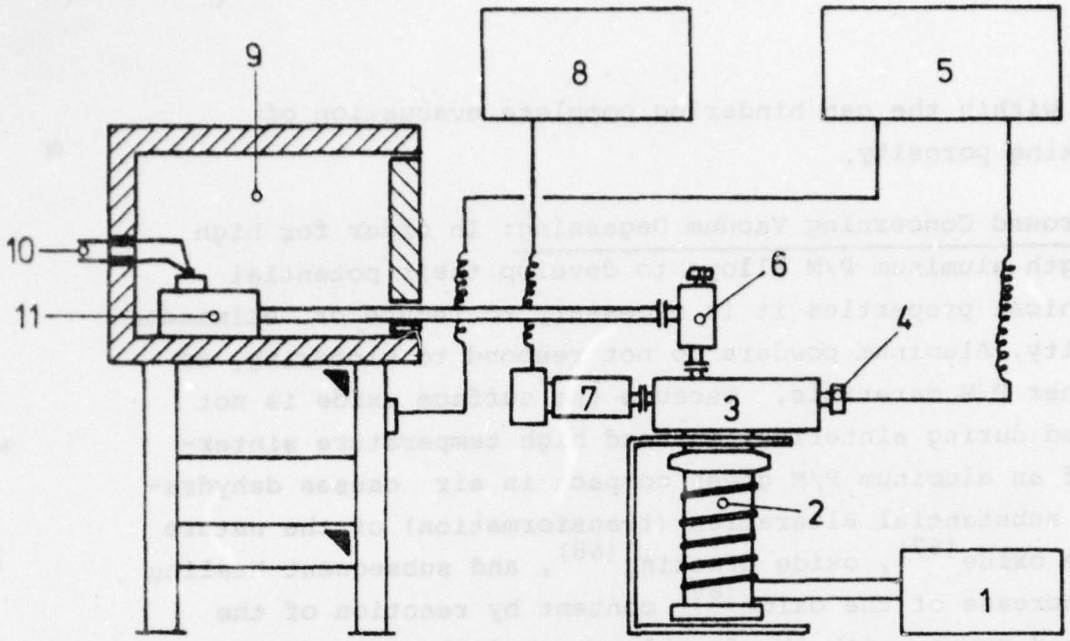

EVACUATION SYSTEM SCHEMATIC

1 MECHANICAL (VACUUM) PUMP

2 DIFFUSION (VACUUM) PUMP

3 VACUUM CHAMBER (Vac. Chamber)

4 PRESSURE GAUGE

5 CONTROL UNIT

6 VALVE

7 ANALYTICAL ION GAUGE

8 ION GAUGE CONTROL UNIT

9 FURNACE

10 THERMOCOUPLE

11 ENCAPSULATED PRODUCT

Figure 2: Schematic representation of the evacuation system used for both 2024 and 7075 canned green compacts.

pressure within the can hindering complete evacuation of slow leaking porosity.

(3.1.) Background Concerning Vacuum Degassing: In order for high strength aluminum P/M alloys to develop their potential mechanical properties it is necessary to reduce or eliminate porosity. Aluminum powders do not respond to sintering, as do other P/M materials, because the surface oxide is not reduced during sintering. Instead high temperature sintering of an aluminum P/M green compact in air causes dehydration, substantial alteration (transformation) of the nature of the oxide[67], oxide cracking[68], and subsequent healing and increase of the oxide[69] content by reaction of the released oxygen with the freshly exposed aluminum. However, the above described sintering is accomplished without sufficient strength increase and porosity reduction. Consequently, several elevated temperature (600 K to 850 K) degassing treatments have been investigated for aluminum P/M production: flowing dry atmospheres with low oxygen contents, flowing inert atmospheres (nitrogen and argon), and a partial vacuum.

For low and moderate tensile strength aluminum P/M alloys (< 450 MPa), liquid phase sintering of precompacted,blends of elemental powders in a flowing dry, low oxygen content or dry inert atmosphere followed by hot working (powder forging) is sufficient to produce acceptable strength levels[18, 21]. Liquid phase sintering allows for rapid diffusion of alloy elements and "cracking and peeling off"[66] of the oxide film to promote the sintering process. However, liquid phase sintering treatments can not provide the properties demanded for high strength aluminum P/M products. Even when extensive hot working operations are employed and densities approach 100 % of the calculated theoretical density, liquid phase sintered products still contain a small (< 1 %) amount of porosity. In addition, liquid phase sintering has a deleterious effect on the mechanical properties of the high strength alloys because of the brittle eutectic that results in the grain boundaries.

For high strength aluminum P/M alloys acceptable properties have been developed by high temperature (700 K to 850 K) degassing in a flowing, dry inert atmosphere[22, 25]. However, Lyle et al.[21] reported finding significant traces of hydrogen within the final P/M product and nitrogen/argon on fracture surfaces of these products. Further work by Cebulak and Truax[22] and Cebulak[23] following the efforts of Dromsky and Lenel[68] on SAP, demonstrated significant fracture toughness (NTS/YS) and ductility improvements resulting from a vacuum (133 Pa)[24e] preheat process. These improvements were especially remarkable in the short transverse direction of extruded products. Lyle and Cebulak[26] reported that porosity is not a significant factor in the structure of P/M products produced by vacuum preheating.

Roberts[4, 5] has investigated reduction of water, hydrogen contamination and pore elimination by vacuum degassing (10^{-2} Pa) at moderate temperatures (600 K to 700 K) so as not to cause deleterious agglomeration of the dispersoid transition elements. The investigation was not directed at fine powders but rather at powders in the 150 to 44 μm range so as to reduce the total contaminated surface oxide area. Although excellent longitudinal properties were obtained, transverse ductility was poor - possibly from insufficient extrusion deformation of 8.5:1 (88 %) with -100 +325 mesh powders - and longitudinally oriented internal porosity was not eliminated by the vacuum treatment.

(3.2.) Evacuation System: The vacuum system consists of a Leybold-Heraeus D60A mechanical pump with a 60 m^3/hr rating and a Leybold-Heraeus PD1000 diffusion vacuum pump rated at 1000 L/sec, figure 3. Vacuum pressure measurements are made in the vacuum chamber at room temperature with a THERMOVAC TM 20 constant resistance conductivity vacuum gauge from 10^5 Pa to 10^{-1} Pa and with a IONIVAC IM 20 hot-cathode ionization gauge from 10^0 Pa to 10^{-8} Pa. The pressure gauges are connected to a Leybold-Heraeus COMBIVAC IT 20 master unit for control and pressure read out. The COMBIVAC IT 20 master control

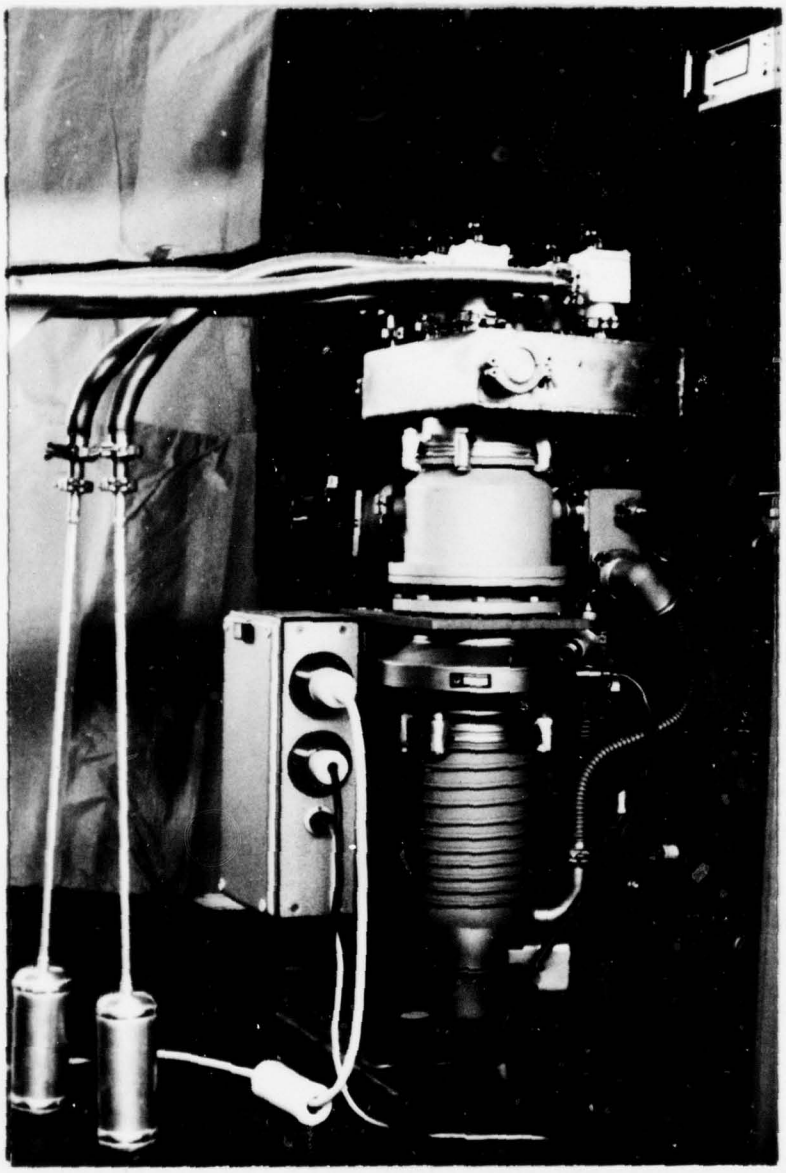

Figure 3: Evacuation system with flexible steel hose connected to two canned green compacts (lower left). The system has six hose connections with valves, four flexible hoses shown here are leading direct to the furnace (not shown). The canned green compacts shown are the shape used for HIPing.

unit contains a "Torrostat S 20" pressure switch which allows auxiliary, pressure-dependent on/off switching based on two programmable pressure settings.

(3.2.1.) Pressure Measurement: The physical phenomenon utilized for pressure measurement in thermal conductivity vacuum gauges is that the thermal conductivity of a gas, within certain limits, is dependent on the gas pressure. For constant resistance thermal conductivity vacuum gauges, such as the THERMOVAC TM 20, the sensing filament located within the gauge tube forms one branch of a Wheatstone bridge circuit. The heating potential applied to this bridge is controlled so the resistance and therefore the temperature of the sensing filament remains constant independent of the rate of heat transfer from the filament. Since the rate of heat transfer from the sensing filament to the gas increases with rising gas pressure, the potential applied to the permanently balanced bridge is a measure of the pressure.

With respect to the IONIVAC IM 20, a precise, constant electron current is emitted by a hot cathode which ionizes the surrounding gas particles. The resulting positive ion current being proportional to the pressure, or number of gas molecules available for ionization.

(3.2.2.) Measurement of Out-gassing Products: Out-gas products are monitored with the aid of a Centronic type 12 Analytical Ion Gauge, AIG 50. The ion gauge has both total and partial pressure measurement capabilities. The AIG 50 ion gauge operates in the pressure range from 10^{-2} Pa to 10^{-7} Pa and in the mass range from 2 to 50 a.m.u. The gauge head is mounted on the vacuum chamber and as such pressure measurements are made at room temperature. For partial pressure measurements, the ionizer is designed so that, by potential inversion, the ion beam enters a quadrupole mass filter so only ions of the selected mass number reach the Faraday cup collector. For total pressure measurements, all the ions produced are collected on a separate electrode. The mass peak resolution over the

whole mass range at 50 % peak height is $M/\Delta M > M$.

In addition to periodic total pressure measurements with the analytical ion gauge, a two channel linear SERVOGOR 2S plotter is used to continuously record the vacuum pressure as measured by the IONIVAC IM 20 gauge in the vacuum chamber and the furnace temperature. Along with the furnace's built-in thermocouple, the temperature is recorded from a Type K Chromel-Alumel thermocouple embedded in a 40 mm dia. by 40 mm long 2024 aluminum alloy block placed in the furnace next to the can being evacuated.

(4) Homogenization: The green compacts are simultaneously subjected to homogenization and vacuum preheat treatments. After the alloy's respective SHT temperature is reached, homogenization and further evacuation are conducted according to the following schedule, figure 4:

2024 - 24 h at 766 K
7075 - 16 h at 733 K + 24 h at 743 K.

After the homogenization treatment has been completed, the hot, aluminum evacuation tube is hammered flat along approximately a 70 mm section, starting approximately 40 mm before the can. The section is subsequently pinched in three places, with the apparatus in figure 5, and is finally severed with this apparatus at the middle pinch. The pinched tube is immediately welded to insure a partial vacuum is maintained in the can. During this complete operation the vacuum pressure is monitored to insure that a leak is not developed during hammering or pinching. The final vacuum pressure at the time of closure in the vacuum chamber is 10^{-4} Pa.

(5) Hot Pressing/Compaction: The hot compaction operation is accomplished either in an extrusion press against a blind die or by impact extrusion in a high energy rate forming (HERF) Dynapak machine with a thick copper disc placed between the die and compact.

The canning material is machined away (turned) after this compaction step and before extrusion.

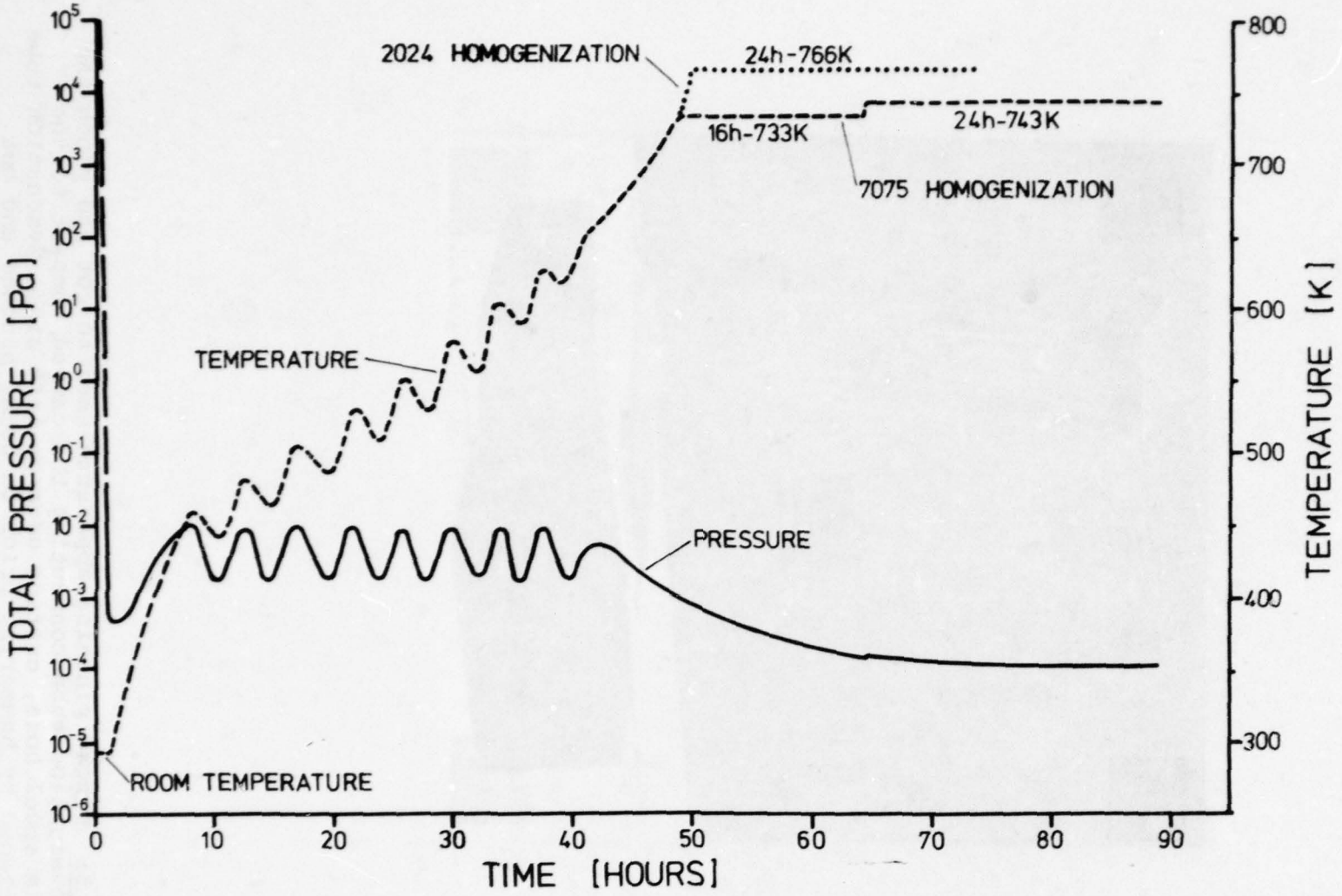

Figure 4: Results of a typical combined evacuation-homogenization vacuum preheat treatment. Heat-up rate is limited by automatic pressure switching control. Partial pressure measurements are from vacuum chamber (RT), not in the can.

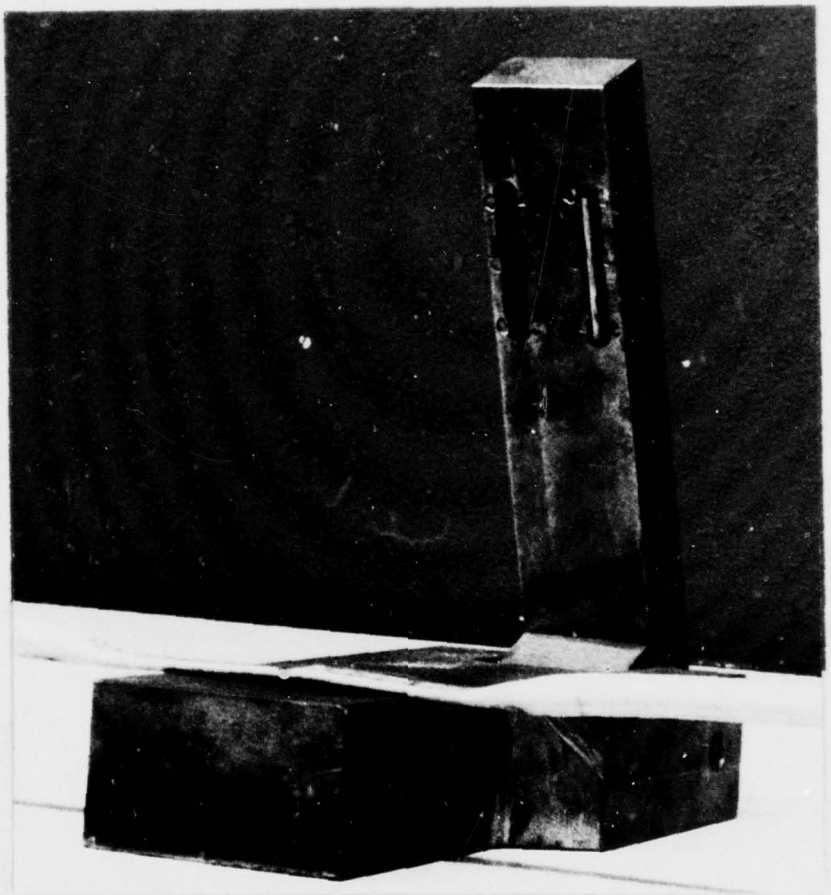

Figure 5: Hinged pinching apparatus used to cut and pinch the AlMg3 evacuation tube connecting the canned compact to the flexible steel hose, cutting edge on left side. Evacuation tube is flattened by hammering prior to being pinched and cut. (Prior pinching of the tube on each side of the cut is not visible.)

(5.1.) Extrusion Press: A 634 MPa, 80 mm ø (diameter) press at the Vereinigte Aluminium Werk's (VAW) Leichtmetall-Forschungsinstitut in Bonn is used for hot compaction. A dwell time of 10 min under full pressure (634 MPa) at a temperature of 753 K for the 2024 alloy and 723 K for the 7075 alloy is employed. The hot can is given a coating of graphite lubricant as it is placed in the extrusion container. Without lubricant the compacted product (billet) has a tendency to deform into a "U" shape when ejected from the press. The welded evacuation tube nipple is slightly bent over on to the top of the can and placed in the press against the blind die/flange. The green compact is SHT in a circulating air furnace at the alloy's respective SHT temperature just prior to compaction, with a soaking time according to the compact diameter[70]: for the 76 mm ø compacts 210 min. at 766 K for 2024 and 743 K for 7075. Compaction is conducted on the same day the evacuation tube is pinched and sealed. This practice is intended to minimize the effect of slow vacuum leaks which could be developed during sealing and go undetected. To date only 76 mm ø x 200 mm canned green compacts have been compacted by this process.

It is important to note that for both hot pressing/compaction and extrusion, the extrusion press container and the green compact, or billet in the case of extrusion, are preheated to the referenced preheat temperature. The extrusion container is resistance heated while the canned green compact is preheated in a circulating air furnace. The extrusion billet is preheated to the extrusion temperature, after the can is removed, inductively.

(5.2.) HERF Hot Compaction: This compaction process employs DFVLR's Dynapak and is similar to that described above for the extrusion press with the following exceptions: no dwell time is possible with the Dynapak, canned green compacts are 50 mm ø x 60 mm or 76 mm ø x 95 mm, a die with a 15 mm thick half hard copper disc is inserted between the die and canned compact, a Dow Corning "Molykote" spray lubricant is applied to the die surface and the extrusion container, and an energy

of $2.155 \cdot 10^4$ Joule. The deliverable Dynapak energy is adjustable between $2.155 \cdot 10^4$ and $6.66 \cdot 10^4$ Joule. The intent of the copper disc is to provide initial flow resistance and thereby insure full densification, while allowing excess energy to be absorbed in deformation of the disc through a die. A slight amount of macroscopic metal flow therefore occurs in material compacted by this process. The die is 20 mm ø for the 50 mm ø compaction and 34.5 mm x 18.5 mm for the 76 mm ø.

The Dynapak's extrusion container is flame heated, figure 6.

(6) Hot Working: A hot working operation is applied to the billet by extrusion to provide additional strength and ductility. The extrusion billet is inductively preheated to the extrusion temperature and is extruded through an unlubricated 180° die. The extrusion pressure is initially adjusted to yield a defect free surface. The ram speed which is controlled by the extrusion pressure, is maintained constant at the highest speed/pressure which produces the defect free surface. (In removing the canning material, the billet is reduced in size from 80 mm to approx. 70 mm in diameter and 160 mm to 135 mm in length.) Extrusion was performed under various conditions as reported in the Results Section of this report.

For HERF impact extrusion, the Dynapak energy is again adjusted for $2.155 \cdot 10^4$ Joule as for HERF hot compaction. A 16 mm ø, conical die with a 110° included angle is lubricated, as is the extrusion container, with MOLYKOTE. The extrusion container is 43 mm ø and therefore provides a 7.14 : 1 direct extrusion ratio (86 % reduction in area).

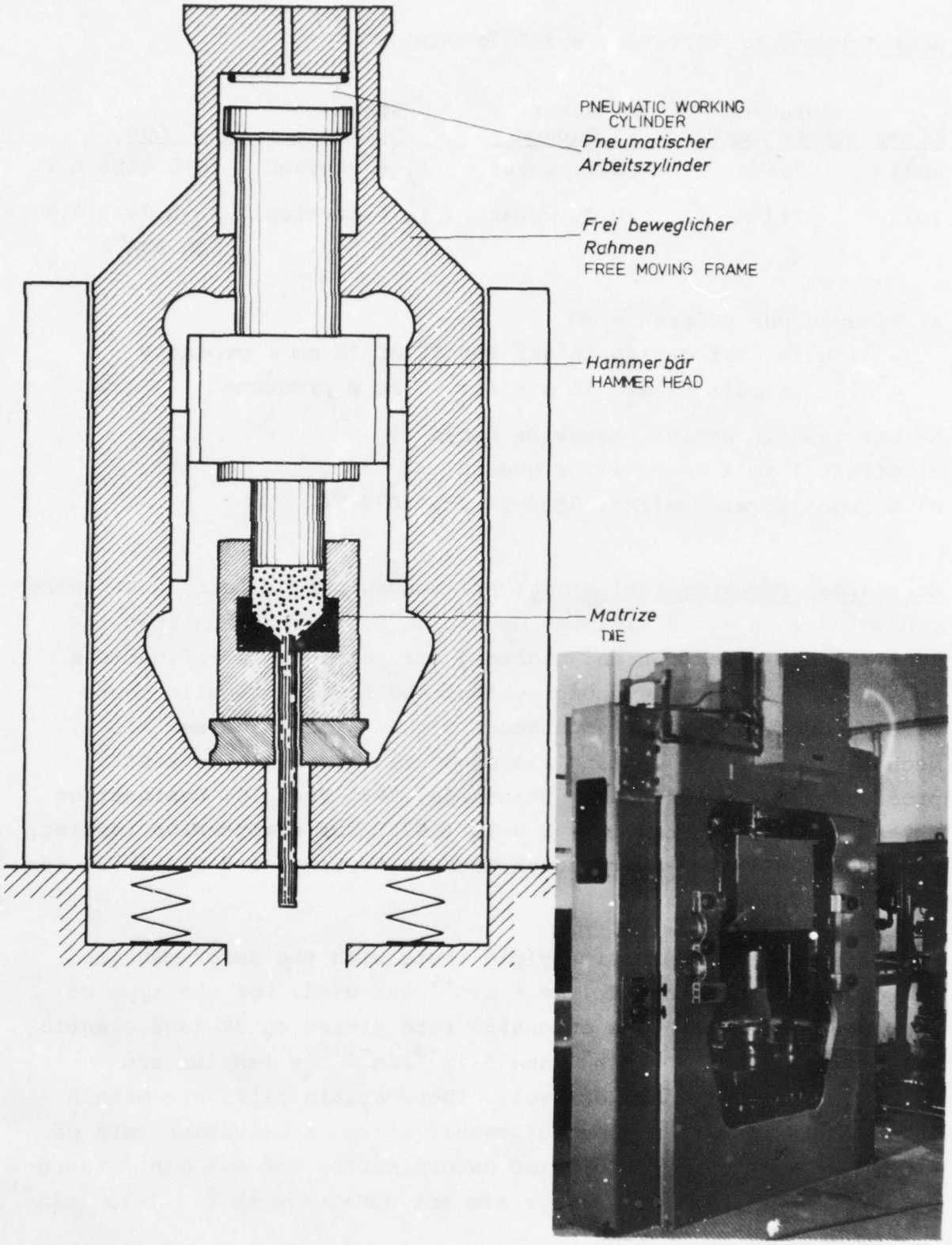

Figure 6: Schematic presentation and picture of DFVLR's Dynapack HERF impact extrusion apparatus. The protection cylinder (middle o picture) travels with the Hammer Head to cover the container/die during impact, protection cylinder not shown in schematic.

(7) Heat-Treatment: 2024-T351 and 7075-T651

Alloy	Solution Treatment [a,b]	Water Quench	Stress Relief [c,d]	Age
2024	766°K	R.T. water	$1\frac{1}{2}$ % stretch	7-10 days R.T.
7075	743°K	R.T. water	$1\frac{1}{2}$ % stretch	3- 5 days R.T. + 24h 394°K

a) Time as per reference 70
   - 1 h in salt or $1\frac{1}{2}$h in air for 16 or 18 mm ø products
   - $2\frac{1}{2}$h in salt or $3\frac{1}{2}$h in air for 70 mm ø products

b) SHT in salt unless otherwise noted

c) Within 1 to 2 hours after quench

d) Without stress relief: 2024-T4 and 7075-T6

(8) Mechanical Property Evaluation: All mechanical property tests were conducted with, as a minimum, duplicate test specimens from the longitudinal direction and machined according to specifications in Appendix A. Tensile, compression, and notched tensile tests were conducted at room temperature with a Zwick machine. All mechanical property testing was conducted according to test procedures outlined in ASTM Standards, 1975 Part 10: Designation E 8-69 for tension testing, E 9-70 (1973) for compression testing, E 338-68 (1973) for sharp notch tension testing, and E 466-72T for fatigue testing.

For tension and compression-yield tests with the Zwick machine, a crosshead extension of 1 mm · min^{-1} was used. For the type of specimens examined, this extension rate yields an average elastic strain rate $\dot{\varepsilon} = 1 \cdot 10^{-2} min^{-1}$ and $5 \cdot 10^{-3} min^{-1}$ for tension and compression testing respectively. These strain rates are within the ASTM Standards' maximum allowable stress application rate of 690 MPa · min^{-1} for yield point determination and 0.5 min^{-1} thereafter. At RT, aluminum alloys are not sensitive to $\dot{\varepsilon} < 1 \cdot 10^{-2} min^{-1}$.

For sharp notch tension testing a crosshead extension of 0.5 mm · min^{-1} was employed. For the sharp notch tension specimen examined, this extension rate yields an average strain rate $\dot{\varepsilon} = 5\ 10^{-3} min^{-1}$.

Sharp notch testing of aluminum alloys at room temperature are reported as not being appreciably sensitive to the rate of loading provided strain rates normally used for tensile testing are employed. This testing is performed to provide a NTS/YS ratio, an accepted, accurate measure of fracture toughness in aluminum alloys. In general, NTS/YS ratios exceeding 1.25 indicate high toughness properties.

The notch fatigue tests, K_t=3 were conducted with an Amsler resonance fatigue machine operating at a frequency of 100 cps. All tests were conducted in lab air at r = 0.1.

Progress and Results

1. Powder Characterization

The various prealloyed powders used for this investigation were air atomized. Atomized powders were chosen because they are: readily available commercially, solidified with a high solidification rate (10^2 to 10^4 K sec^{-1}), easily producible with medium* to fine** average particle diameters (APDs), and irregularly shaped. Figures 7,8 show the fineness of the solidification structures which have an average 2.4 µm dendrite spacing. The dendrite arm spacing (DAS) ranges from approx. 1.2 to 3.5 µm for 2024 particles and to 3.75 µm for 7075 particles, figure 9. The powders were also examined with a CAMBRIDGE STEREOSCAN S4 30KV(max.) scanning electron microscope and found to be irregular, slightly elongated, rounded and have some porosity, figure 10. The size distribution for the 7075 alloy L powder with an 88 µm APD is shown in figure 11, and for the 2024 alloys D through G powders with 117, 82, 44, and 36 µm APDs respectively, in figure 12.

2. Powder Compaction

2.1. Cold Isostatic Compaction

The effect of prior cold (room temperature) isostatic compaction on final mechanical properties was investigated for 2024-T351 alloy E. A comparison was made between P/M products produced by 25 : 1 direct extrusion (96 % red. in area) at 753 K, from green compacts of 80 % density (isostatic pressed) and 58 % tap density (vibration compacted). Mechanical property data from both products show no significant effect of the cold isostatic compaction, however from the 4 samples tested a slight ductility increase appears to have resulted from the isostatic compaction.

Compaction (T351)	UTS	0.2% YS	0.2% CYS	R.A.	e (in 4D)	NTS/YS
	(MPa)			(%)		
Isostatic	494	382	393	27.8	17.0	1.42
Vibration	492	382	392	24.5	15.6	1.40

* - 100 + 325 mesh (149 to 45 µm)
** - 325 mesh (11 µm)

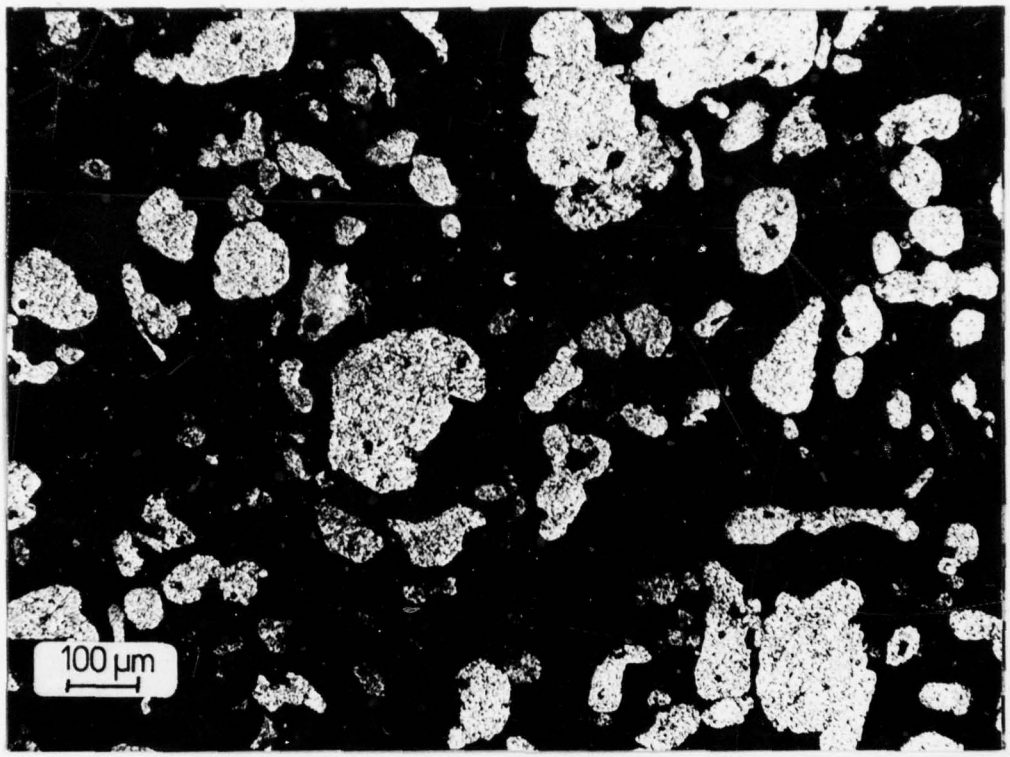

100x

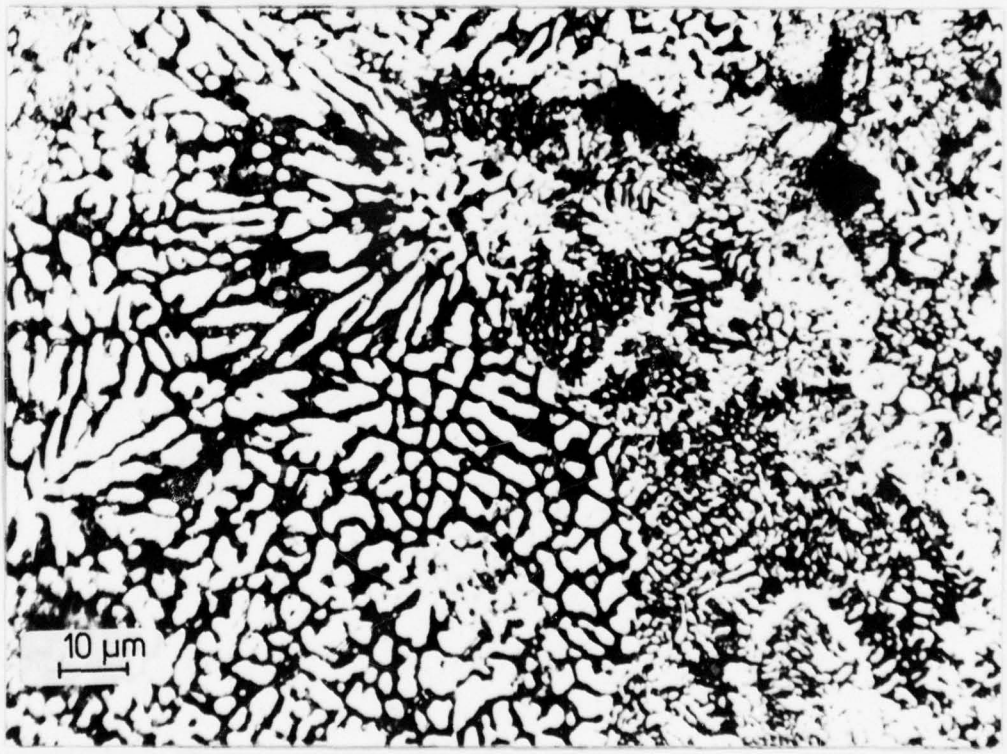

1000x

Figure 7: Representative sample of the dendrite arm spacing (DAS) in "as atomized" 2024 alloy E powder. Partial central porosity and rounded surfaces are noticeable in the embedded and polished powder (above). The DAS size range is observed in the 80 % dense, cold isostatically pressed green compact (below).

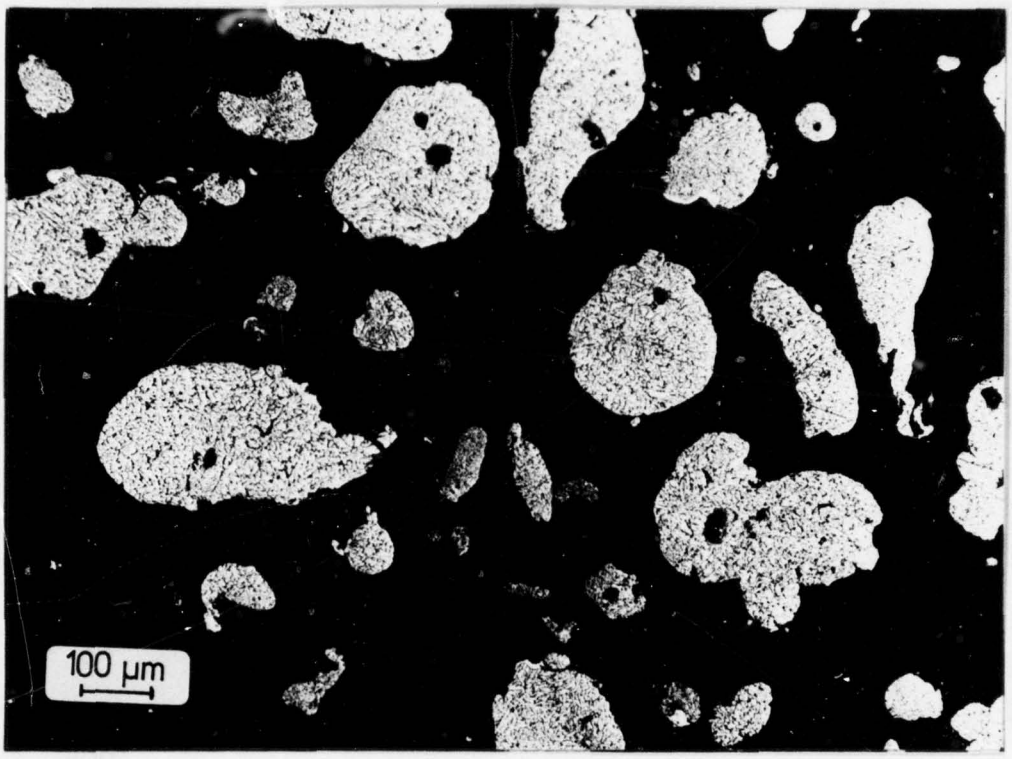

100x

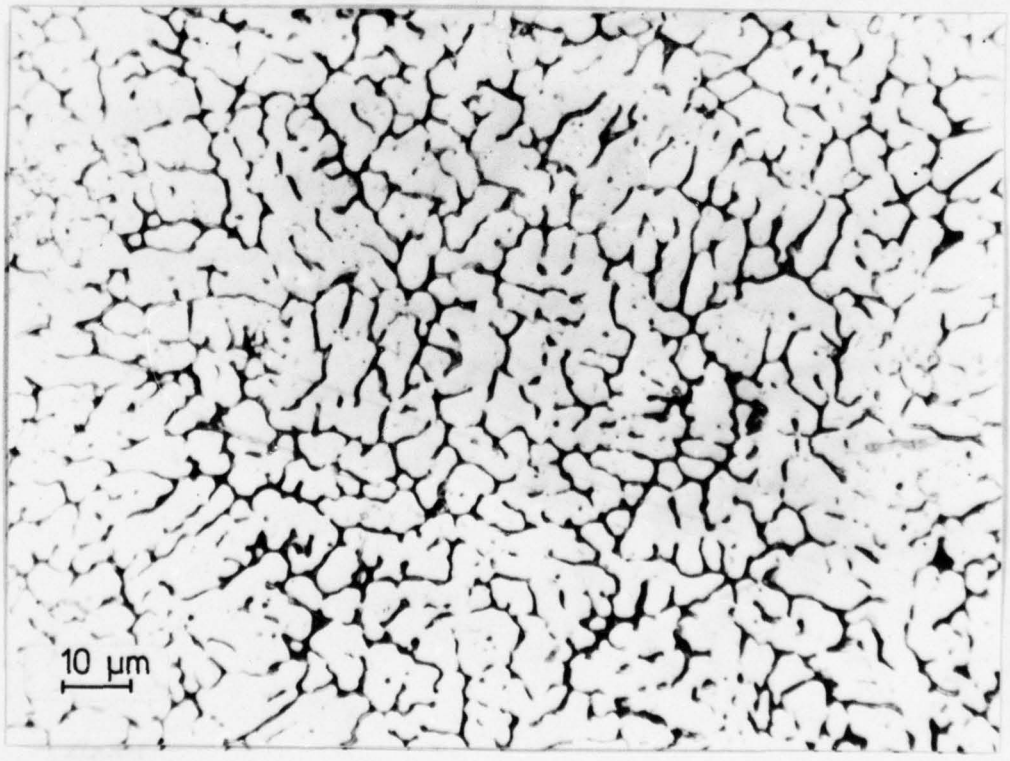

1000x

Figure 8: Representative sample of the dendrite arm spacing (DAS) in "as atomized" 7075 alloy L powder. Partial porosity can be seen in the embedded and polished powder (above), especially noticeable in the larger particles. The large size distribution between the 2024, figure 7, and 7075 powders is readily apparent.

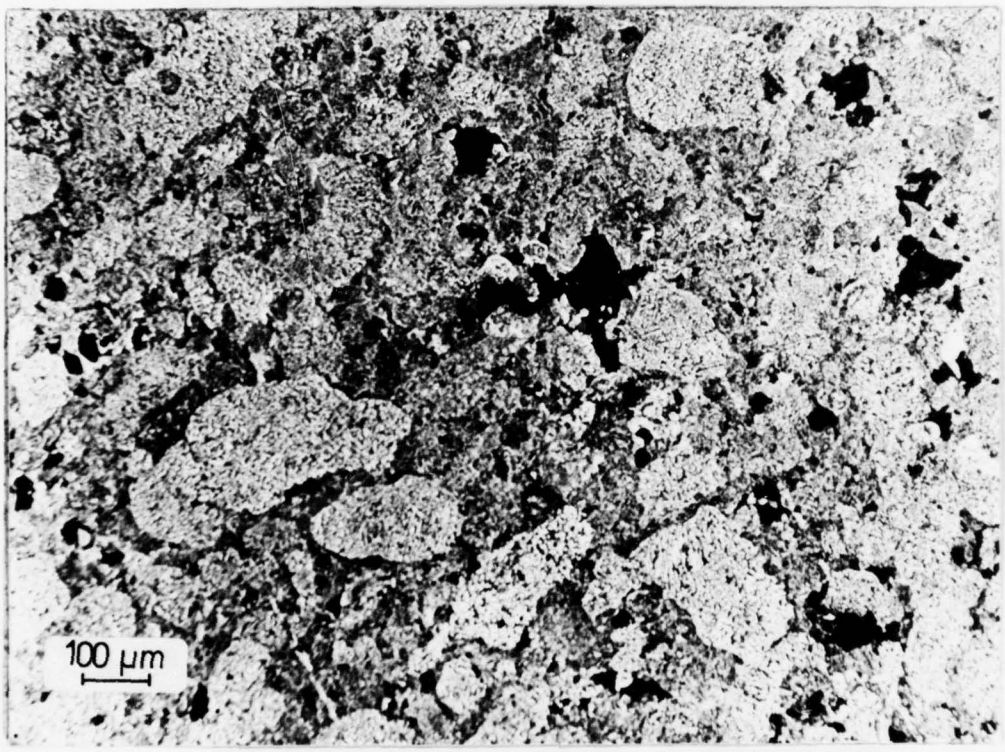

100x

Figure 9: Representative structure of the 80 % dense cold isostatically pressed green compact. Sample shown for the 2024 P/M alloy E is representative also of the 7075 P/M structure.

2024

(APD 44 µm)

500x

7075

(APD 88 µm)

200x

Figure 10: Representative SEM pictures for characterization of the irregular, slightly elongated 2024 (above) and 7075 (below) powders. As a whole, no significant difference exists between the 2024 and 7075 powder shapes, the 2024 picture (above) was selected because of the surface detail that is provided by the particle in the lower left of the picture.

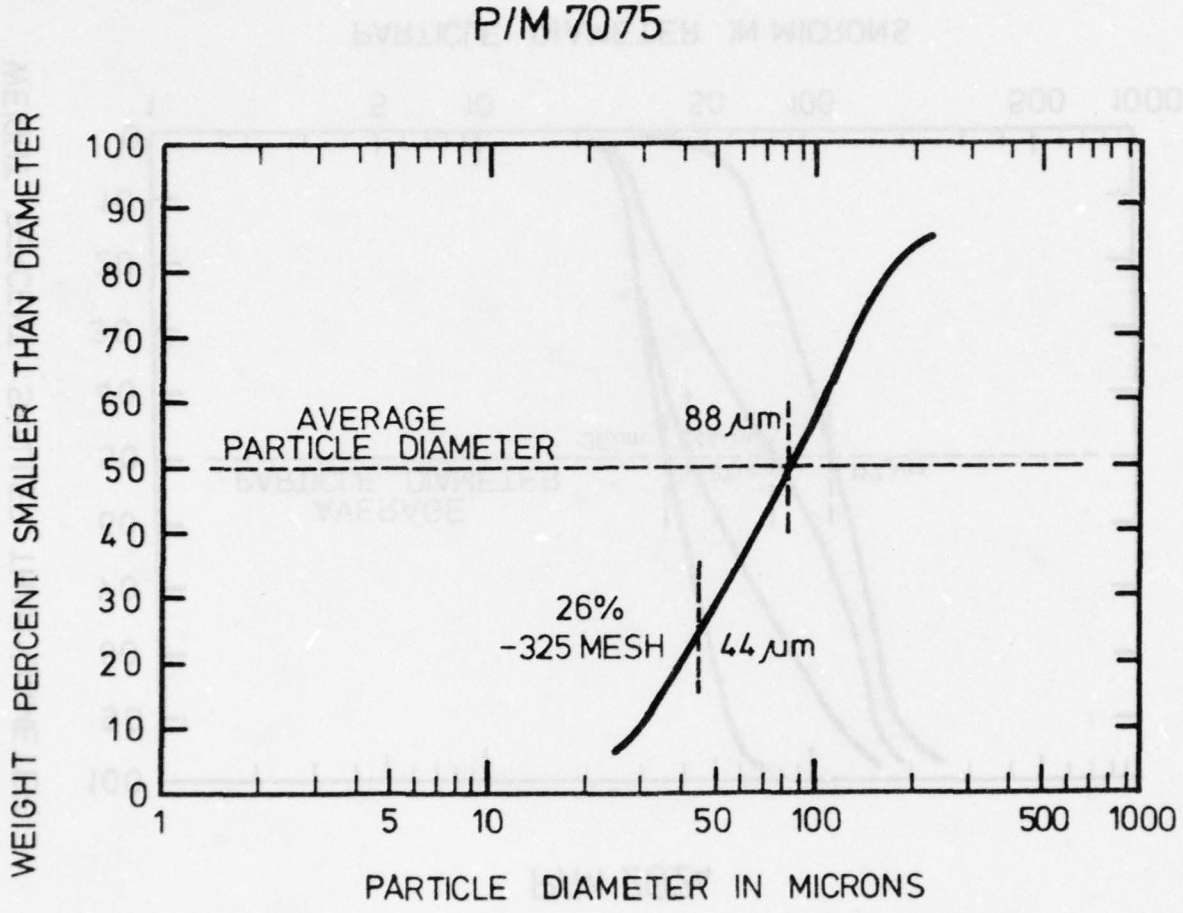

Figure 11 Powder size distribution from screen and micromesh sieve analysis for 7075 alloy atomized powders (alloy L).

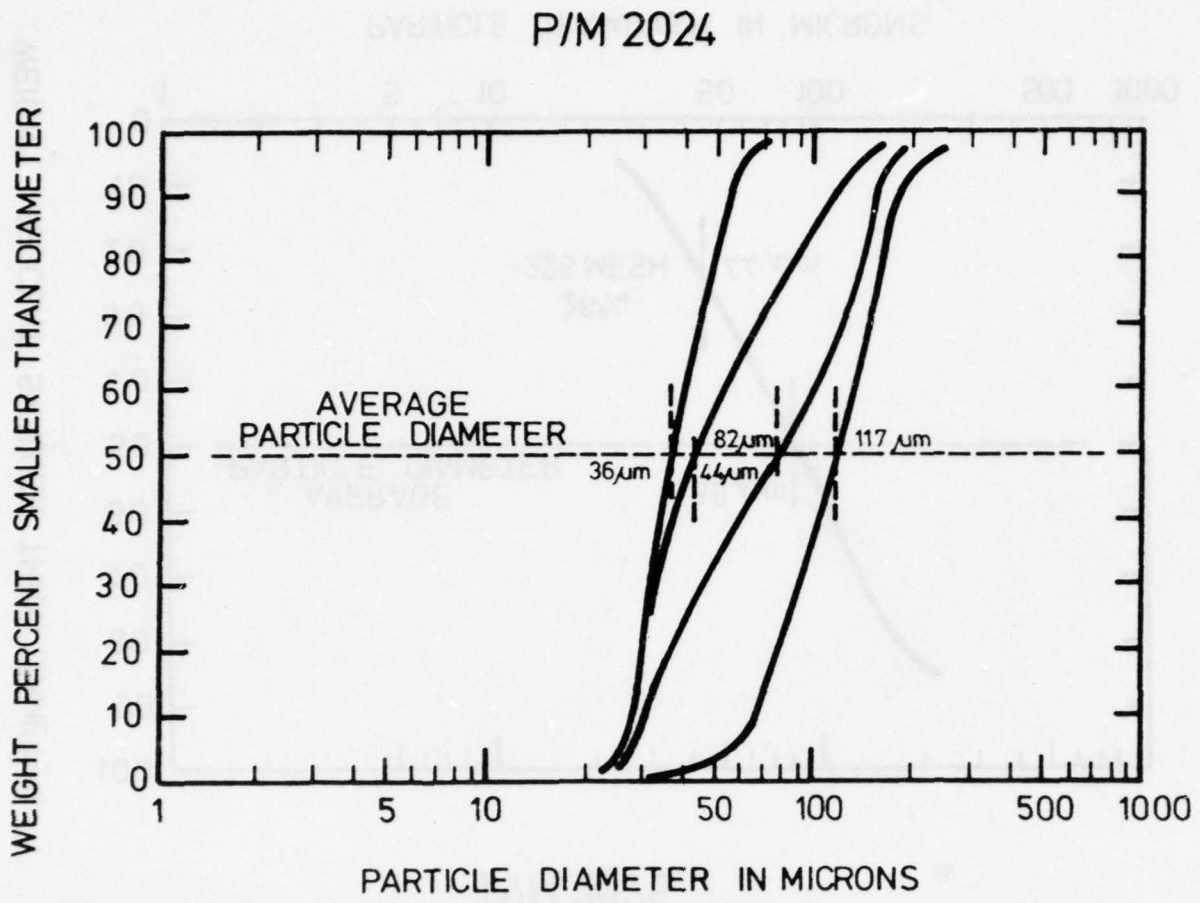

Figure 12 Powder size distribution from screen and micromesh sieve analysis for 2024 alloy atomized powders. The 36 µm and 117 µm APD powders (2024 alloys G and D, respectively) were screened from the 82 µm APD alloy (2024 alloy E). The % - 325 mesh fraction is 66 %, 50 %, 28 %, and 3 % for the 36 µm (alloy G), 44 µm (alloy F), 82 µm (alloy E) and 117 µm (alloy D) APD powders respectively.

2.2. Hot Isostatic Compaction

An investigation of the 2024 alloy E response to hot isostatic pressing (HIPing) was conducted. The powder was cold isostatically pressed, canned, and evacuated in the manner previously described for hot compaction. The canned green compact was HIPed at 713 K for 2h under a pressure of 132 MPa, figure 13. Subsequent property investigations revealed a non-ductile product having a density of $2.63_2 \cdot 10^3 kg \cdot m^{-3}$ (94.3 % dense) and a tensile yield strength equal to the material's 188 MPa ultimate strength. In addition, 1 mm Ø blisters were observed on the surface of products which were SHTed.

The tensile fracture surface of the HIPed product appears very similar to the cold isostatic pressed surface as viewed in the SEM, figure 14. It is apparent that significant densification, particle shearing and rewelding of fresh metal surfaces, has not taken place. In particular, the smaller particles have not been subjected to sufficient shearing and extension of the metal to metal contact area, but rather restructured to form semi-continuous, low density planes or weak zones.

2.3. Hot Unidirectional Compaction

P/M products from the 2024 alloy E were produced without any hot working (deformation) operation after hot pressing and examined in the T351 condition. This production procedure follows steps 1 through 8 previously outlined but omits step 6 - hot working.

The P/M products were compacted by:

(1) unidirectional hot pressing* in the VAW extrusion press at 753 K with 615 MPa applied for 10 min (dwell) yielding a 71 mm Ø x 144 mm billet - after removal of canning material - and a density approaching 100 %, and

*A slight amount of buckling of the can occurred along the first 40 mm from the blind die causing an extra 2 mm to be removed from the diameter along this length.

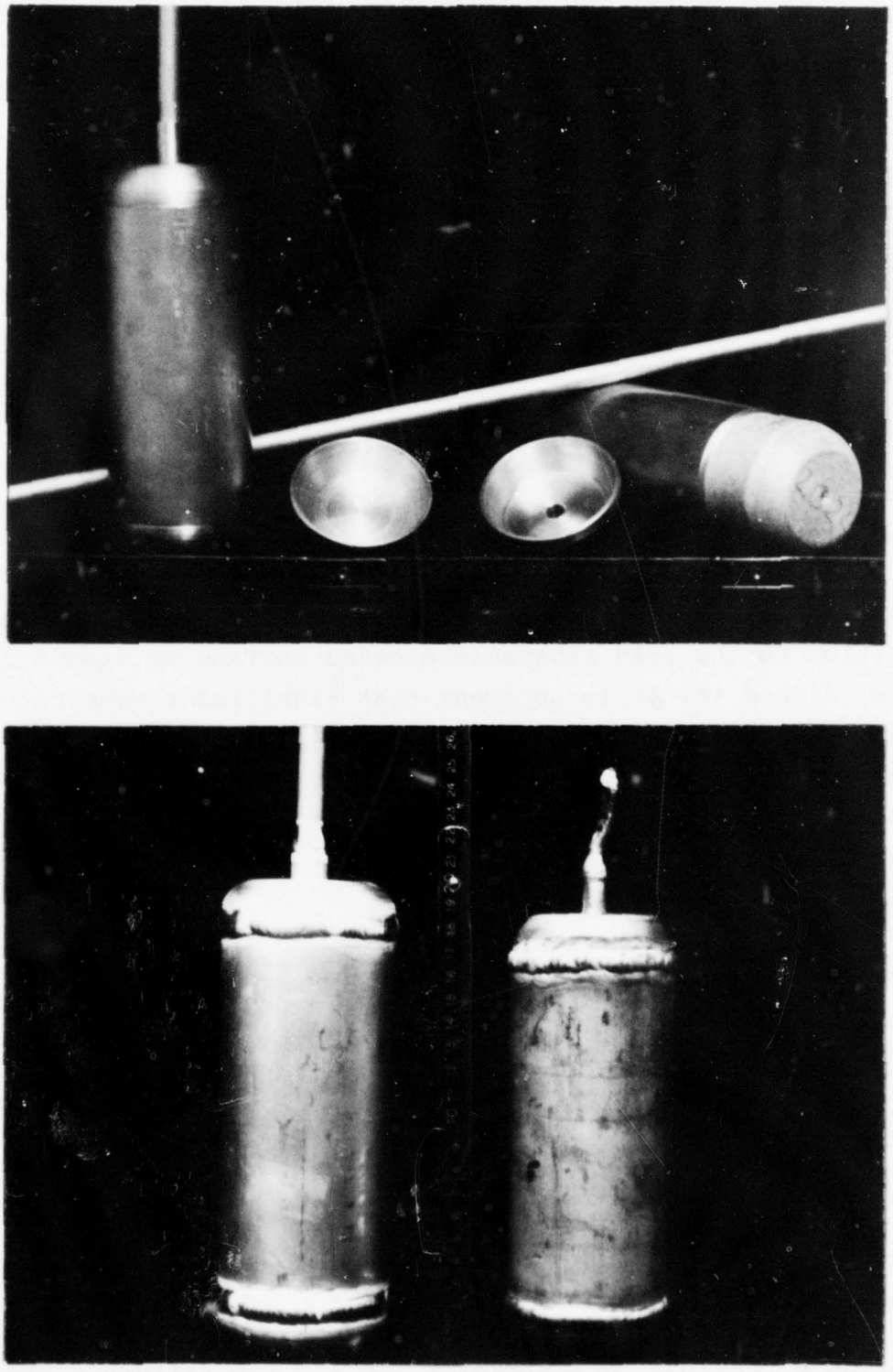

Figure 13: The upper picture shows a 2024 alloy E green compact and special HIP can shape [material AlMg3] prior to double welding, can as assembled at left (above). In the lower picture the shape and size of the HIP can is shown before (left) and after HIPing at 713 K for 2 h under a 132 MPa pressure.

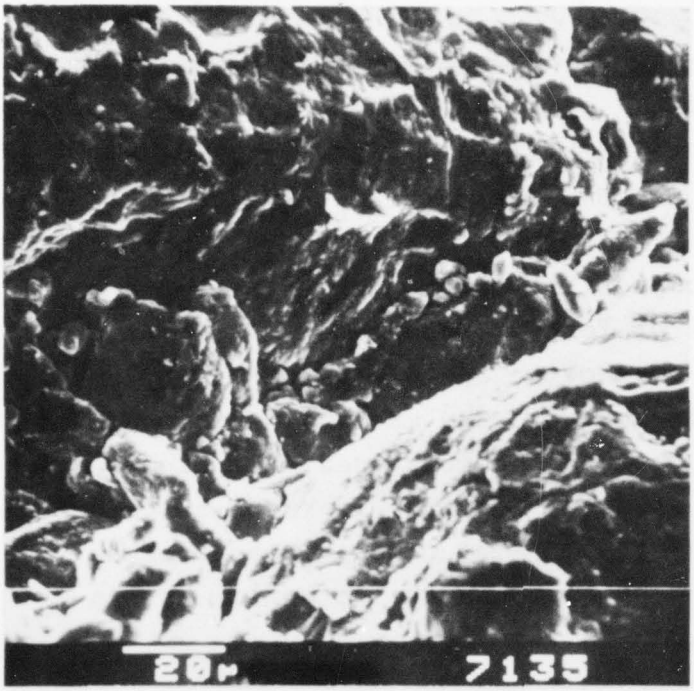

tensile fracture surface of a non-ductile hot isostatically pressed product

93 % dense

UTS = 0.2% YS = 188 MPa

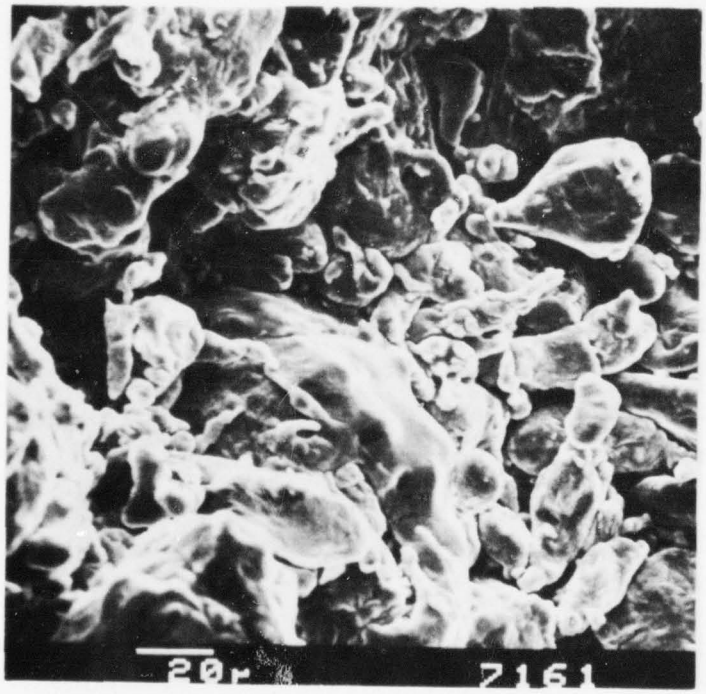

cold isostatically pressed

80 % dense

Figure 14: SEM fractographs of 2024 alloy E powder after hot isostatic pressing (above) and cold isostatic pressing (below). Zones of weakness caused by low density planes are readily apparent in the HIP structure. Surface buldges in cold pressed powder are possibly due to internal gas pressure in the central porosity, figure 7. Similarity in material surfaces shows lack of oxide breakage and metal to metal welding for both conditions.

(2) HERF unidirectional hot impact compaction with DFVLR's Dynapak at 753 K with $4.75 \cdot 10^6$ Joule$\cdot$m^{-2} ($5.00 \cdot 10^7$ Joule$\cdot$m^{-3}) yielding a 69 mm Ø x 62.5 mm billet - after removal of canning material - and a density of $2.80_6 \cdot 10^3$kg$\cdot$m^{-3}.

These two methods of hot compaction were chosen to simulate the two general classifications of forging processes - impact forging by HERF hot impact compaction and press forging by hot pressing - in order to investigate the material's response to conventional, economical manufacturing processes. The slower deformation process, press or creep forging, is known to produce superior mechanical properties in I/M aluminum alloys whereas the impact or hammer forging process has the potential for increased rate of production.

Table 2 lists the properties of these hot compacted products and figures 15 and 16 display their notched fatigue behavior for a stress concentration factor (K_t) of 3. The notched fatigue strength at 10^7 cycle of 125 MPa for the hot pressed product represents a significant fatigue strength advantage over the impact compacted product. A more definitive fatigue strength at 10^7 cycles for the impact compacted product was prevented because of the limited number of test specimens which could be obtained from one impact compacted sample, however, it is significant that for hot impact compaction at $4.75 \cdot 10^6$ Joule$\cdot$m^{-2} the notched fatigue properties are not as good as the hot pressed product's properties. Furthermore, the hot pressed products' fatigue strength is significantly better than I/M products for the same heat treatment - 125 vs 105 MPa - as will be discussed later under extrusion of 2024 P/M.

SEM Fractographic examination of tensile specimens from the hot pressed product, figure 17, shows that a considerable increase in the degree of metal/metal area has been produced over the HIP process, figure 14. Even though an outline of some of the prior powder particles and possible slight porosity is evident, the hot pressed product's strength approaches that of the 25 : 1 extruded product's strength. The typical I/M transgranular dimple

Compaction process	UTS (MPa)	0.2% YS (MPa)	e (4D) (%)	R.A. (%)	density ($10^3 \cdot kg \cdot m^{-3}$)	NTS/YS
pressed 2024*-T351						
longitudinal	473	377	15.4	11.7	2.79_7	1.37
transverse	477	374	15.0	11.2	2.79_7	1.43
impact 2024*-T4	449	323	14.3	9.6	2.80_6	-

*alloy E - 82 µm APD

Table 2: Properties of Unidirectional Hot Compacted P/M Products. (All properties measured in the longitudinal direction (L) unless otherwise indicated. For extrusions, (L) is the same as the extrusion direction.)

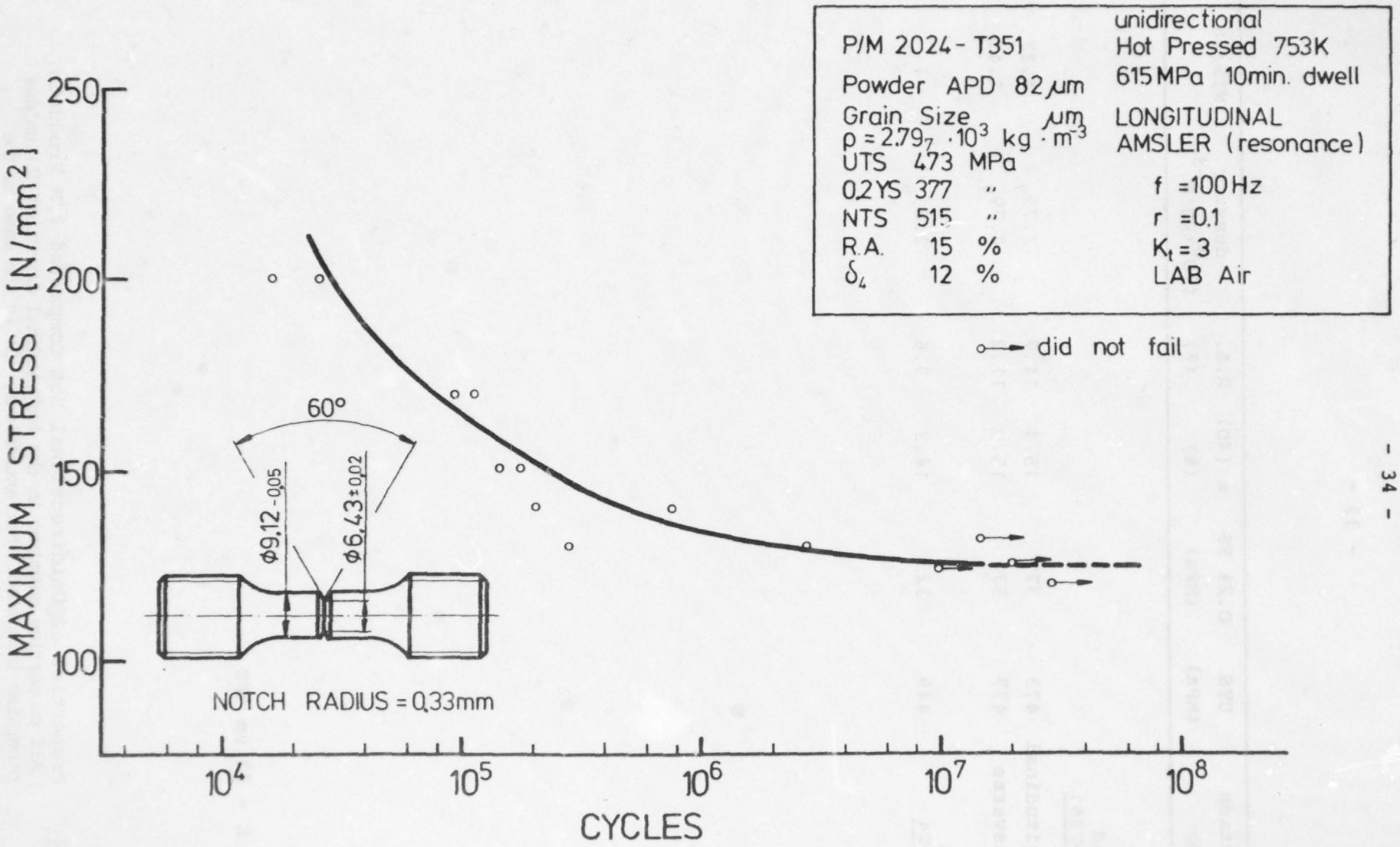

Figure 15 Notch fatigue performance of axial stressed P/M 2024-T351 alloy E hot pressed products showing a fatigue strength of 125 MPa at 10^7 cycles.

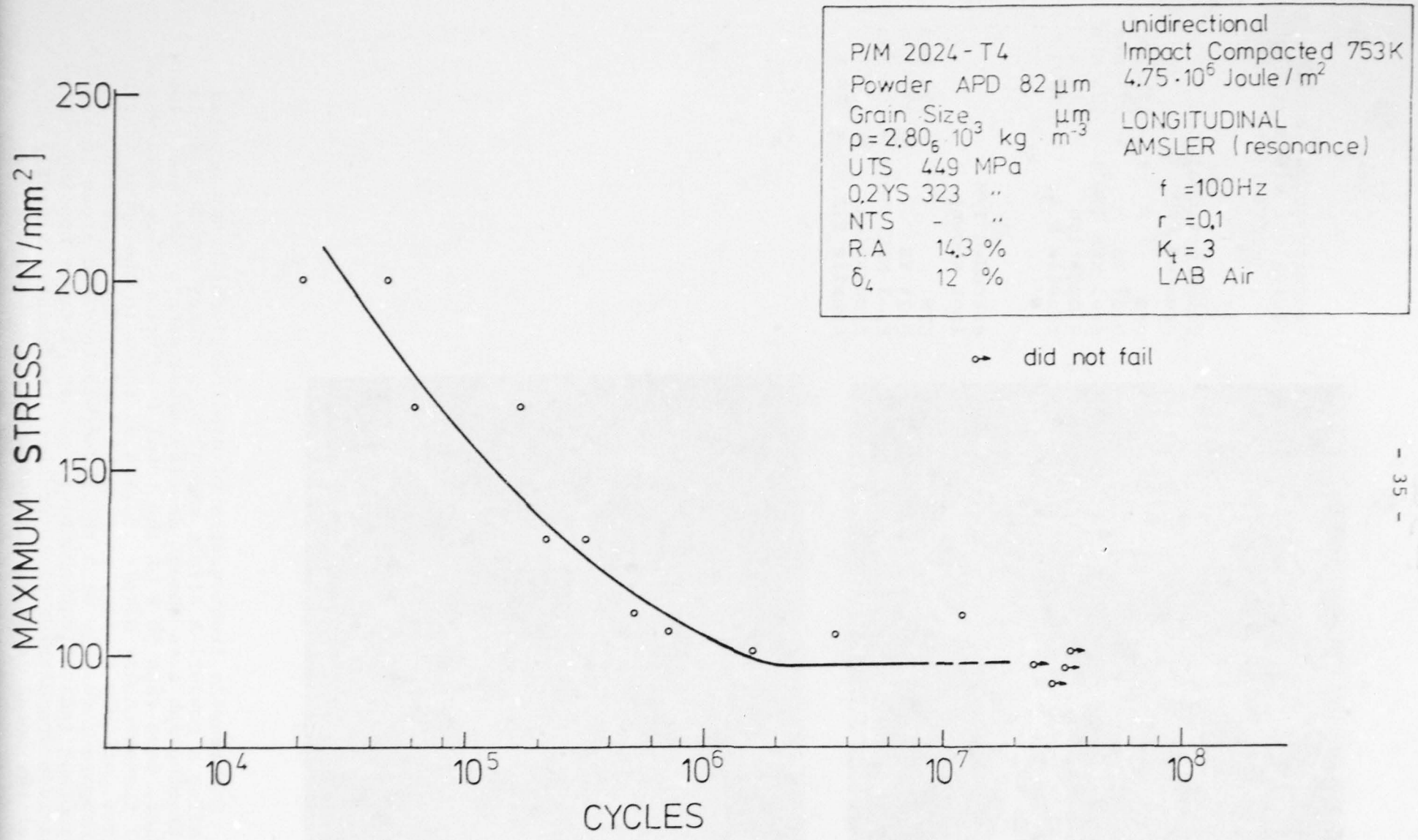

Figure 16 Notch fatigue performance of axial stressed P/M 2024-T4 alloy E from impact compacted products showing a maximum fatigue strength of 95 MPa at 10^7 cycles.

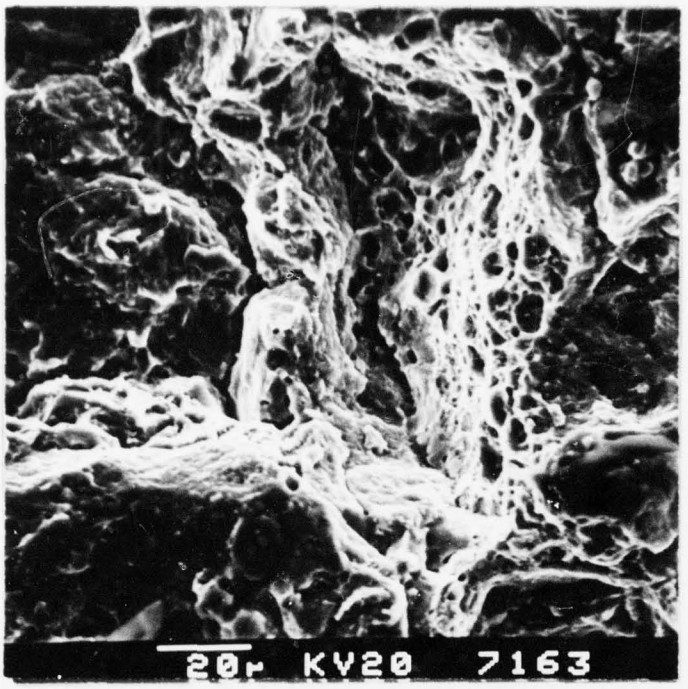

Property comparison for
equivalent yield strengths
2024-T351

unidirectional hot
pressed P/M

UTS	= 473 MPa
0.2% YS	= 377 MPa
K_t=3 NFS (10^7)	= 125 MPa
elongation	= 12 %
tensile R.A.	= 15 %

extruded I/M
(not shown)

UTS	= 492 MPa
0.2% YS	= 377 MPa
K_t=3 NFS (10^7)	= 105 MPa
elongation	= 20 %
tensile R.A.	= 28 %

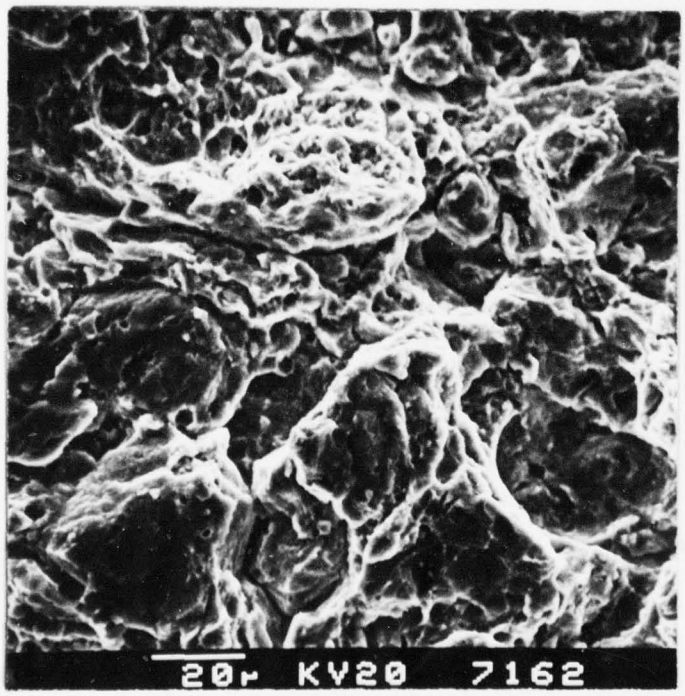

Figure 17: SEM tensile fractographs of unidirectionally hot pressed 2024-T351 alloy E powder. A slight amount of porosity can be seen in the lower fractograph even though density measurements indicate a 100 % dense product. Less than 50 % of the total fracture surface area was of the typical transgranular dimple rupture as shown in the upper fractograph. Powder particle's size, shape, and surface area appearance in Figure 10 compare favorably with the rather featureless areas in the lower fractograph indicating incomplete powder particle bonding. This featureless intergranular/particle fracture represented slightly more than 50 % of the total fracture surface area.

fracture structure represents less than 50 % of the fracture area of the hot pressed tensile specimen. This nonhomogeneous fracture structure indicates that insufficient shearing of the oxide surface and welding of metal to metal surfaces, necessary to produce a coherent material, has occurred.

3. Hot Working

Substantial metal flow is imparted to the hot compacted material primarily to increase the ductility and toughness, however, significant increases in strength and therefore fatigue can also be obtained from hot working. As used here, hot working is therefore not a primary consolidation process, but is used to produce material of theoretical density having a severely worked structure.

3.1. 2024

3.1.1. Hydraulic Extrusion Pressing

The primary hot working method used for this investigation has been press extrusion. It was selected because it produces uniform metal flow. An investigation of extrusion processing parameters - % reduction and preheat temperature - was conducted to obtain optimum properties from sound P/M products. Two additional extrusion parameters, the influence of lubrication and die angle, were not investigated. Earlier work of Gurney et al.[49,54] showed that only when no lubrication was applied, were sound, extruded P/M products consistently produced. The square edge die, which is the common industry practice for extrusion of aluminum[71c] and which has been demonstrated by Jäncke[56] and Sheppard and Chare[42,46,57] to be effective for aluminum P/M, was directly employed for this investigation.

The percent reduction studies ranged from 90 % to 98 % reduction in area and were conducted at the usual hot extrusion temperatures for unrecrystallized I/M 2024, between 693 K and 753 K. Figure 18 shows the results of this study as evaluated by strength and ductility, and figure 19 the notch tensile strength and notch tensile strength yield strength ratio (NTS/YS). The highest

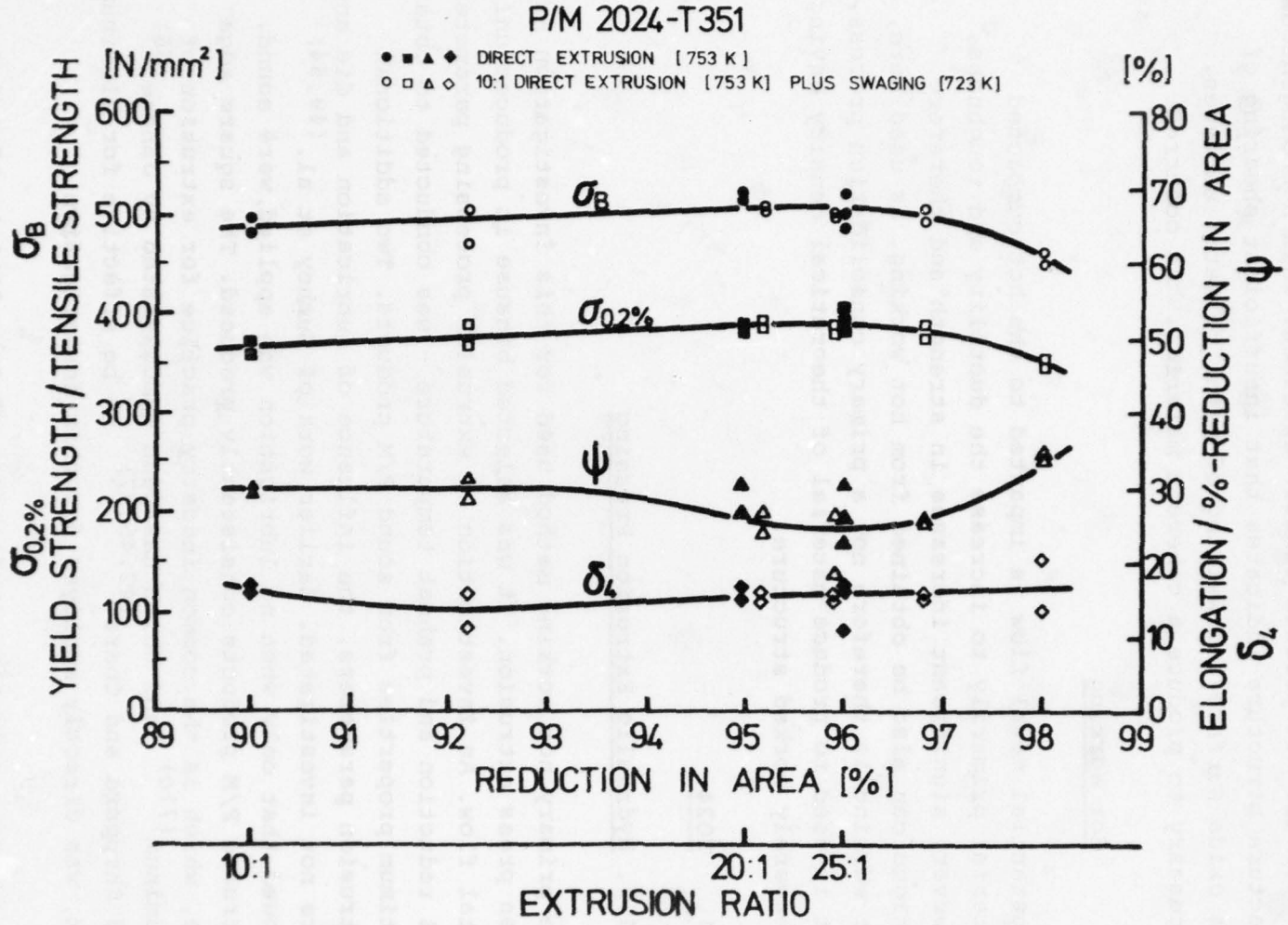

Figure 18 Strength and ductility mechanical property evaluation of 2024 P/M alloy E's response to extrusion deformation, elongation (δ_4) measured along four times tensile specimen's diameter.

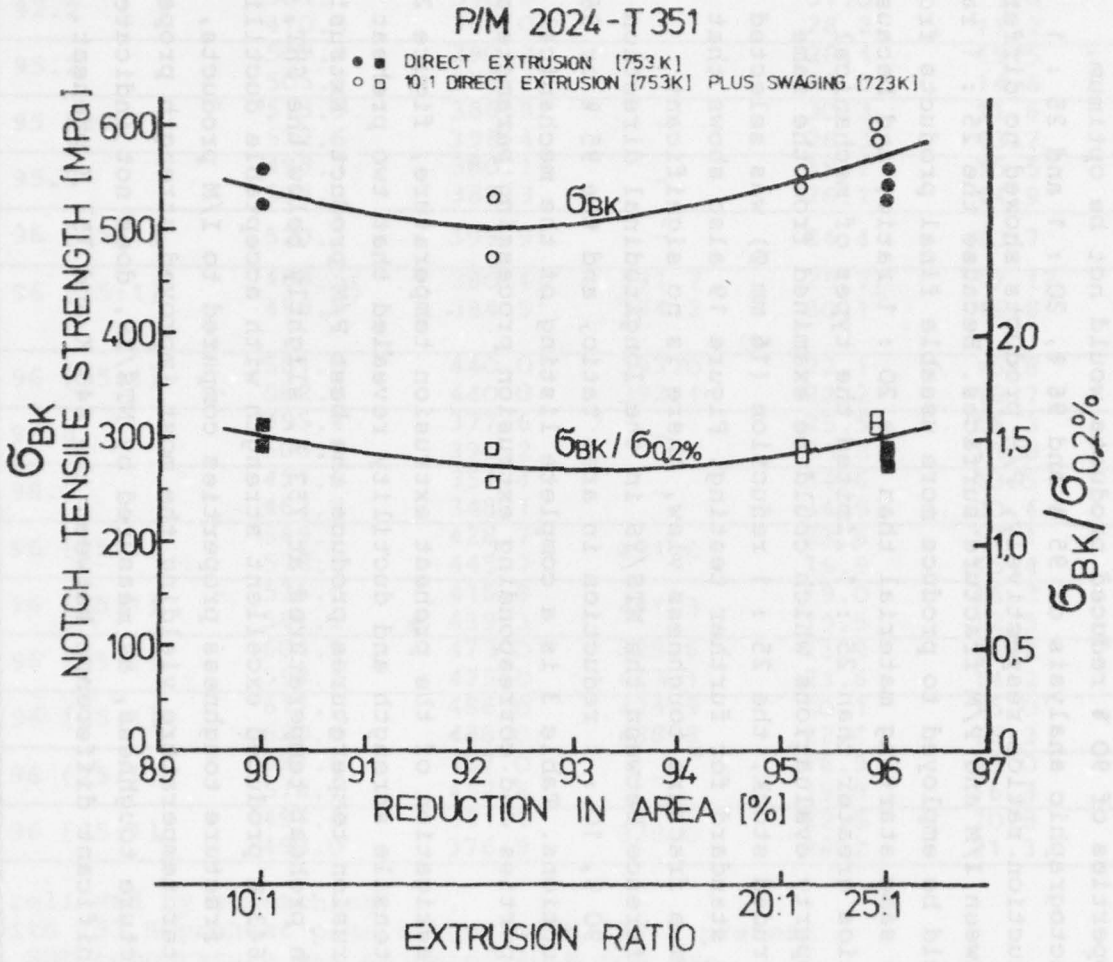

Figure 19: Variation of longitudinal fracture toughness, as measured by ASTM notch tensile testing techniques, with extrusion ratio for 2024 alloy E, 82 µm APD. Commercial I/M product's show comparable values for 25 : 1 extrusion of NTS between 526 to 555 MPa and the corresponding range of NTS/YS ratios of 1.44 to 1.53.

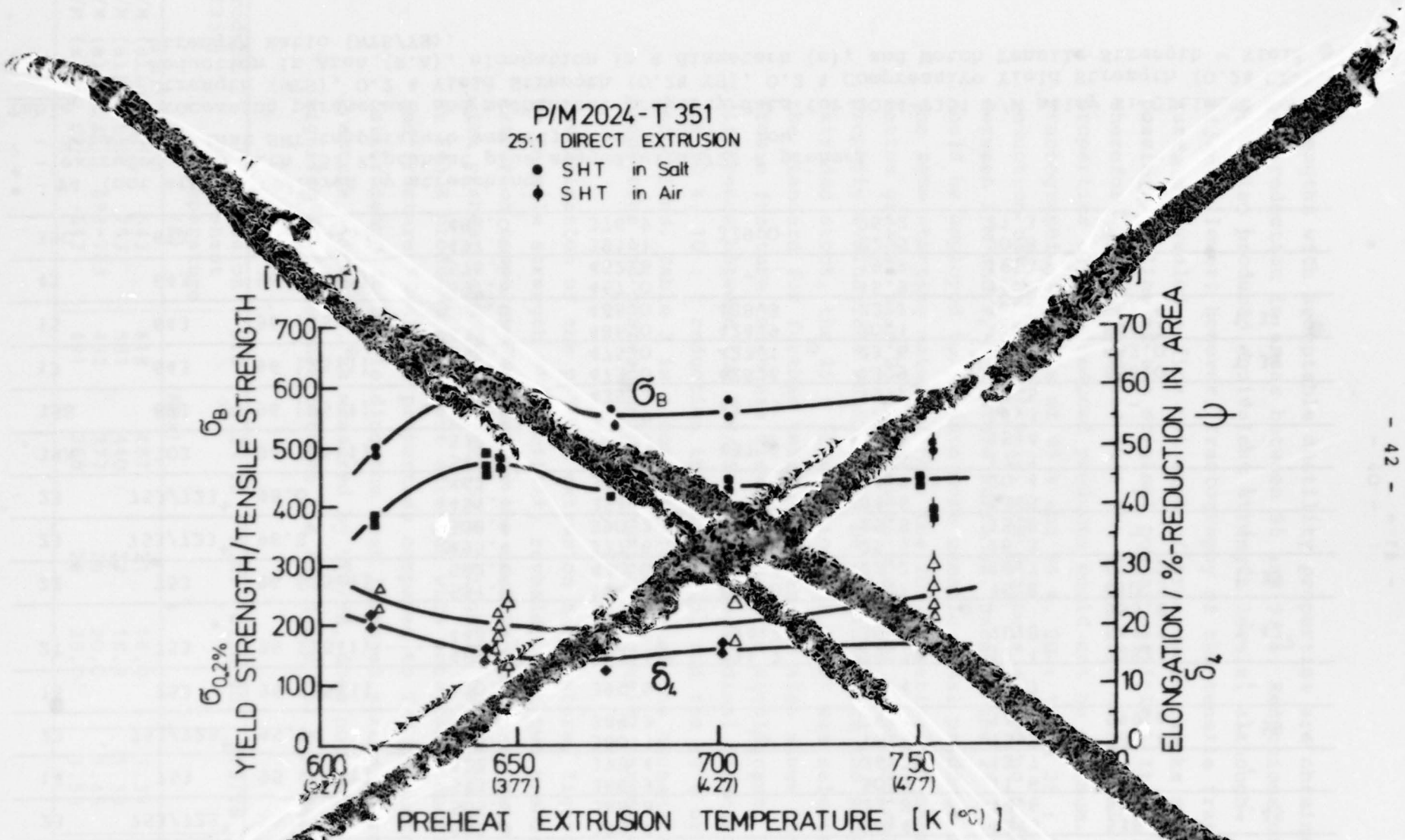

Figure 20: Variation of tensile strength (UTS and 0.2 % YS) and ductility (elongation in [illegible] meters and R.A.) with preheat extrusion temperature for 2024 P/M alloy E. Extrusions are [illegible] a [illegible]: 1 ratio, typical 2024-T351 I/M values for this ratio are UTS = 490 MPa, 0.2 % [illegible] 75 MPa, e = 20 %, and R.A. = 28 %.

strengths with acceptable ductility properties are obtained with reduction in areas between 95 and 97 %. Reductions of 90 % also produced equivalent strength levels, although slightly lower; however, fractography of the tensile fracture surface revealed a fine net work of transverse cracks and a possible outline of the original powder particles. It is therefore to be predicted that the transverse mechanical properties of 90 % reduced products would not be optimum. Fractographic analysis of 95 % and 96 %, 20 : 1 and 25 : 1 reduction ratios respectively, P/M products showed no differences between I/M and P/M fracture surfaces. Because the 25 : 1 ratio could be employed to produce more useable final products from the same starting material than the 20 : 1 ratio, and because ratios greater than 25 : 1 limited the types of mechanical property evaluations which could be examined from the same extruded stock, the 25 : 1 reduction (16 mm Ø) was selected as the standard for further testing. Figure 19 also shows that from a fracture toughness view, there is no significant difference between the NTS/YS in the longitudinal direction for 90 %, 10 : 1 reduction in area ratio, and the 95 % or 96 % reductions. Table 3 is a complete listing of the mechanical properties and corresponding extrusion processing parameters.

Investigation of the preheat extrusion temperature, figure 20, by tensile strength and ductility revealed that two preheat extrusion temperatures produce the best P/M product. Extrusion with preheat temperatures at 753 K, slightly below the SHT, and at 643 K produced excellent strength with acceptable ductility and fracture toughness properties compared to I/M products, the latter temperature yielding the most improved strength properties. Fracture toughness, as measured by NTS/YS, does not indicate any significant difference between the 643 K and 753 K preheat.

Product (T351)	Extrusion preheat temperature (K)	UTS (MPa)	0.2% YS (MPa)	R.A. %	e(in 4D) %	NTS/YS	E (MPa)
P/M (alloy E)	643	618	487	21	16.0	1.37	-
P/M (alloy E)	753	581	440	22	16.3	1.39	74,200
I/M (alloy A)	693-723	492	377	28	20.0	1.45	73,500
I/M (alloy C)	643	491	368	26	25.0	1.53	-

Charge No.	Processing Parameters: preheat temp. (K)	Processing Parameters: reduction in area (%)	Mechanical Properties (longitudinal) L): UTS (MPa)	0.2% YS (MPa)	0.2% CYS (MPa)	R.A. (%)	e (%)	NTS (MPa)	NTS/YS
23	753	90 [10:1]	498.7 483.0	374.4 360.1	-	29.9 29.3	16.6 16.0	556.5* 522.8*	1.52
23	753/723+	92.2	504.7 470.3	390.0 367.0	-	31.0 28.2	15.8 11.2	530.4* 472.2*	1.37
23	753/723+	95.2	509.9 505.6	390.2 388.8	-	26.4 23.8	15.5 14.6	538.8* 553.2*	1.45
14	753	95 [20:1]	513.9 522.6	386.9 398.4	-	30.3 26.3	11.6 13.7	-	-
23	753/723+	95.9	498.7 504.2	380.1 389.3	-	18.2 26.1	15.5 14.9	583.4* 599.0*	1.59
16	753	96 [25:1]	520.7	399.9	-	24.4	10.7	-	-
21	753	96 [25:1]	489.5? 498.9?	380.4? 384.5?	391.7 394.2	25.7? 30.1?	17.1? 16.8?	528.3? 541.1? 555.8?	1.42?
22	753	96 [25:1]	581.0 582.0	440.0 440.0	393.0 392.4	22.1 22.2	15.8 16.7	610.3 612.2	1.39
23	753/723+	96.8	495.4 508.4	377.6 390.2	-	25.5 25.8	16.3 15.8	-	-
23	753/723+	98.0	451.6 463.2	354.4 348.1	-	34.6 34.9	13.5 20.4	-	-
39A	703	96 [25:1]	549.5 578.6	428.7 445.7	431.6	23.6 16.9	17.1 15.4	-	-
39B	673	96 [25:1]	536.6 561.2	415.9 439.3	431.3	19.0 19.5	16.3 12.5	-	-
13	643	96 [25:1]	604.5 598.5	473.0 475.0	428.6 427.1	13.9 23.6	14.2 14.2	656.0 652.0	1.38
15	643	96 [25:1]	617.8 620.0	486.0 488.0	424.9 438.8	20.1 22.1	15.0 16.3	666.7 667.8	1.37
41	643	96 [25:1]	597.6 576.3	467.0 452.8	-	16.9 19.9	15.0 16.3	-	-
39C	613	96 [25:1]	497.6 493.0	381.1 376.9	329.0	22.5 26.2	20.8 21.3	-	-

* - T4 (not stress relieved by stretching)
\+ - extruded 10:1 with 753 K preheat plus swaged with 723 K preheat
? - determined that SHT temperature was adjusted 40 K too low

Table 3: Processing parameters and mechanical property data for 2024-T351 P/M alloy E: Ultimate Tensile Strength (UTS), 0.2 % Yield Strength (0.2% YS), 0.2 % Compressive Yield Strength (0.2% CYS), Reduction in Area (R.A), elongation in 4 diameters (e), and Notch Tensile Strength - Yield Strength Ratio (NTS/YS).

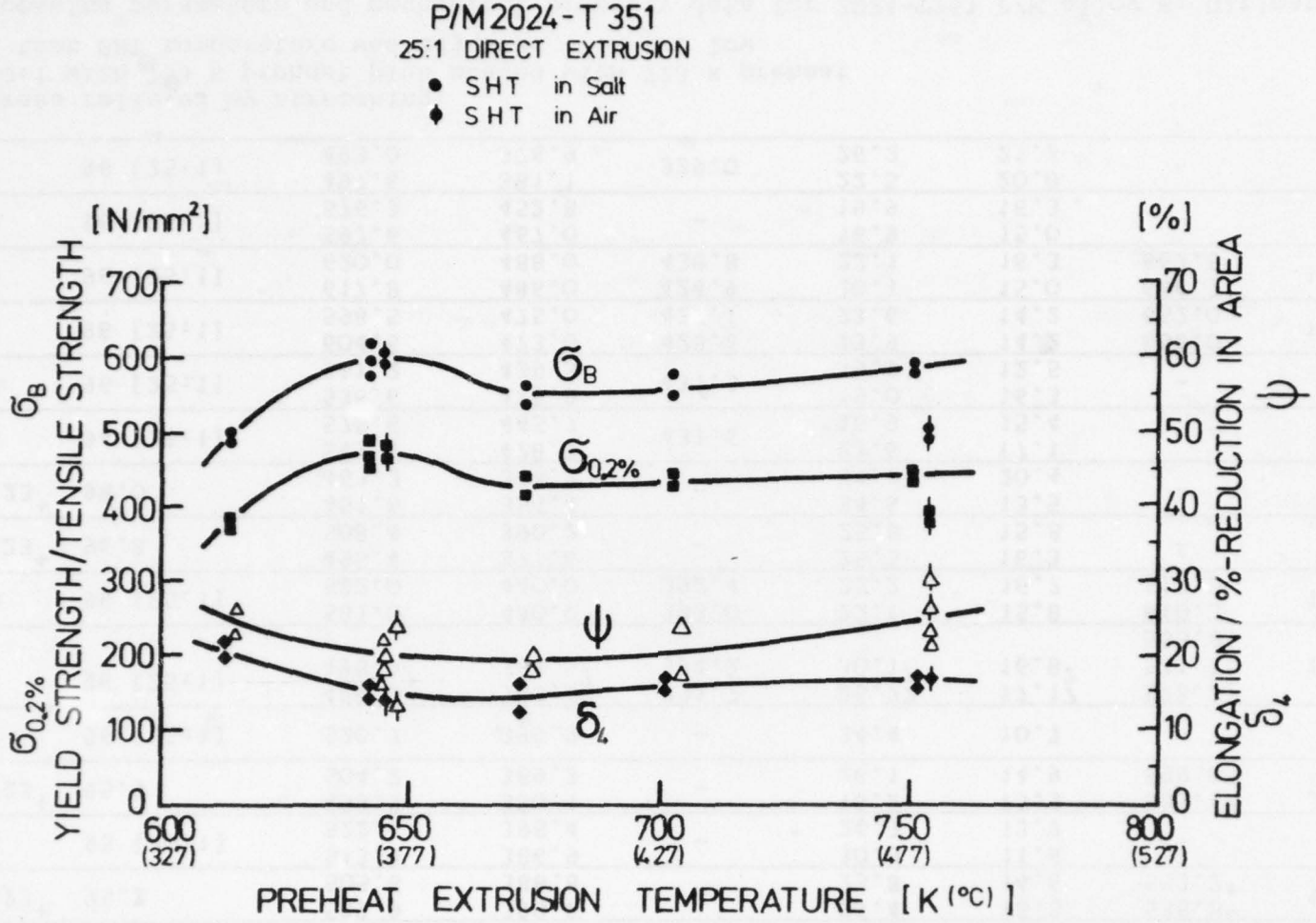

Figure 20: Variation of tensile strength (UTS and 0.2 % YS) and ductility (elongation in 4 diameters and R.A.) with preheat extrusion temperature for 2024 P/M alloy E. Extrusions are for a 25 : 1 ratio, typical 2024-T351 I/M values for this ratio are UTS = 490 MPa, 0.2 % YS = 375 MPa, e = 20 %, and R.A. = 28 %.

Tensile test results for the 643 K preheat extrusion treatment were investigated from three products to insure that property improvements do indeed result from this preheat temperature.

The compressive yield strength was also investigated as a function of preheat temperature, and as expected follows the same trend as tensile strength, figure 21. The longitudinal stress relief, stretching, increases the longitudinal tensile yield strength, but due to the Bauschinger effect the longitudinal compressive yield strength is reduced. Consequently, the compressive yield strength values shown here can be increased by about 3 % if the $1\frac{1}{2}$ % stretch is not employed, i.e. a T4 treatment. The effect can be increased to about 5 % if the $1\frac{1}{2}$ % stretching is done after the aging treatment or practically eliminated if stretched between SHT and an artificial aging treatment.

product (T351)	extrusion preheat temperature (K)	0.2 % CYS (MPa)	E(comp) (MPa)
P/M alloy E	643	432	75,700
P/M alloy E	753	393	
I/M alloy A	693-723	280	73,400
I/M alloy C	643	287	

The optimum P/M processing treatment imparts a 44 % increase in the compressive yield strength over I/M treatments.

Concerning notch fatigue behavior, K_t=3, the P/M products produced with the optimum extrusion processing parameters demonstrated significant 33 % improvement over the I/M alloy products, figures 22-25. The results indicate a fatigue strength at 10^7 cycles of 140 MPa for the P/M alloy E product extruded at 643 K versus 105 MPa for the various I/M alloys. This represents a significant improvement in the high cycle fatigue (HCF) behavior for this alloy with a T351 treatment.

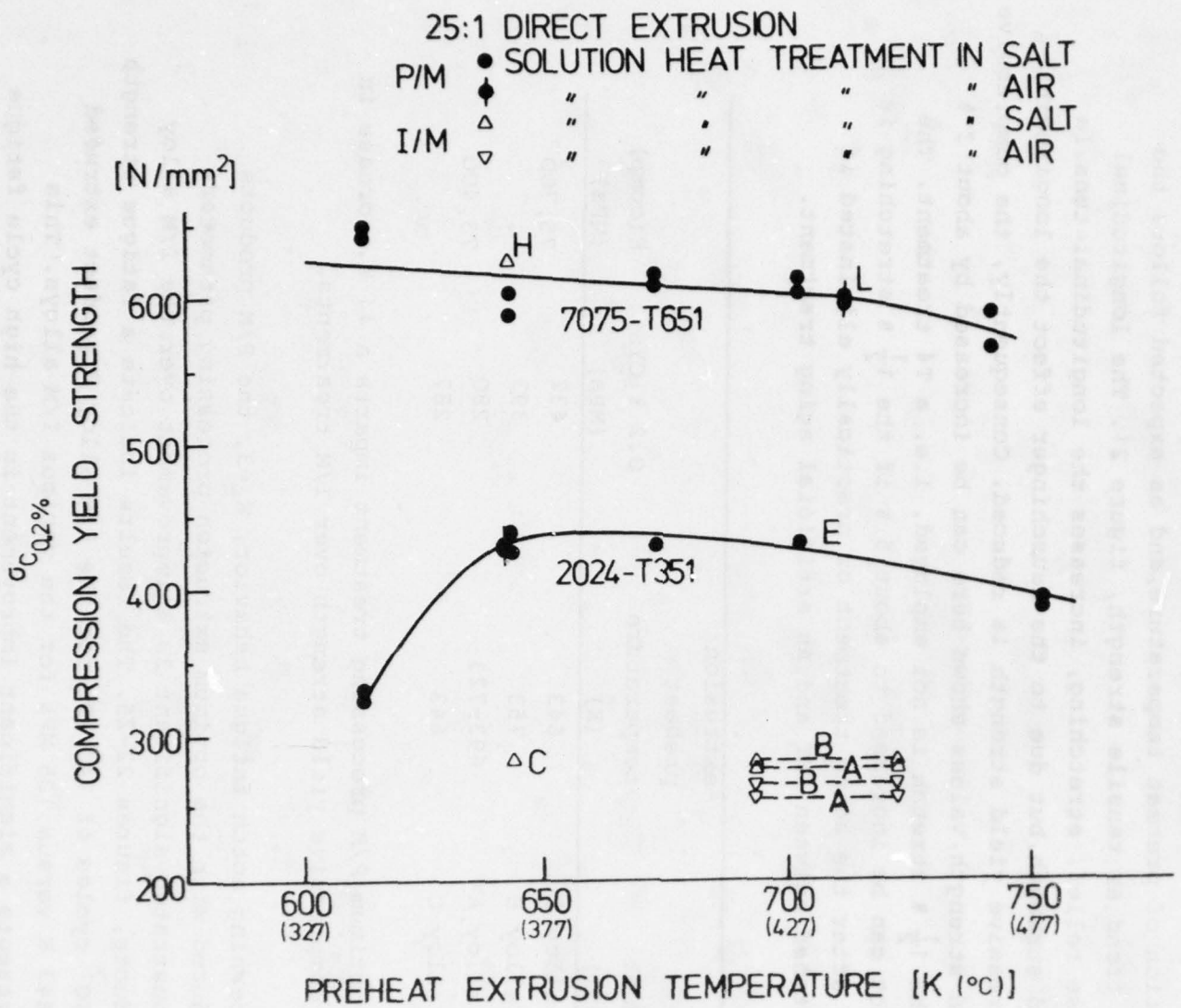

Figure 21: Variation of compressive yield strength (0.2 % CYS) with preheat extrusion temperature (25 : 1 extrusion ratio) for: 2024-T351, P/M alloy E and I/M alloy A, B and C; and 7075-T651, P/M alloy L and I/M alloy H.

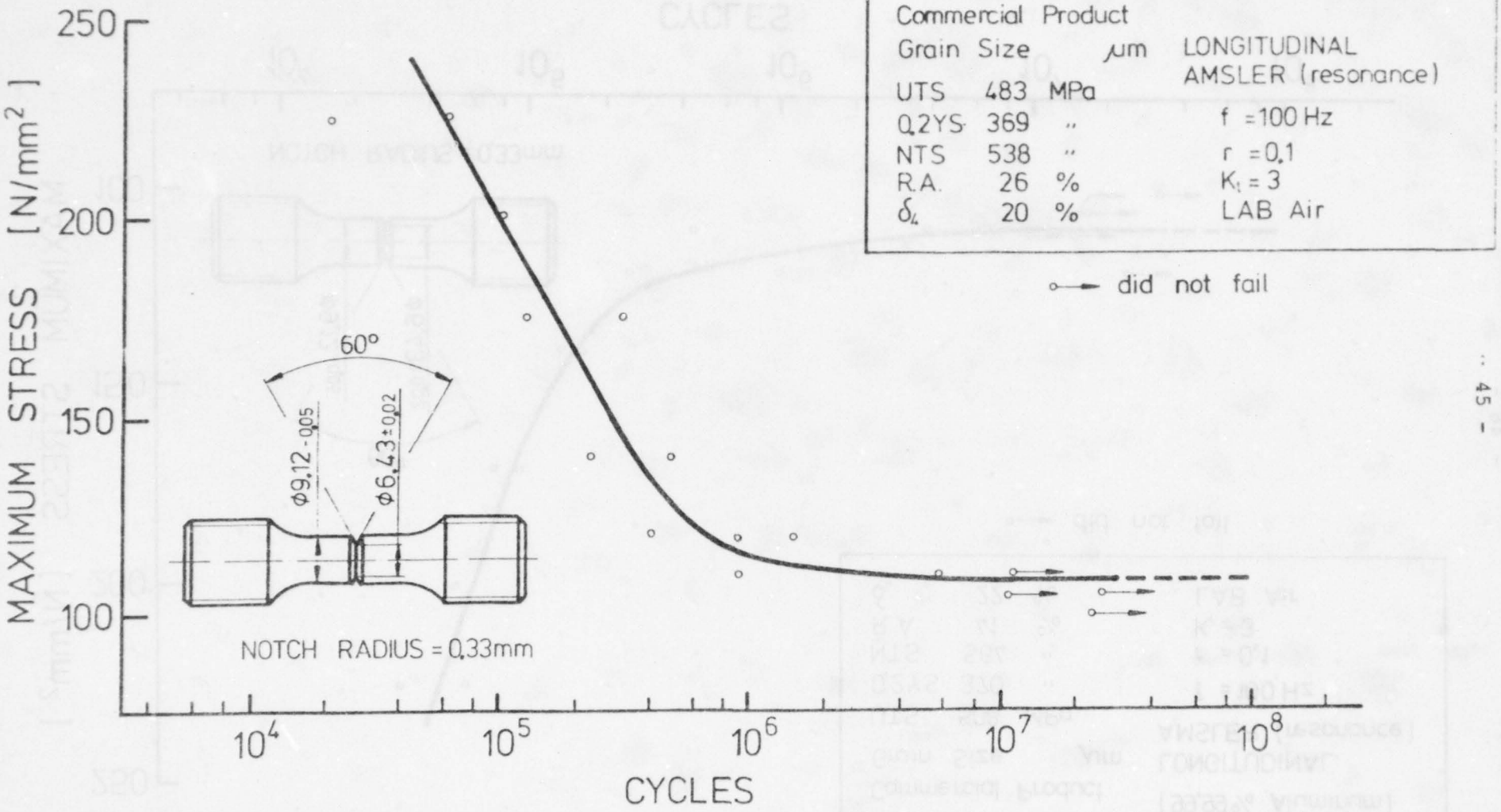

Figure 22: Notched axial-stress fatigue response of I/M 2024-T351 alloy A extruded products having a fatigue strength between 105 and 110 MPa at 10^7 cycles.

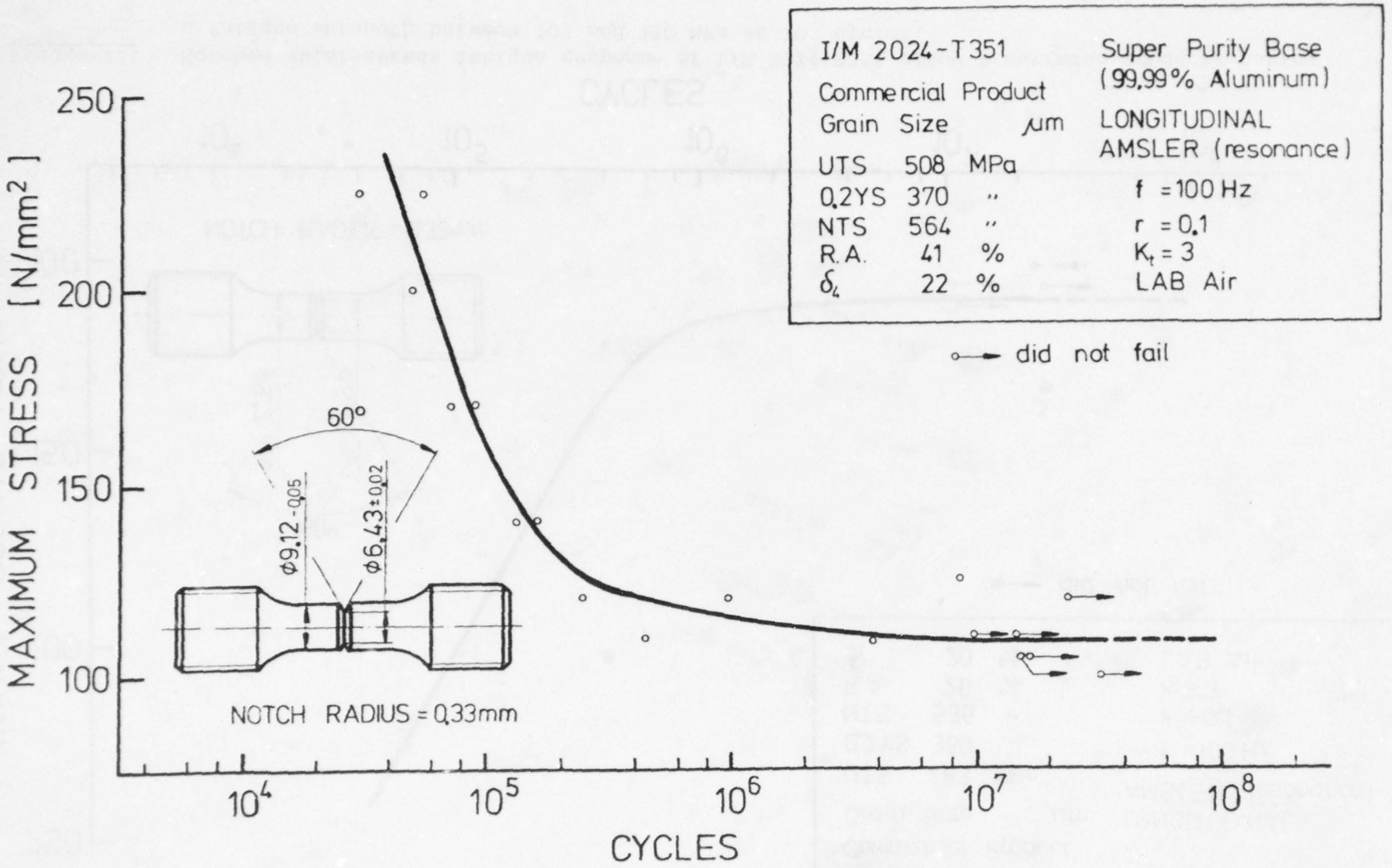

Figure 23: Notched axial-stress fatigue response of I/M 2024-T351 alloy B extruded products having a fatigue strength between 105 and 110 MPa at 10^7 cycles.

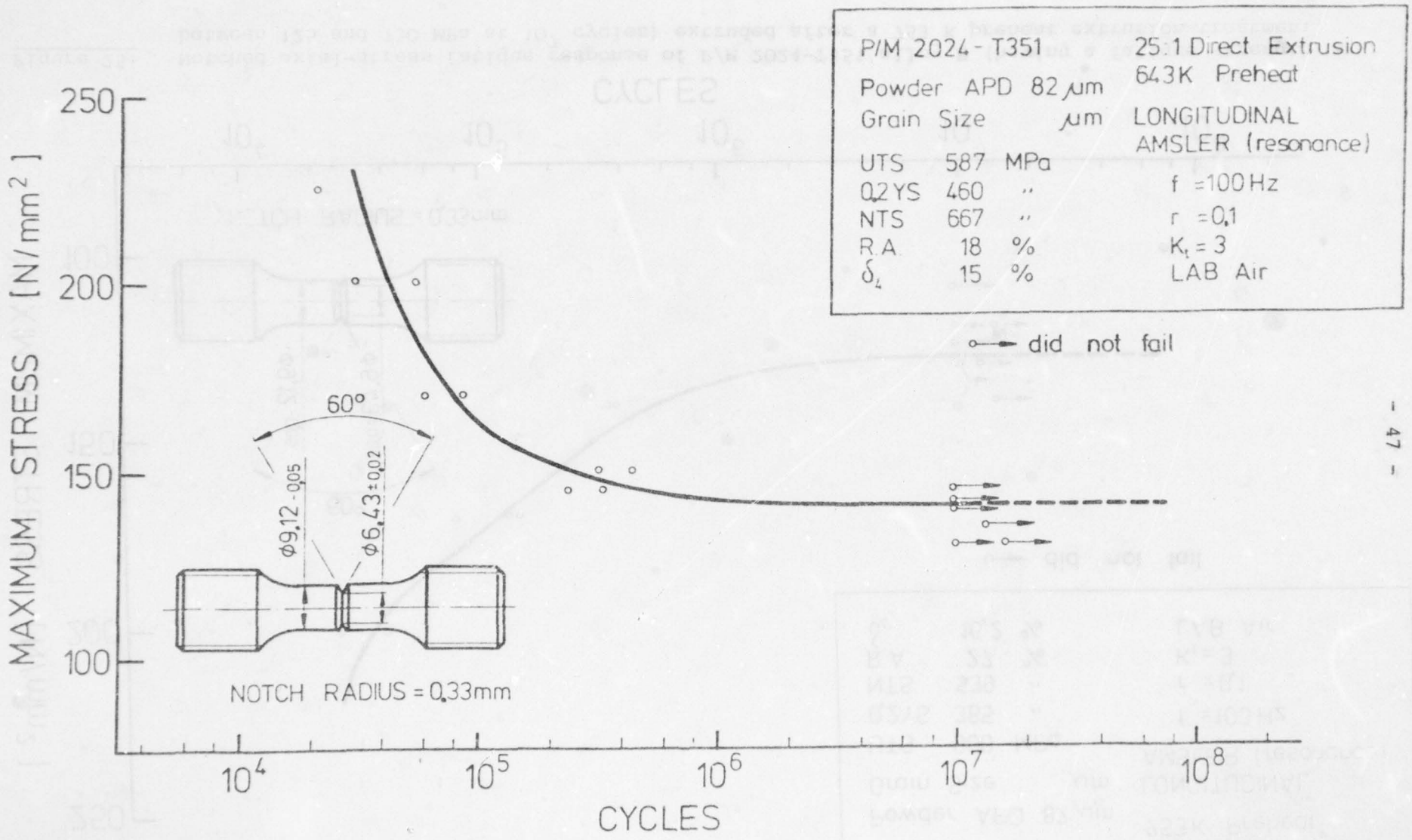

Figure 24: Notched axial-stress fatigue response of P/M 2024-T351 alloy E (having a fatigue strength of 140 MPa at 10^7 cycles) extruded after a 643 K preheat extrusion treatment.

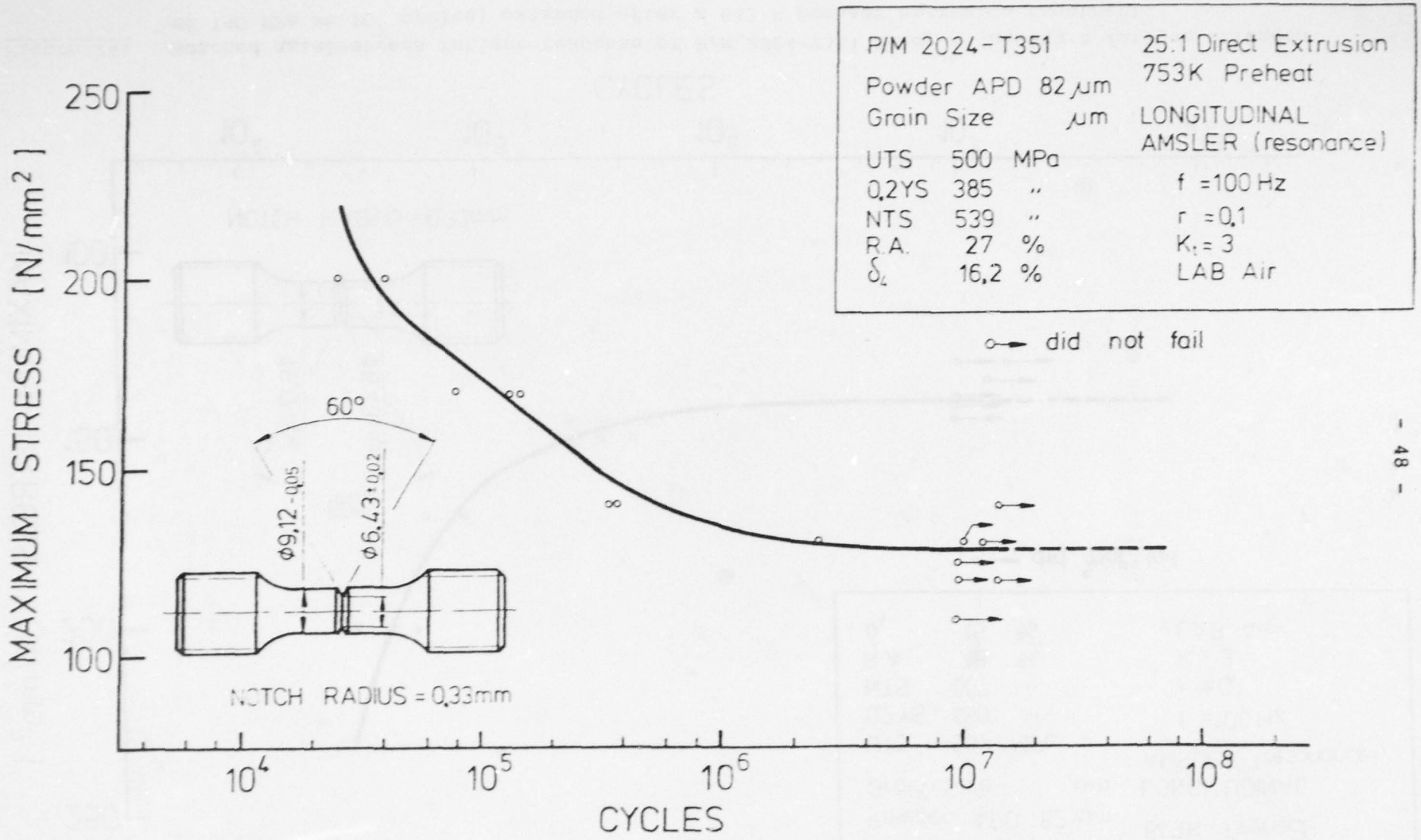

Figure 25: Notched axial-stress fatigue response of P/M 2024-T351 alloy E (having a fatigue strength between 125 and 130 MPa at 10^7 cycles) extruded after a 753 K preheat extrusion treatment.

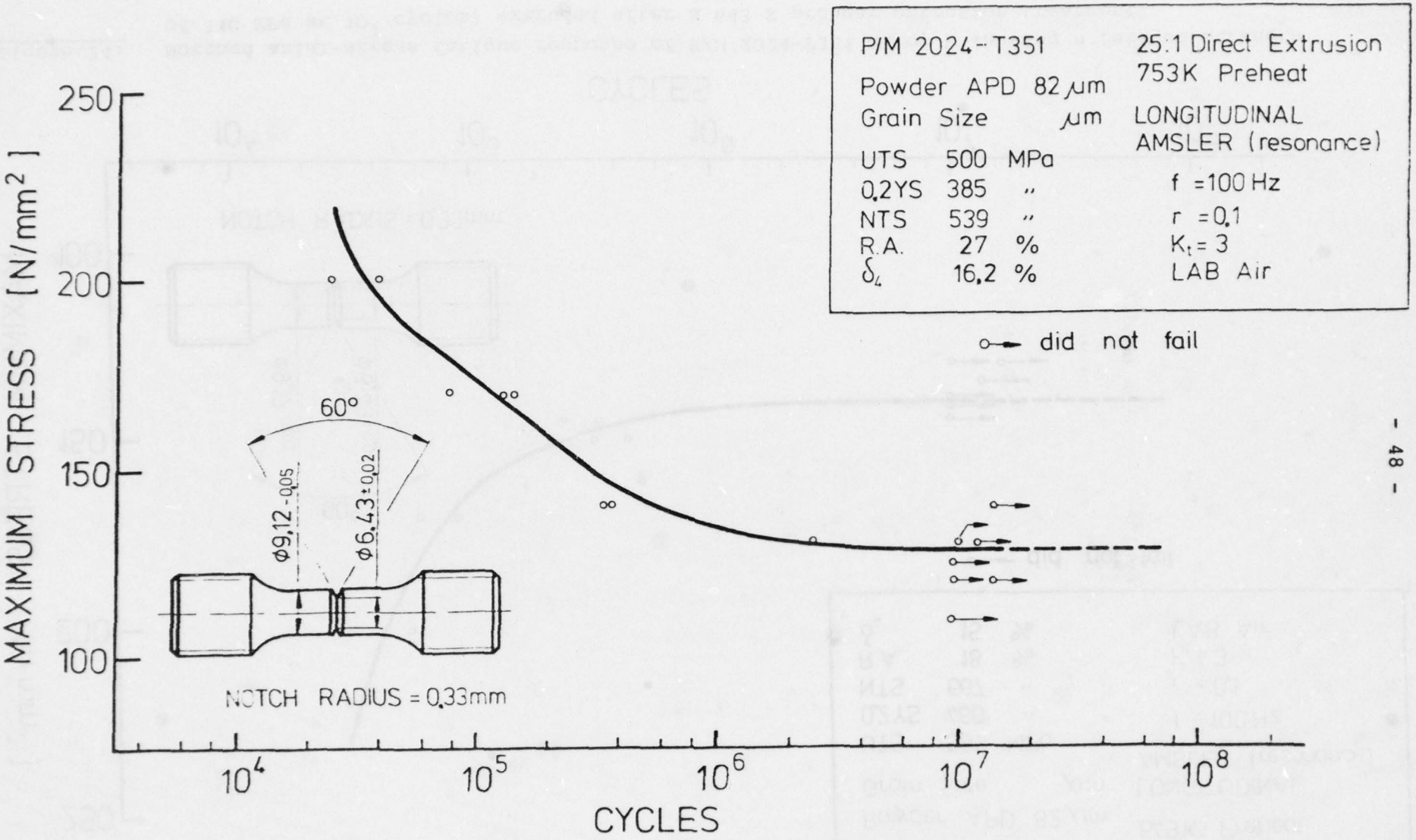

Figure 25: Notched axial-stress fatigue response of P/M 2024-T351 alloy E (having a fatigue strength between 125 and 130 MPa at 10^7 cycles) extruded after a 753 K preheat extrusion treatment.

The slight differences in the insoluble intermetallic phase, iron and silicon contents, between I/M alloys A and B did not develop any observable trend for the notch fatigue run out stress, figure 22 and 23. Both alloys appear to have a 105 MPa fatigue strength level at 10^7 cycles under the conditions tested. From the limited number of test specimens investigated, the following observations can be made concerning the I/M alloys tested:
(1) the degree of scatter above the 120 MPa stress level is much smaller for the super purity base material, alloy B, and
(2) in the LCF to HCF transition range, $5 \cdot 10^4$ to $5 \cdot 10^5$ cycles, the scatter tends to show a better mean fatigue response for the commercial purity base alloy, alloy A.

The P/M alloy appears to have a much flatter fatigue response compared to the I/M alloys. Since the P/M alloy's fatigue strength was increased, this flatness appears to produce a slightly poorer LCF response for the P/M products, figures 24 and 25. Because only a few LCF fatigue specimens were tested, the extent of the LCF response degression, if any, cannot be quantified. This LCF difference may indeed only be the width of the scatter band at these higher stress levels.

In a manner similar to the tensile properties, the fatigue strength for the P/M products was found to be dependent on the preheat extrusion temperature. Fatigue specimens from material extruded after the 643 K preheat treatment exhibited a fatigue strength of 140 MPa at 10^7 cycles, figure 23, while a fatigue strength between 125 and 130 MPa (at 10^7 cycles) was exhibited by specimens from the P/M extrusion product preheated to 753 K, figure 24.

Preliminary fatigue results of specimens from control I/M alloy C, which was also 25 : 1 extruded with a 643 K preheat, are in good agreement with the fatigue strength range of the other I/M alloys tested. Thereby substantiating the HCF improvement of 2024 P/M over I/M independent of extrusion preheat temperature.

3.1.1.1. Product Surface Finish

Excellent extruded product surface finishes were obtained for all extrusion processing conditions examined. Typical direct extrusion product speeds for 16 mm Ø bars are:

preheat temperature K	extruded product speed mm/min.	
753	385	
643	130	(constrained by press capacity)

3.1.1.2. Thermomechanical Treatment

The natural aging response of 2024 P/M alloy E to a thermomechanical treatment (TMT) was investigated to determine if the extruded P/M materials hardening response had been exhausted. This investigation was deemed of interest because of the jump in strength properties of the naturally aged P/M material compared to I/M materials.

In 2XXX series commercial aluminum alloys,precipitation is nucleated on dislocations. The 2XXX series aging response is therefore accelerated by strain hardening of the SHTed material. Consequently, the dislocation density of the P/M product was increased by stretching directly after SHT. Results shown below indicate that the hardening potential of the naturally aged extruded product has not been exhausted as an additional 22 % increase in yield strength by finer precipitation is possible. Indeed further increases in strength by artificial aging are also possible. Although not tested in a TMT condition, it is to be expected that the compression yield strength will also show similar improvements.

condition (25:1 extrusion)	extrusion preheat temperature (K)	deformation (stretch) (%)	UTS (MPa)	0.2% YS (MPa)	RA (%)	e (%)	NTS/YS
T351	753	1.5	581	440	22.1	16.3	1.39
T357	753	7.7	611	539	11.4	9.7	1.08

An attempt to optimize the material's response for TMT has not been undertaken. However, it is anticipated that further strength increases can be obtained if a 643 K extrusion preheat temperature were employed. The decrease in longitudinal fracture toughness, as measured by the NTS/YS ratio, is to be expected from the increased yield strength and decreased ductility. Even though the NTS/YS value has dropped below 1.25, the material retains an acceptable, although poorer fracture toughness.

3.1.2. HERF Impact Extrusion

A limited HERF impact extrusion study with 2024 P/M alloy E was also performed. All impact extrusions were conducted with a 643 K preheat temperature and with percent reductions of 83.2 % and 85.4 %. Products of greater percent reductions, trials of 88 %, 90.4 %, and 95.5 % reductions, were examined and found to contain deep circumferential cracks around the newly extruded surface. These cracks result from the high deceleration stresses at the end of the impact extrusion cycle. Die angles other than 180° were employed to reduce the deceleration effect but without much success.

Mechanical properties of P/M products produced by means of HERF impact extrusion were in general not as improved as by hydraulic press extrusion. Consequently, the greater hot working portion of this investigation was accomplished by press extrusion instead of impact extrusion.

Condition	processing reduction in area (%)	UTS	0.2% YS	0.2% CYS	R.A.	elong.	NTS/YS	E
		(MPa)			(%)			(MPa)
P/M-T351	83.2	492	370	284	34.8	21.7	1.44	71,400
P/M-T351	85.4	482	362	317	41.4	26.7	1.49	
P/M-T851	85.4	473	430	-	48.0	14.0	1.44	-
I/M-T351	85.4	473	361	260	41.0	23.3	1.49	-
I/M-T851	85.4	480	450	-	22.0	7.0	1.44	-

In general, for the same processing treatments the impact extruded P/M products display better properties than I/M products. The P/M T851 heat treatment is suspect because of the high ductility values and rather low UTS compared to P/M T351 values.

3.1.2. Effect of APD

The influence of the initial powder size was investigated with 2024 P/M alloys D, E, and G having the same chemical composition and APDs of 117, 82, and 36 µm, respectively. The results of this investigation have proven inconclusive, as shown in table 4. The P/M products from which test specimens were machined, were all direct extruded with a 25 : 1 ratio and a 753 K preheat temperature, and given a T351 heat treatment. Alloy E, 82 µm APD, has slightly higher strength and lower ductility properties than the other two alloys. This is due to the higher oxygen content for alloy E. The NTS/YS fracture toughness indicator shown here is not very sensitive to the increased oxygen content as the oxide particles are elongated in the test direction and therefore cannot be expected to have very much influence on the longitudinal NTS/YS ratio. The notched fatigue strengths for the 117 and 36 µm APD alloys appear to be increased over the higher strength 82 µm APD alloy; in fact, the fatigue strengths approach the 140 MPa value found for optimal processing conditions of the 82 µm APD alloy E, i.e. 743 K preheat.

Investigation of the influence of APD is continuing. Alloy F, 44 µm APD, will be compacted, extruded, and examined in order to clarify the trends observed to date. In addition,oxygen content analysis of all three alloys will be repeated by neutron activation analysis. Of particular interest is the exceedingly low oxygen content found for the 36 µm APD alloy. This finding is in direct contradiction to the highest oxygen content being normally associated with highest particle surface area, or lowest APD, and with the density measurements, table 4. Since the three alloys have identical chemical composition and since the density of aluminum oxide is approximately 45 % greater than that of aluminum, the lowest density, not the highest, should correlate with the lowest oxygen content as determined for the 36 µm APD powder.

2024 alloy	APD (μm)	UTS (MPa)	0.2% YS (MPa)	0.2% CYS (MPa)	R.A. %	elong (in 4D) %	NTS/YS	K_t=3 fatigue strength at 10^7 cycles (MPa)	oxygen[1] content (w/o)	density 10^3 $kg \cdot m^{-3}$
D	117	557	399	398	26.8	21.3	1.35	135*	0.134	2.79_6
E	82	581	440	393	22.1	16.3	1.32	125-130	0.195	2.79_3
G	36	547	390	383	27.9	21.3	1.39	130-135*	0.012	2.80_0

*estimated from preliminary results

[1]as determined by photon activation analysis

Table 4: Properties of P/M 2024 alloys with various initial average particle diameters (APD). All P/M products were 25 : 1 direct extruded with a 753 K preheat temperature and were tested in the T351 condition. Alloys D and G were sieved from alloy E.

3.2. 7075

3.2.1. Hydraulic Extrusion Pressing

Press extrusion was the only hot working process used to investigate the 7075 P/M alloy. The processing parameter investigation was conducted in a manner similar to that for the 2024 P/M alloy except the 25 : 1 direct extrusion ratio was employed without further investigation. The straightforward selection of the 25 : 1 ratio was based on the results of Gurney et al.[49,54] for 7075 rotating electrode produced powder (REP) and the earlier findings for 2024 P/M alloys since commercial processing practices for both 2024 and 7075 I/M alloys are similar[71c,72].

In contrast to the response of P/M 2024 over the 753 K to 613 K extrusion range investigated, results indicate the strength properties of P/M 7075 continue to slightly increase as the extrusion preheat temperature is decreased in increments of 30 K, figure 26 and table 5. However, it appears that for preheat temperatures lower than 580 K strength properties will decrease in a manner similar to that found for P/M 2024 and Gurney's findings. This upward trend in strength as the preheat temperature decreases from 743 K to 613 K, in contrast to P/M 2024, can be explained by the enhanced recrystallization resistance of the I/M 7075 alloy over the I/M 2024 alloy. The compression strength response of the 7075 P/M alloy L to extrusion preheat temperature, figure 21, is similar to the tensile strength response.

Over the range of preheat temperatures investigated, the fracture toughness indicator NTS/YS remains constant. As the yield strength increased with decreasing preheat temperature, the notch tensile strength also increased, figure 27. The vacuum degassing of the 7075 P/M alloy developed good longitudinal fracture toughness, but not outstanding values as have been reported[23] for the vacuum preheat processing of Al-Zn-Mg-Cu-Co P/M alloys.

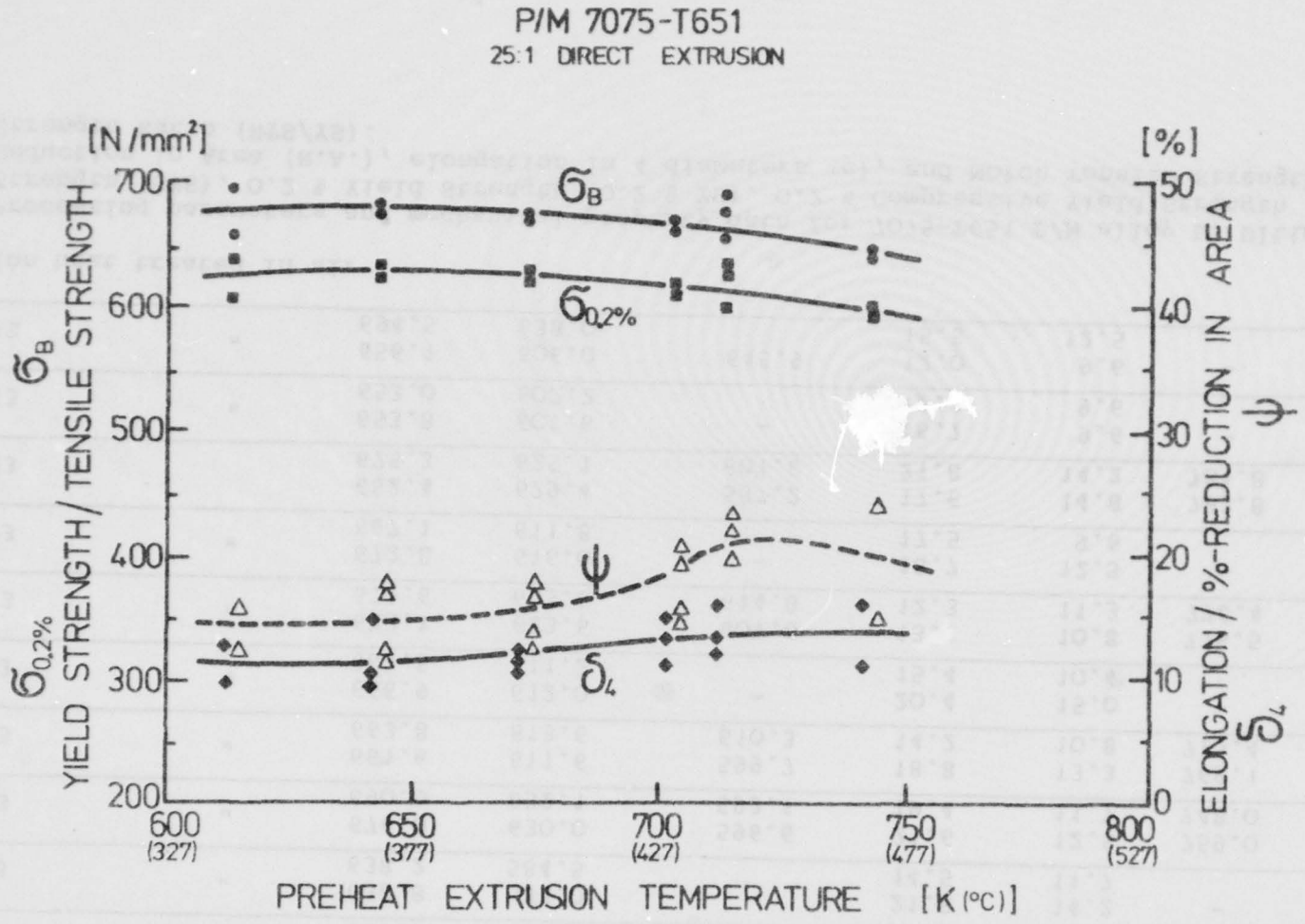

Figure 26: Variation of tensile strength (UTS and 0.2% YS) and ductility (elongation in 4 diameters and R.A.) with preheat extrusion temperature for 7075 P/M alloy L. Extrusions are for a 25 : 1 ratio. Typical 7075-T651 I/M values from Hyatt reference 75, are: UTS = 570 MPa, 0.2% YS = 500 MPa, and e = 8 %.

Charge No.	Processing Parameters		Mechanical Properties						
	preheat temp. (K)	reduction in area (%)	UTS	0.2 % YS (MPa)	0.2 % CYS	R.A. (%)	e	NTS (MPa)	NTS/YS
35	743	96 [25:1]	642.2 643.0	593.0 594.5	584.2 561.4	14.7 23.8	11.0 16.0	731.0 742.1	1.23 1.24
35L	743	"	638.8 638.2	583.0 584.5	-	21.8 14.5	14.2 11.7	-	-
30	713	"	676.0 690.0	630.0 632.1	596.6 593.1	21.6 19.4	12.5 11.7	759.0 748.0	1.20 1.19
36	703	"	661.6 663.8	611.6 613.6	599.7 610.3	18.8 14.2	13.3 10.8	769.1 773.4	1.26 1.26
36L	703	"	666.9 663.5	612.0 611.2	-	20.4 15.4	15.0 10.4	-	-
37	673	"	673.1 671.6	623.6 623.6	607.6 614.8	13.3 12.3	10.8 11.3	776.5 776.4	1.26 1.26
37L	673	"	672.8 667.1	616.0 611.8	-	18.7 17.5	12.5 9.6	-	-
38	643		682.4 675.3	629.4 625.1	587.2 601.6	17.6 21.8	14.8 14.2	782.8 781.8	1.25 1.25
38L	643	"	653.8 653.0	601.6 602.2	-	16.7 12.0	9.6 9.6	-	-
31A	613	"	656.1 694.5	606.0 638.0	645.9	12.0 15.5	9.6 12.5	-	-

L - Solution heat treated in air

Table 5: Processing parameters and mechanical property data for 7075-T651 P/M alloy L: Ultimate Tensile Strength (UTS), 0.2 % Yield Strength (0.2 % YS), 0.2 % Compressive Yield Strength (0.2 % CYS), Reduction in Area (R.A.), elongation in 4 diameters (e), and Notch Tensile Strength - Yield Strength Ratio (NTS/YS).

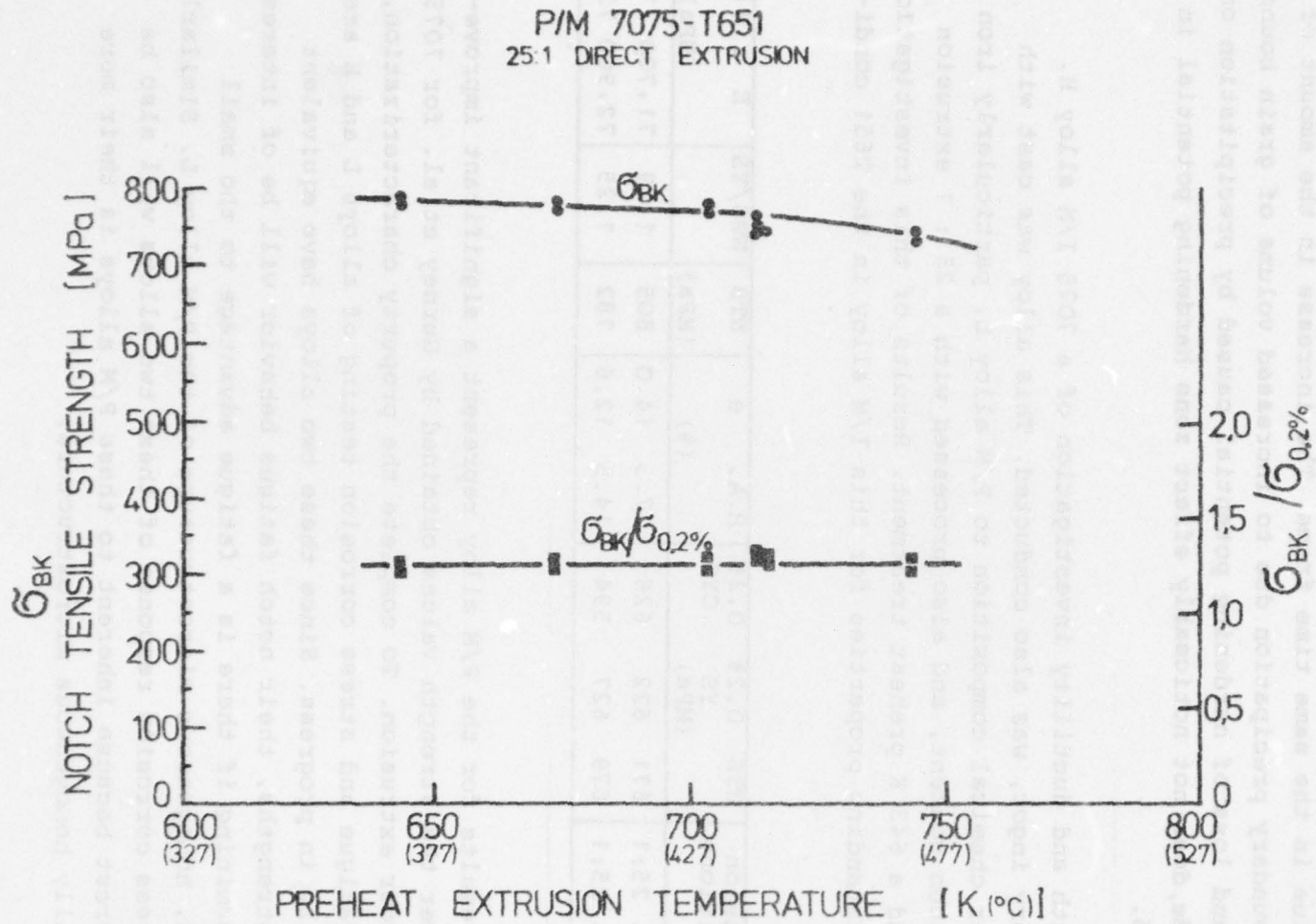

Figure 27: Variation of longitudinal fracture toughness, as measured by ASTM notch tensile testing techniques, with preheat extrusion temperature for 7075-T651 P/M alloy L extruded 25 : 1. I/M alloy C was extruded with a preheat temperature of 643 K, 25 : 1, and had properties similar to the P/M values: NTS = 805 MPa and a NTS/YS ratio of 1.29.

An investigation of the P/M alloys artificial aging response was conducted by hardness measurements to investigate if there is a difference in the artificial aging character, figure 28. Of particular interest was the effect of oxide and fine grain size. The P/M alloy's aging response was found to be similar with that of an 7075 I/M alloy. Both alloys reached the same maximum hardness value in the same time frame. The increase in the amount of grain boundary precipation due to increased volume of grain boundaries, and loss of hardening potential caused by precipitation on the oxide, does not noticeably effect zone hardening potential in P/M 7075.

A strength and ductility investigation of a 7075 I/M alloy H, laboratory ingot, was also conducted. This alloy was cast with a similar chemical composition to P/M alloy L, particularly iron and silicon content, and also processed with a 25 : 1 extrusion ratio and a 643 K preheat treatment. Results of this investigation show outstanding properties for this I/M alloy in the T651 condition.

alloy 7075-T651	extrusion conditions	UTS	0.2% YS (MPa)	0.2% CYS	R.A. (%)	e (%)	NTS (MPa)	NTS/YS	E (MPa)	E(comp) (MPa)
H (I/M)	643K, 25:1	671	622	626	17.3	14.0	805	1.29	71,700	71,400
L (P/M)	643K, 25:1	679	627	594	14.5	12.6	782	1.25	72,900	73,300

These results for the P/M alloy represent a significant improvement over the strength values obtained by Gurney et al. for 7075 REP powder extrusion. To complete the property characterization, notch fatigue and stress corrosion testing of alloys L and H are currently in progress. Since these two alloys have equivalent yield strengths, their notch fatigue behavior will be of interest in determining if there is a fatigue advantage to the small grained, homogeneous microstructure of the P/M alloy L. Similarly, the stress corrosion response of these two alloys will also be of interest because inherent to these P/M alloys is their more chemically homogeneous microstructure.

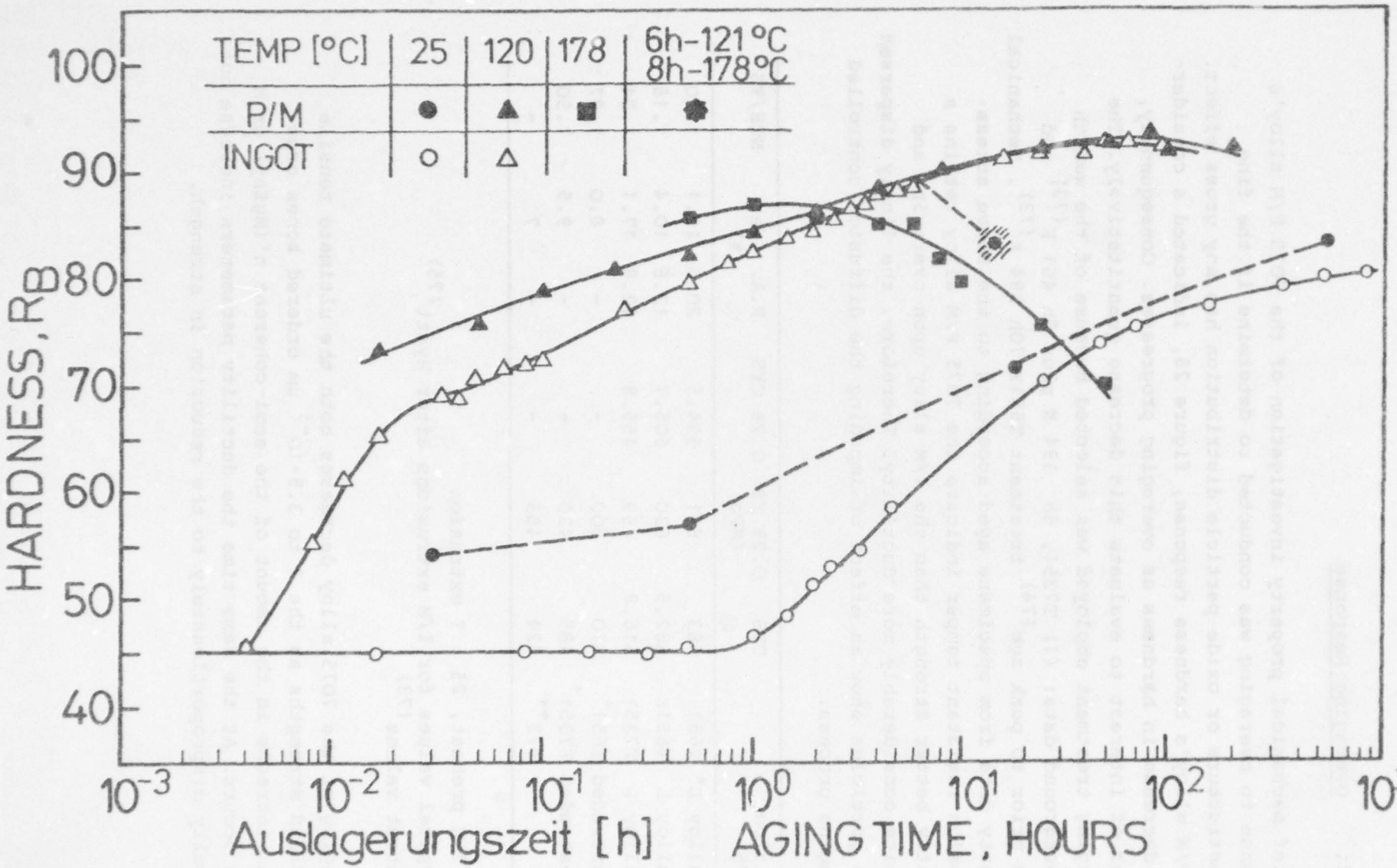

Figure 28: Artificial aging response of P/M and I/M 7075 products.

3.2.2. Overaging Response

A brief mechanical property investigation of the 7075 P/M alloy's response to overaging was conducted to determine if the fine microstructure or oxide particle distribution has any gross effect. The P/M alloy's hardness response, figure 28, indicated a considerable decrease in hardness as overaging progresses. Consequently, it was of interest to evaluate this decrease quantitatively. The overaging treatment employed was selected because of the wealth of background data: (1) T7351, 6h 394 K plus 8h 451 K[73] and (2) a prior to peak age[74] treatment T651X 70h 394 K[73]. Mechanical property data from specimens aged according to the above stress corrosion resistant temper indicate the 7075 P/M alloy retains a slightly better strength than the I/M alloy upon overaging and exhibits considerably more ductility. Therefore, the finely dispersed oxide particles show an effect of impeding the diffusion controlled overaging process.

Condition 7075		UTS	0.2% YS (MPa)	0.2% CYS	R.A. (%)	e	NTS/YS
P/M alloy L*	T651	683	631	594.5	20.5	12.1	1.20
P/M alloy L	T651X	682.5	630	606.7	12.6	10.4	1.18
P/M alloy L	T7351	516.8	469	455.8	42.8	17.1	1.34
I/M extruded	T651+	570	500	-	-	8.0	1.27
I/M extruded	T7351+	485	420	-	-	9.5	1.50
I/M	T73++	524	455	-	-	7	-

* 713 K preheat, 25 : 1 extrusion
\+ typical values for I/M extrusions after Hyatt[75]
++ patent values[73]

Overaging of the 7075 alloy decreases both the ultimate tensile and yield strengths as the 2 to $3.5 \cdot 10^{-3}$ µm ordered zones grow and an increase in the amount of the semi-coherent $\eta'(MgZn_2)$ or M phase occurs. At the same time the ductility parameters increase but typically disproportionately to the reduction in strength.

Contrary to these expected results, the P/M alloy exhibits a considerable increase in ductility and retention of strength as overaging progresses. The longitudinal fracture toughness of the P/M alloy is acceptable but considerably below typical values of extruded 7075 I/M. A significant part of this results from the high overaged strength.

4. Density

Density measurements were made for most of the variations in P/M processing, table 6. In addition, a 2024 and a 7075 control sample were produced by separately melting and casting a piece from extruded products of alloy E and alloy L under argon. The control was hot worked, sectioned, and metallographically examined before density determinations. In this way the control sample would reflect the density for the identical alloy content of the P/M products.

Results indicate that all P/M products with the exception of the aforementioned HIP product attained 100 % full density. Each value represents a minimum of two measurements with the uncertainty shown by subscripting the last decimal digit. Exact volume measurements were made by the displacement of water.

Values for the specially cast I/M alloys C and H, with compositions similar to the P/M alloys, have been included for comparison purposes.

Because of the disparity between the indication from the measured density value and the SEM fractograph for the hot pressed 2024 product, it is necessary to supplement the density values with examination of a polished, unetched sample in the SEM when 100 % density is indicated. Examination of the polished sample with SEM allows for easier interpretation between porosity and completely or partially removed nonmetallic inclusions/insoluable intermetallics.

Alloy	State	Density 10^3 ($kg \cdot m^{-3}$) measurements	Density 10^3 ($kg \cdot m^{-3}$) average
P/M 2024 E	HIP	2.639 2.632	2.63_6
P/M 2024 E	hot pressed	2.791 2.802	2.79_7
P/M 2024 E	impact compacted	2.8006 2.8128 2.8067	2.80_6
P/M 2024 E	90 % reduced	2.790 2.797	2.79_4
P/M 2024 E	95.5 % reduced	2.788 2.797	2.79_3
P/M 2024 E	98 % reduced	2.790 2.807	2.79_9
Control 2024 E	70.6 % reduced 87.2 % reduced	2.789 2.788 2.786	2.78_8
P/M 2024 D	96 % reduced	2.793 2.799	2.79_6
P/M 2024 G	96 % reduced	2.799 2.801	2.80_0
Control 7075 L	87.2 % reduced	2.805 2.809	2.80_7
P/M 7075 L	impact compaction	2.799 2.795	2.79_7
P/M 7075 L	96 % reduced	2.812 2.819	2.81_6
I/M 2024 C			2.78_6
I/M 7075 H			2.80_5

Table 6: Results of density measurements

5. Analysis of Out-Gas Products

Earlier work by Otto[30] concerning high strength P/M products concluded that vacuum hot compacting at a temperature above the SHT temperature must be employed in order to avoid hot shortness during subsequent hot working and to allow full transverse mechanical properties to be developed. Roberts[4] and Gurney[49,54] have attempted to develop high strength aluminum P/M products with excellent properties by evacuating a canned green compact and compacting at moderate temperatures, between 590 K and 644 K, to avoid deleterious agglomeration of the finely dispersed, small dispersoid particles. These dispersoid particles result from the transition alloying elements - namely chromium in 7075 and manganese in 2024 - added to enhance corrosion resistance, improve thick section precipitation response by reducing quench sensitivity, and inhibit recrystallization and grain growth. However, both Roberts and later Gurney have reported that even though a good vacuum of $1.3 \cdot 10^{-2}$ Pa or better was obtained and the extruded billet appeared sound, the transverse properties of heat-treated products would not be optimum due to either the observed microscopic porosity or presence of transverse and longitudinal cracks. Further, Roberts found by nuclear magnetic resonance (NMR) techniques that the water contamenation was reduced to an undetectable level after 1 hour at 616 K and $4 \cdot 10^{-2}$ Pa. Consequently, it was of interest for this report to analyse selective out-gas products to determine why vacuum preheating at the SHT temperature or above yielded good transverse properties, while attainment of a good vacuum at moderate temperatures, which eliminated the water content, failed to yield good transverse properties.

Out-gas products analysed by partial pressure determinations were water vapor, oxygen, hydrogen, and nitrogen. Hydrogen was especially of interest because it is the only gas having measurable solubility in aluminum. The dissolved hydrogen content in the aluminum matrix should not be a significant factor of concern if proper melting and atomizing practices are followed. However, the surface oxide which forms during solidification is very reactive and physically adsorbs water as well as chemically forms hydrates of water. When the powder is reheated some of the water reacts with aluminum or magnesium to form hydrogen. Since a source of hydrogen is therefore

present within the oxide, it was important to analyse its partial pressure temperature response as well as that of the water vapor. If significant solubility of hydrogen within the aluminum powder had occurred, diffusion of atomic hydrogen and evolution of molecular hydrogen would occur during the high temperature stage of the vacuum preheat treatment.

Analysis of nitrogen was a control measurement which reflected the entrapped gas content and interconnection of porosity with temperature. Analysis of nitrogen partial pressures reflected evacuation trends of the original entrapped gases versus those which resulted from the release and partial disassociation of the oxide's chemically and physically bonded water.

Partial pressure analyses of the 2024 and 7075 canned green compacts revealed similar trends, figures 29 and 30. For the 7075 green compact, the water vapor's recorded maximum partial pressure of $1.3 \cdot 10^{-6}$ Pa occurs at a temperature of 473 K. With continued evacuation and heating, a partial pressure reduction to $2 \cdot 10^{-9}$ Pa at 659 K is attained; further heating to 823 K only reduces the water vapor's partial pressure to $1.5 \cdot 10^{-10}$ Pa at a total pressure of 10^{-4} Pa. (The equilibrium partial pressure for water vapor in the evacuation system was determined to be $6.4 \cdot 10^{-11}$ Pa at a total pressure of 10^{-4} Pa.) These findings are in agreement with the results of Roberts[4], as discussed earlier.

The results of the water partial pressure analysis for the 2024 compact are similar to that for the 7075 compact. They also show a significant drop in partial pressure between 543 K and 659 K from the 10^{-6} Pa maximum to the 10^{-9} Pa level. Slight further partial pressure decreases are obtained at the 766 K SHT temperature but they are not significant in comparison to the reduction obtained between 543 K and 659 K.

The results for both alloys with regard to water, oxygen, and nitrogen show similar trends. That is, in the temperature range from 543 K to 659 K the near maximum in interconnected porosity is reached and the greatest reduction of partial pressures for these out-gas products is attained.

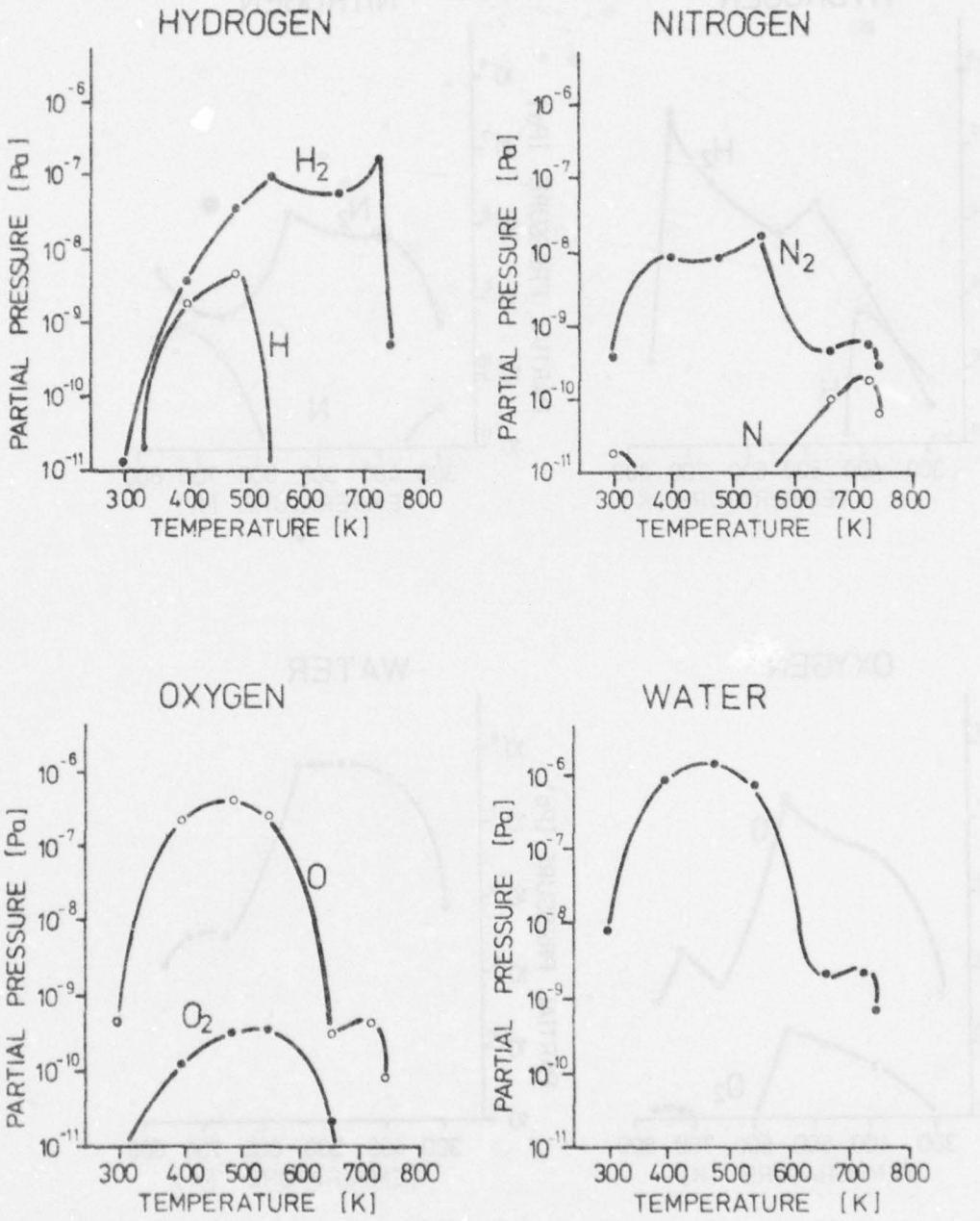

Figure 29: Quasi-steady-state partial pressure determination of hydrogen, nitrogen, oxygen and water vapor at various temperatures during vacuum preheating of an 80 % dense canned 7075 P/M alloy L compact.

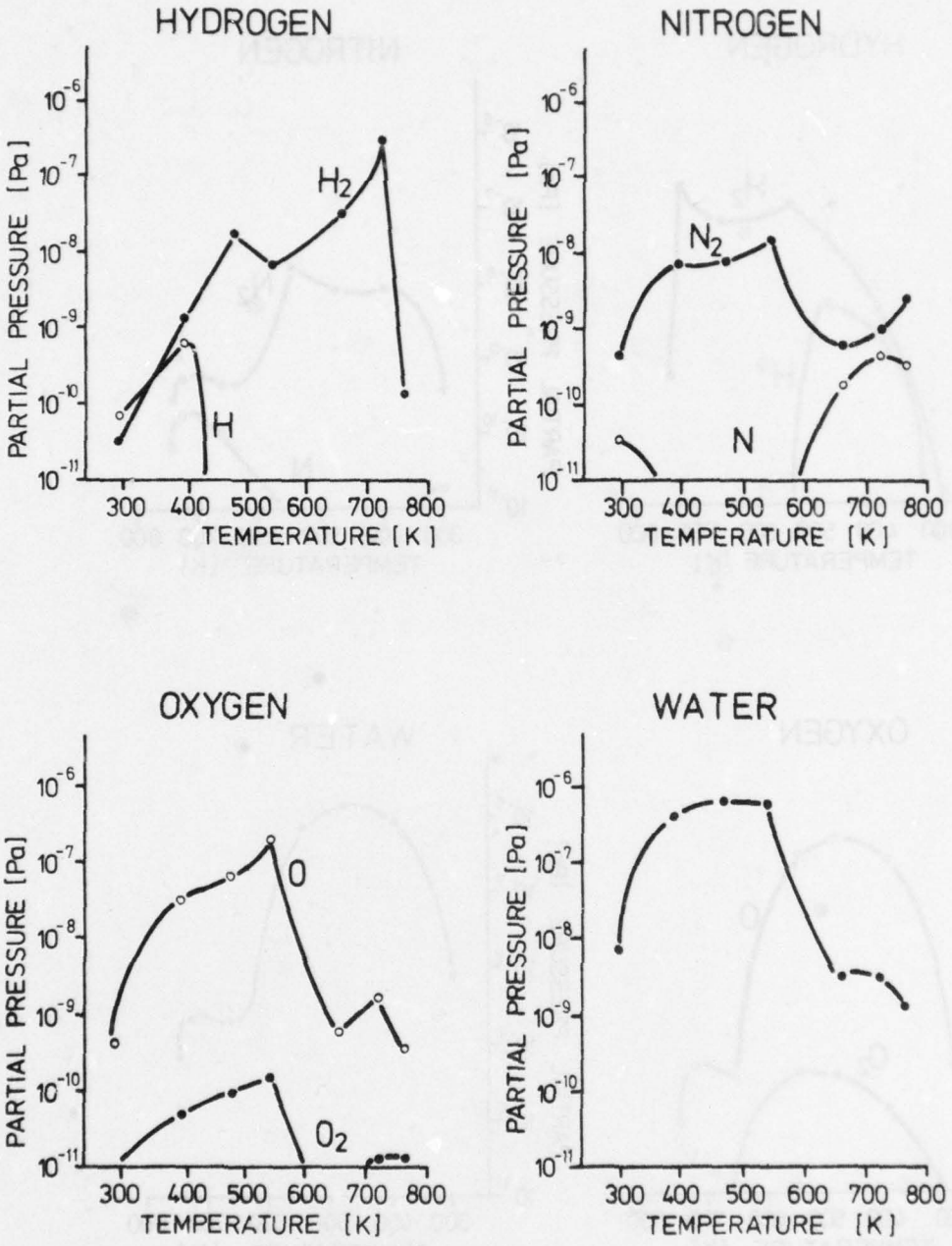

Figure: Quasi-steady-state partial pressure determination of hydrogen, nitrogen, oxygen, and water vapor at various temperatures during vacuum preheating of an 80 % dense canned 2024 P/M alloy E compact.

With regard to hydrogen, the maximum partial pressure of $2.7 \cdot 10^{-7}$ Pa in 2024 and $1.6 \cdot 10^{-7}$ Pa in 7075 was recorded at 723 K. From these recorded maximums, both alloys showed sharp drops in hydrogen partial pressure at their respective SHT temperatures. These sharp partial pressure decreases are $1.3 \cdot 10^{-10}$ Pa at 766 K for 2024, and $4.9 \cdot 10^{-10}$ Pa at 743 K for 7075. For 7075, heating to 783 K showed slight further hydrogen partial pressure reductions to $1.6 \cdot 10^{-10}$ Pa which thereafter remained constant up to 823 K. Consequently, the majority of hydrogen has been removed at the respective SHT temperatures, and it is necessary to vacuum preheat near the SHT temperature range, the higher the temperature the better, in order to adequately reduce the alloy's gas content.

For both alloys the relationship between atomic and molecular oxygen was reversed from that which is predicted by the thermodynamic equilibrium partial pressure relationship between the two. Additional analyses with a second ion gauge confirmed this relationship, and a brief theoretical thermodynamic analysis of the complex relationship between the partial pressures of the various reacting gases and tendency for further oxidation did not reveal an explanation for this inverse relationship.

Repeated partial pressure analysis (not shown) served to confirm the general shape of the curves shown in figures 29 and 30. With the addition of new data points to these figures, all curves tended to be of the rounded shape displayed in figure 29 for water and oxygen partial pressures. Additional measurements for temperatures up to 823 K (not plotted) show very little further decrease in partial pressures than those already shown at the respective alloy's SHT temperature, except for the partial pressure of water in the 7075 compact which decreased to $1.5 \cdot 10^{-10}$ Pa at 823 K from $7.3 \cdot 10^{-10}$ Pa at the 743 K SHT temperature.

5.1. Evacuation Pressure Analysis

Throughout this report it has been emphasized that pressure measurements have been made at room temperature in the vacuum chamber rather than in the compact. Consequently, it was of interest to

determine the variation of vacuum pressure with distance: (1) within the compact, and (2) along the evacuation line from the compact to the vacuum chamber. This determination was of special interest because of the potential evaporation of zinc and magnesium at the evacuation temperatures and pressures employed in this investigation, figure 31.

An investigation of a 7075 canned green compact showed there was a vacuum pressure attenuation of five orders of magnitude between the vacuum chamber and a distance behind the compact equal to the length (and diameter) of the evacuation tube on the front of the can, figure 32. Further evaluation revealed slightly less than an order of magnitude pressure attenuation between the vacuum chamber and the end of the flexible steel evacuation hose (25 mm Ø in x 600 - 750 mm) and approximately a further order of magnitude pressure attenuation along the aluminum evacuation tube (8 mm Ø in x 550 - 600 mm) from the steel hose connection to the front of the 80 % dense green compact (70 mm Ø in x 200 mm). The flexible steel hose is necessary to allow movement of the can for pinching and cutting, while the length of the evacuation tube is necessary to protect the synthetic VITILAN vacuum O-ring between the steel hose and aluminum tube from excessive temperature and also to provide enough length to insure that the compact is in a uniform temperature zone in the furnace.

Consequently, a total vacuum pressure in the vacuum chamber of 10^{-4} Pa is indicative of approximately 10^{-2} Pa at the front of the green compact and approximately 1 Pa ($7.5 \cdot 10^{-3}$ torr) at the far end of the compact. This difference is not considered significant for development of full properties from the compact, as Otto[30] has shown that full properties can be developed without property differences for vacuum pressures* between 2.6 Pa and $1.33 \cdot 10^{-2}$ Pa.

*The location of the pressure reading devices were not specified.

Figure 31 indicates that at the temperatures and pressures employed for this investigation, evaporation of magnesium and zinc could be expected. However, a wet chemical analysis for an extruded product which had received the long time homogenization - vacuum preheat treatment showed no difference in zinc and magnesium compositions from the prealloyed 7075 powder melt composition. In addition, microprobe analysis showed no differences along the transverse direction for cross sections removed at various distances along the extruded bar. Therefore, if evaporation had occurred, it was not sufficient to significantly affect the final properties of the products investigated.

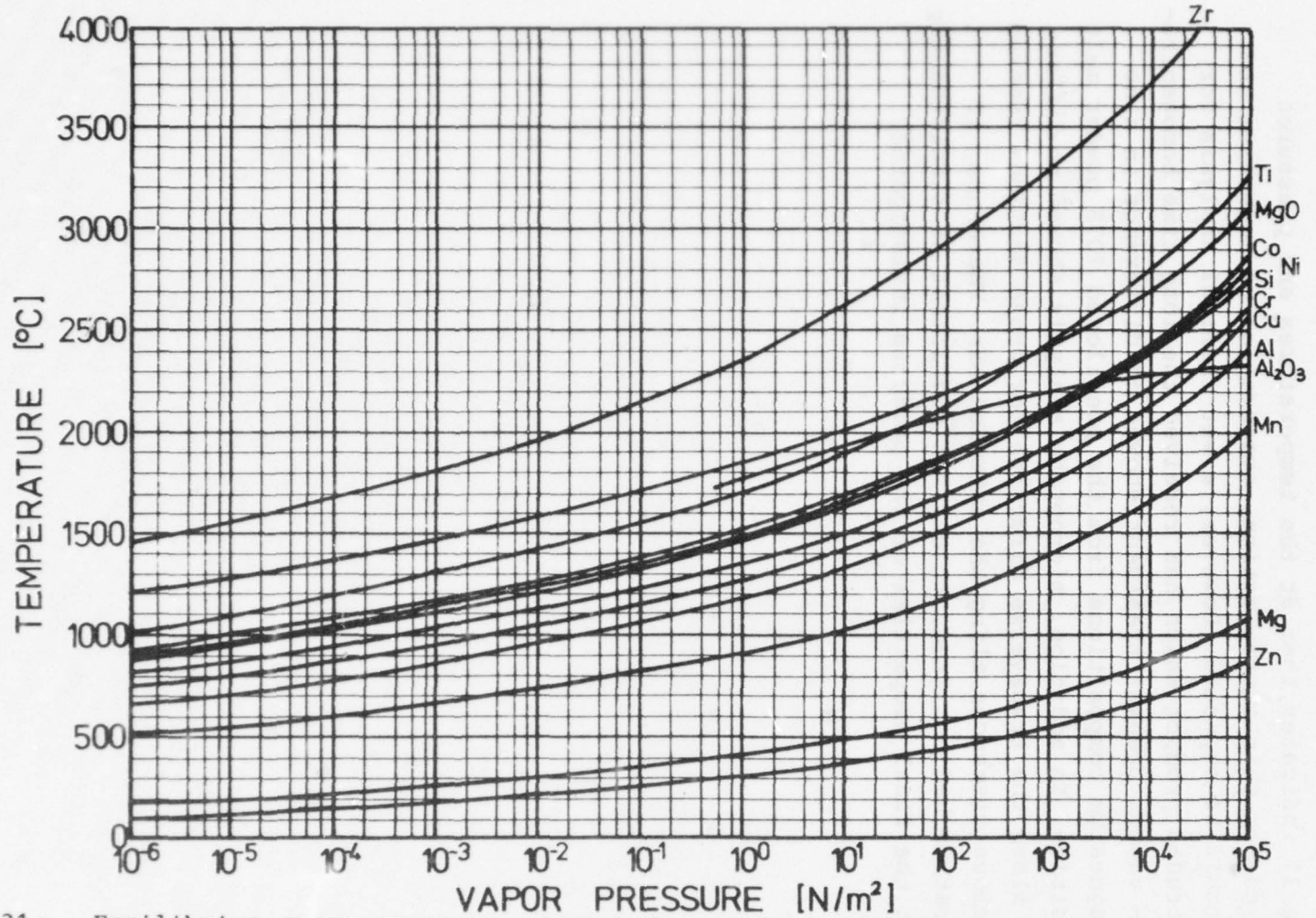

Figure 31: Equilibrium vapor pressure - temperature relationship for various elements, Al_2O_3 and MgO. (A compilation of values from: Honig, R.E. RCA-Review. June 1953, pp.195-204; Stull and Sinke. Thermodynamic Properties of the Elements. Amer. Chem. Soc.: Washington, D.C., 1956; and, Samsonov, G.V. Oxide Handbook. Univ. of Kiev - IFI Plenum: New York - Washington - London, 1973. (Translated from Russian by C.N. Turton and T. Turton.))

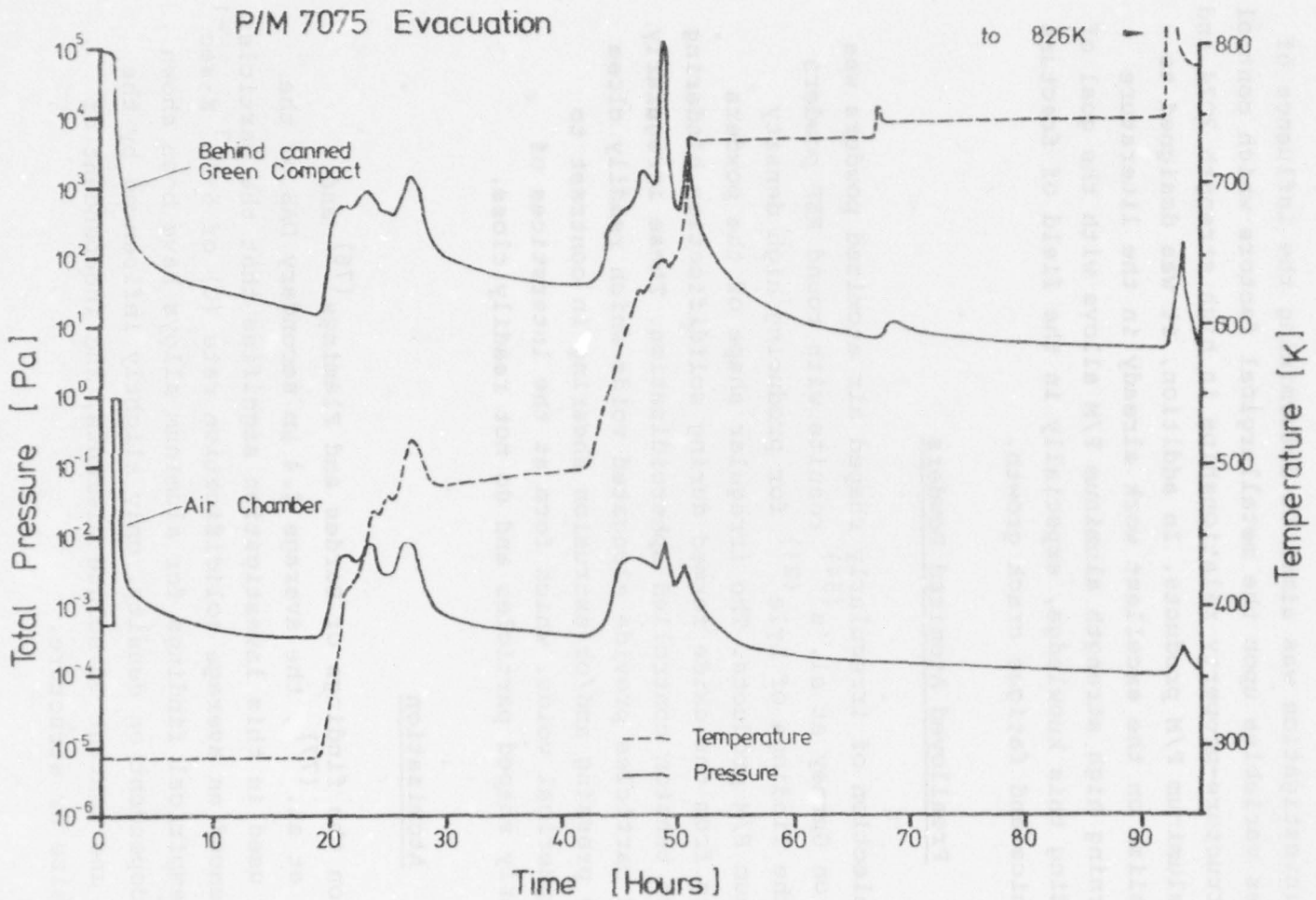

Figure 32: Total pressure - temperature - time relationship for a canned 7075 P/M alloy L vacuum preheated from room temperature to 826 K. Room temperature pressure measurements were made in the vacuum system's vac. chamber and at a distance behind the green compact (outside the furnace) equal to the length of the aluminum alloy AlMg3 evacuation tube (0.55 m).

Discussion

This investigation was aimed at determining the influence of process variables upon the metallurgical factors which control the structure-property relationships in high strength 2024 and 7075 aluminum P/M products. In addition, it was designed to capitalize on the excellent work already in the literature concerning high strength aluminum P/M alloys with the goal of extending this knowledge, especially in the field of fracture mechanics and fatigue crack growth.

1. Prealloyed Atomized Powders

The selection of irregularly shaped air atomized powders was based on Gurney et al.'s[54] results with round REP powders and the findings of Lyle[21] for producing high density aluminum P/M products. The irregular shape of the powders results from the oxide formed during solidification hindering surface tension controlled spheroidization. These irregularly shaped particles provide elongated voids which readily close during pressing and/or extrusion shearing in contrast to near spherical voids, which form at the interstices of regularly shaped particles and do not readily close.

1.1. Atomization

Based on the findings of Bardes and Flemings[76] and Matyja et al.[77], the average 2.4 μm secondary DAS of the powder used in this investigation signifies that the particles experienced an average solidification rate (U) of $5 \cdot 10^3$ $K \cdot sec^{-1}$. These empirical findings for aluminum alloys have been shown to be dependent on density, only slightly influenced by the nature and content of solute elements, and independent of grain size or structure.

The small DAS and fine interdendritic network of the powder particles' solidification structure, figure 7, is a result of the high degree of supercooling which occurred during the

atomization process. The supercooling results from the high solidification rate and is responsible for a finer, more uniform dispersion of the intermetallic constituents in the P/M product than in the I/M products investigated. The effect of this fine solidification structure on mechanical properties depends on the alloy system.

1.1.1. 2024 Alloy

Atomization can reduce the growth of or even eliminate some of the second phase intermetallics. Lebo and Grant[48] have shown that microsegregation and formation of the brittle AlCuFeMn intermetallic second phase in 2024 can be essentially suppressed by splat cooling ($U = 10^4$ to 10^6 $K \cdot sec^{-1}$ and respective DAS = 3 to 0.67 µm). Even though the volume fraction of second phase particles between their I/M and P/M products remained unchanged, P/M strength parameters increased up to 18 % without any loss of ductility. Results of the current investigation with atomized powders ($U = 5 \cdot 10^3$ $K \cdot sec^{-1}$ and DAS = 2.4 µm) indicate that considerable suppression of the AlCuFeMn also occurs. An average 32 % increase in strength for P/M relative to I/M products occurs with a disproportionately small decrease in ductility (R.A. decreases from 26 % to 21 %). However, SEM fractographs of tensile fractures indicate that the oxide is not thoroughly dispersed in the extruded product from splat cooled powders. Coarse shears are associated with oxide film fragments from original splat foils, whereas the tensile fracture of extruded products from atomized powders is completely highly dimpled and characteristic of a highly ductile structure. In addition, the splat cooled powders contained approximately twice as much insoluble iron and silicon content, and grain sizes were significantly larger than those of the atomized powder products (168 to 135 µm versus 10 to 2 µm). Nevertheless, in comparison to I/M products, the fine solidification structure of the higher solidification rate 2024 splat cooled powders shows significantly more ductility improvements for equal strength than is shown by the solidification structure of atomized powder products.

1.1.2 7075 Alloy

In the case of 7075, solidification rates from 10^3 to 10^6 $K \cdot sec^{-1}$ do not cause any significant suppression of the equilibrium (impurity) iron and silicon intermetallic second phases. Instead, high solidification rates produce an interdendritic network of these insoluble intermetallics which results in their fine, uniform dispersion in the final P/M product. The equilibrium dispersoid E phase ($Cr_2Mg_3Al_{18}$) is initially suppressed, but precipitates to a very fine dispersion during subsequent metal processing.

The longitudinal 7075-T651 tensile properties of the extruded laboratory cast ingot (DAS 70 - 100 μm) show no effect of the somewhat coarser, insoluble intermetallic second phase over the tensile properties of the P/M extrusion. Solidification and homogenization studies[78-82] of I/M 7075 have shown that through elimination of undissolved second phases by special ingot processing and limiting iron and silicon contents to 0.01 w/o each, it is possible to maintain strength, reduce anisotropy, and increase ductility related mechanical properties. Specifically, a 7075-T6 alloy relatively free of second phases, shows R.A. values of 26 to 40 % without any grain size refinement (grain sizes of 50 to 200 μm). In comparison to the fine grained 7075 products of the current investigation, it is clear that the fine, undissolved second phase dispersion resulting from atomization, reduces ductility rather than enhancing it (I/M R.A. = 17.3 % and P/M R.A. = 14.5%)

Since the I/M and P/M 7075-T651 alloys used in the current investigation are of equivalent yield strength and chemistry, the ongoing notch fatigue tests will evaluate the influence of the atomized powder's structure on fatigue crack growth. Mulkerin and Rosenthal[82] found no significant difference in 7075-T6 longitudinal smooth fatigue behavior between a product processed to produce an extremely low concentration of undissolved second phase (0.053 v/o) and a commercial alloy. Therefore, if the ongoing notch fatigue tests show different fatigue

performances, it will be an indication that the manner in which the intermetallic second phase is dispersed, influences the crack growth rate.

1.2. Prealloying

When P/M technology is employed as a manufacturing technique, the mechanical properties that can be developed from prealloyed atomized powder surpass those which can be obtained from elemental blended powders. The fine solidification structure of the prealloyed powder develops superior properties to those which result from alloying by diffusion. Bhattacharyya and Kulkarni[65] have isothermally forged a component from -100 mesh (149 μm) elemental blended 7075 alloy powder. They have found longitudinal tensile properties in the artificially aged T6 condition which are only slightly better than those which were developed in the current investigation by vacuum hot pressing the lower strength 2024 alloy and testing in the naturally aged condition.

alloy	powder	UTS (MPa)	0.2% YS (MPa)	elongation (%)
forged 7075-T6	elemental	497	435	8.5
pressed 2024-T351	prealloyed	473	377	12.0

An examination of the tensile properties of a hot pressed component made from prealloyed 7075 powder is presently being conducted to afford a direct comparison. However, the current results from the lower strength 2024 alloy demonstrate the benefit of the high solidification rate in producing a chemically more homogeneous product. Clearly, the full potential of the high solidification rate process to increase alloyability has not been investigated in order that the influence of minimized macro- and micro-segregation can be investigated.

2. Vacuum Preheat Treatment

To develop high strength, the 2024 and 7075 alloys must be solution treated and quenched. During the SHT porosity, blistering, and delamination can develop if the gas content of the P/M product has not been previously reduced. Lyle and Cebulak[26] have used preheat treatment temperatures slightly higher than the alloy's SHT temperature but below that which causes excessive coarsening of constituent particles.

Following the successful vacuum preheat treatment work of Dromsky and Lenel[68] with aluminum powder, several investigators have attempted to employ this treatment to reduce the gas content of prealloyed powders. However, because there are significant differences between the oxides of the aluminum and prealloyed aluminum powders, the vacuum preheat treatment has not always proven successful in sufficiently reducing the gas content.

Amorphous[83] hydrates of aluminum oxide ($Al_xO_y \cdot n\ H_2O$) form on aluminum powder. Upon heating, this oxide transforms[67] to $\gamma\ Al_2O_3$ and releases its adsorbed and hydrated water content, some of which is evolved as water vapor and some of which reacts with the aluminum[71a] to yield hydrogen. In the case of the prealloyed powders, an amorphous oxide[26] forms as a result of the selective oxidation of the alloying elements. According to thermodynamic considerations, free energy of formation data predicts the oxidation of the 2024 and 7075 major alloying elements in the following order : MgO, Al_2O_3, ZnO, Cu_2O, and CuO. Otto[30] has examined the surface of an Al-Zn-Mg-Cu alloy powder particle by Auger analysis during sputtering of the particle. His findings of increased Mg and Zn concentrations within the first 10^{-8} m of the surface, confirms the selective oxidation of the alloying elements. An additional ductile layer[54] of MgO is subsequently formed[36,69] during the vacuum preheat treatment on top of the initial amorphous oxide, further hindering the release of water vapor and hydrogen. In addition, the preferred selective oxidation

of magnesium serves to further increase the hydrogen gas content. Lyle and Cebulak[25] have reported the presence of hydrogen and either argon or nitrogen in high strength aluminum P/M products fabricated by either flowing argon or nitrogen preheat treatments.

The employment of a vacuum preheat treatment reduces the likelihood of argon or nitrogen being entrapped within the final P/M product. However, the partial pressure analysis reveals that unless a vacuum preheat treatment with sufficient time at or above the SHT temperature is used, a sufficient gas content (predominantly hxdrogen) will be present to cause blistering and delamination during subsequent SHT. Times equivalent to 24 h at 743 K have been determined for 7075 to be sufficient for elimination of blistering and delamination; times equivalent to 24h at 766 K for the 2024 alloy are also sufficient. These times do not represent a minimum evacuation time at the alloy's respective SHT temperature. An additional investigation is planned to determine minimum times.

Jones[64] has reported that vacuum-preheat and subsequent compaction treatments are responsible for porosity reductions as well as improved ductility and fracture toughness properties as a result of breaking down the oxide film. Results of the current study show that vacuum processing is indeed capable of reducing porosity but improvement in fracture toughness has not been found. Investigation of the equal strength 7075 I/M and P/M alloys shows no longitudinal fracture toughness improvement as a result of P/M processing.

3. Mechanical Properties

The longitudinal mechanical properties of the naturally aged 2024 P/M alloy are significantly improved beyond those of the I/M alloy in the artifically aged condition, with the exception of fracture toughness. The reduction in fracture toughness, which is to be anticipated with the large strength improvements, is not critical, as the NTS/YS ratio of 1.37 for the

high strength P/M product is still indicative of a good fracture toughness property. Through optimum processing, the P/M alloy's notch fatigue strength has been improved to the smooth fatigue strength for the I/M alloy (140 MPa). These property improvements are the result of an enhanced precipitation response and a fine grained (2 μm), annealed structure. A micrograph of this fine structure is shown in figure 33.

Unfortunately presentation of a sharp, clear micrograph at this time is not possible. As has been mentioned by Roberts[3a], the fined grain structure presents a significant problem to find an etching reagent which reveals the grain structure without attacking the fine grains. Interpretation of figure 33 can be confusing as it appears that significant porosity remains in the P/M product. Consequently, two other structures which have not been as heavily etched are presented in figure 34 as evidence of the lack of porosity. Figure 34 clearly reveals the fine dispersion of the impurity iron and silicon second phases. The grain growth resistance can nevertheless be recognized in figure 33.

Recrystallization resistance was observed in P/M 2024 up to a 97 % reduction, figure 18, with partial recrystallization and subsequent decrease in textural strength occuring for a 98 % reduction. The longitudinal tensile strength increases shown in figure 18 for reductions from 90 to 96 % result from increased texturing.

The reason for the increased tensile strength of P/M 2024 with a 643 K preheat is presently being pursued metallographically, both optically and with the transmission electron microscope.

Preliminary findings indicate that the degree of partial recrystallization increases in the P/M 2024 as the preheat extrusion temperature decreases. The 2024 P/M alloy appears to be much more recrystallization and grain growth resistant than the I/M alloy.

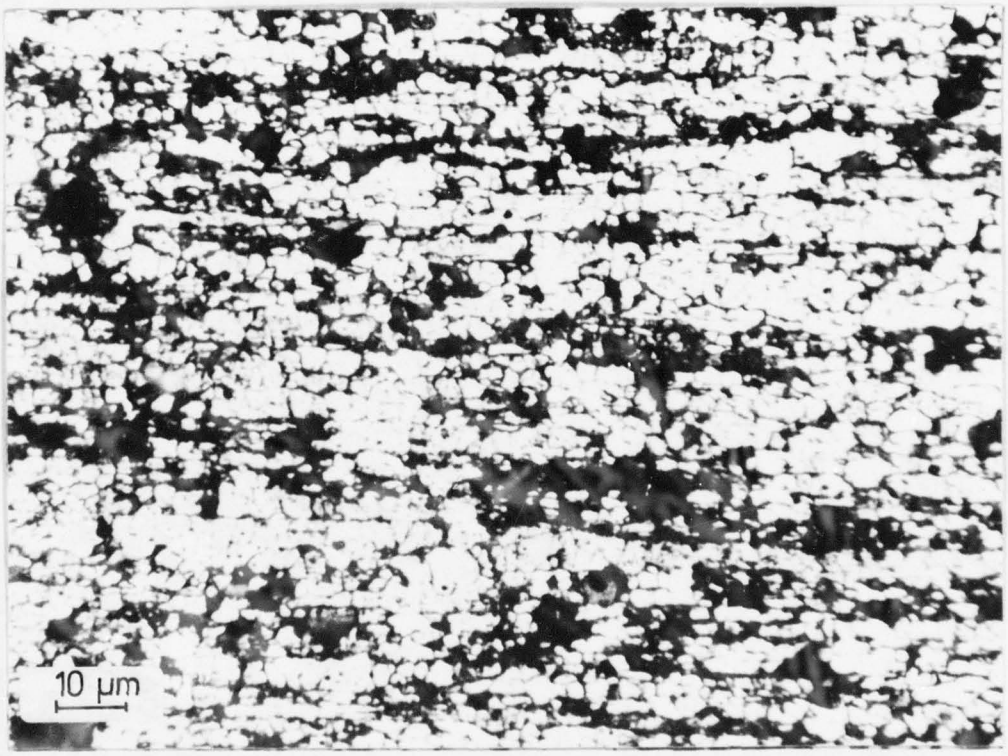

1000x

Figure 33: Representative microstructure of 2024-T351 P/M alloy E extruded 25 : 1 at 643 K. The etching reagent has attacked the fine grained material to produce what appears to be a porous structure, compare with figure 34.

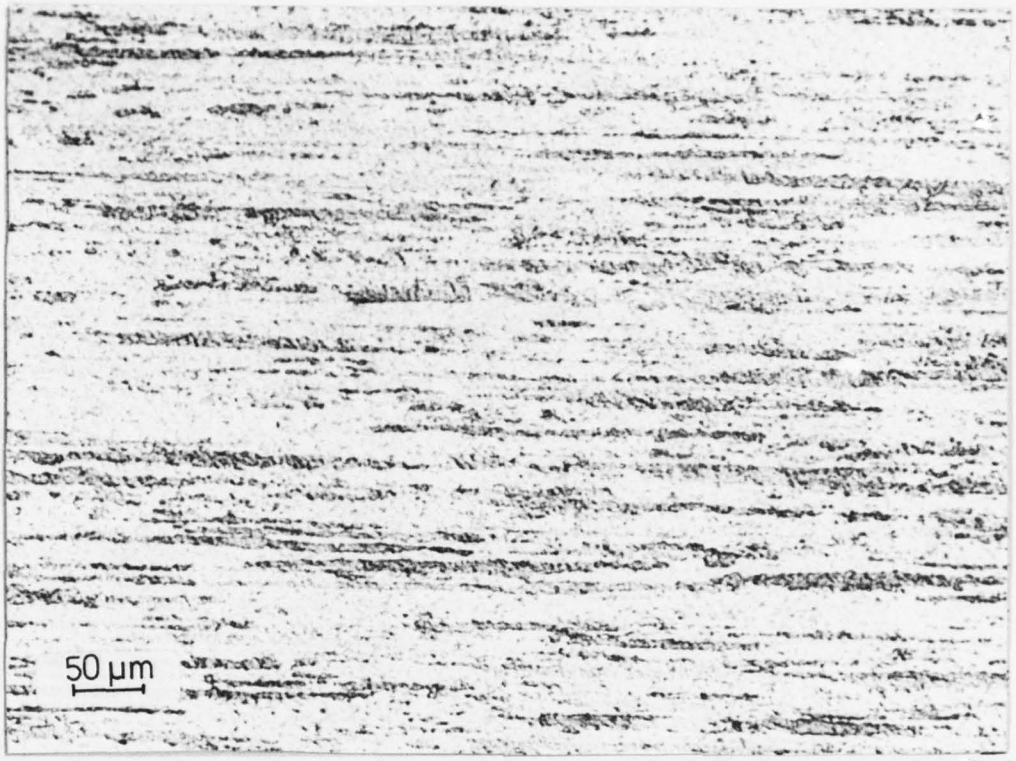

200x

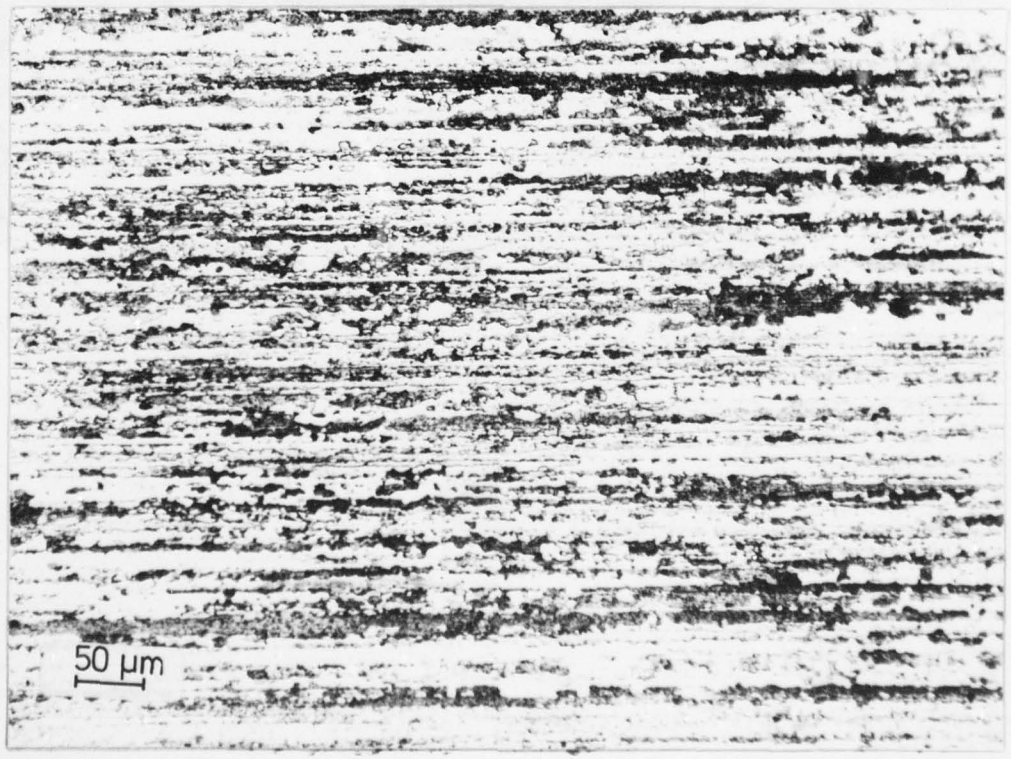

200x

Figure 34: Representative microstructures of 2024-T351 P/M alloy E extruded 25 : 1 at a preheat temperature of 643 K (above) and 653 K (below).

Micrographs of the 7075 P/M alloy also reveal a grain growth resistant structure independent of the preheat extrusion temperature (613 to 743 K), figure 26. The structure retains a very fine grained condition leading to the high strength.

The decrease in ductility properties in figure 26 at a 743 K extrusion preheat temperature is attributed to a slightly flawed structure. At this temperature the material's shear strength was not high enough to accommodate the excessive amount of shear in the matrix near the dispersed oxide particles which occurred during extrusion processing.

As the extrusion preheat temperature decreases from 743 K, the strength increases due to the attenuation of dynamic recovery. The slight strength increases over the range of temperatures investigated appear to result only from substructure strengthening.

The percent deformation investigation was initiated with a 10 : 1 reduction because Roberts[4] reported unsound heat-treated P/M products produced with reduction ratios less than 10 : 1 and because Lyle and Cebulak[25,26] had successfully used the 10 : 1 ratio. However, the isotropic strength properties developed by the 2024 hot pressed product are equivalent to the extruded I/M values; ductility properties of the P/M product are good but about half those of the I/M values. Consequently, it is predicted that only a 6 : 1 reduction will increase the P/M longitudinal strength and ductility properties to approximately the same values obtained for 10 : 1 reduction. A 6 : 1 ratio is the practical minimum employed for commercial 2024 I/M products, and is also reported by Gurney et al.[54] to have yielded sound 7075 P/M extrusions prior to heat-treatment. Gurney has also reported that unidirectionally hot pressed billets from 7075 REP powders have insufficient integrity to allow machining, with failure occuring solely at interparticle boundaries. These results are in sharp contradiction to those of the similarly produced 2024 unidirectionally pressed billet whose notch fatigue behavior is improved over that of the 2024 I/M material (125 MPa

for the P/M product versus 105 MPa at 10^7 cycles). This difference is the result of the greater metal flow and subsequent oxide fragmentation which results from compaction of irregular powders. Even the limited amount of metal flow which occurred in the 2024 HIPed product showed more integrity than can be developed from hot pressing of REP powders.

The 19 % improved notch fatigue behavior of the unidirectionally hot pressed 2024 P/M billet, in comparison with the equal strength I/M product, indicates that an inherent fatigue improvement may result from the fine, atomized solidification structure. A smooth fatigue investigation of equal strength, extruded 2024 P/M and I/M products is planned to distinguish if this fatigue strength improvement is the result of slower crack initiation or growth rate.

The longitudinal notch fatigue behavior of the optimum P/M processing condition for naturally aged 2024 shows an 33 % improvement over the naturally aged 2024 I/M products (140 MPa versus 105 MPa for 10^7 cycles). This represents a significant improvement as no other approaches have been able to increase the notch fatigue behavior of this alloy. Lebo and Grant[48] had reported a 14 % smooth fatigue improvement at 10^6 cycles for splat cooled, naturally aged 2024. However, such improvements can also be accomplished by thermomechanical processing, but without subsequent improvements in the notch fatigue behavior. Similarly, Lyle and Cebulak [20,22,24] have reported smooth fatigue improvements by P/M alloy development, in contrast to equal strength I/M 7075-T6, but the notch fatigue character of these alloys was equal to that of 7075-T6.

As an additional source of information to aid in endurance limit determination, fatigue specimens which did not fail were retested at 170 MPa to determine if microstructural fatigue damage had occurred. In general, specimens initially tested at the endurance limit stress level were "trained", and required a higher number of cycles to failure when retested at the 170 MPa maximum stress level than fatigue specimens which were used to establish the 170 MPa fatigue strength. Specimens which were initially tested at 5 or 10 MPa below the endurance limit stress level, did not appear to have suffered any

fatigue damage, and in general, failed within the normal 170 MPa scatter range. These results have not been recorded on the fatigue diagrams presented within this report.

Conclusion

The results of this investigation verified the expectation that the P/M approach to alloy development can yield high strength aluminum products with improved capabilities. In particular are the high strength and notch fatigue properties developed in the naturally aged 2024 products, and the higher grain growth resistance in both the 2024 and 7075 P/M products. Both alloy's extruded products are characterized by a fine grained structure with a fine, uniform second phase dispersion.

Unidirectional hot pressed 2024-T351 P/M products have strength properties equal to those of I/M, but with 19 % improvements in the notch fatigue behavior at equal yield strengths. Extruded 2024-T351 P/M products have strength properties superior to artificially aged 2024-T851 I/M properties with an 33 % improvement in the notch fatigue performance.

The improved grain growth resistance of these P/M alloys allows retention of a favorable microstructure, and should permit outstanding mechanical properties to be maintained during low temperature metal working operations. Optimum processing conditions for the P/M alloys are:

(1) Air atomization of -100 mesh irregularly shaped powders, preferably with APDs less than 100 µm, to provide a fine grained structure and a fine dispersion of the Mn and Cr constituents.

(2) Long time vacuum preheat treatment at the solution heat treatment temperature to sufficiently reduce the hydrogen

content, or shorter times at higher temperatures (time and temperatures remain to be optimized for each alloy but 24h at the solution heat-treatment temperature is sufficient).

(3) Vacuum pressures of 1 Pa or better allow full mechanical properties to be developed.

(4) Unidirectional hot pressing with 615 MPa and 10 min dwell at 10 K below the solution heat-treatment temperature to develop high strength and a near 100% dense product.

(5) Press extrusion with 20 : 1 or 25 : 1 reduction ratios at a 643 K preheat temperature to develop optimum longitudinal and transverse strength and ductility.

(6) Aging treatments similar to those used for the I/M alloys are also optimum for P/M products.

P/M processing of 7075 has shown similar results, in the longitudinal direction, to those for elimination of second phases by special I/M processing. Namely, from a longitudinal strength point of view, there is no advantage to P/M processing of 7075. However, just as special I/M processing provided fracture toughness and transverse mechanical property improvement in I/M 7075, so is the reduction of anisotropy anticipated in P/M 7075. In addition to the increased recrystallization resistance, it is also expected that the longitudinal notch fatigue strength will be increased.

Future Research Effort

With the research efforts listed below, Phase I - the investigation of the processing property relationship, will be complete and major attention will be devoted to microstructure analysis and the correlation of the processing - property - microstructure interrelationship.

Phase I

- smooth fatigue response at equal strengths for 2024 P/M alloy E and I/M alloy A
- 2024 P/M alloy's response to artificial aging (strength and notch fatigue)
- effect of APD on the mechanical properties of 2024 P/M products (strength, notch fatigue, 4-point bend fracture toughness)
- evaluation of 7075-T6 hot pressed products and notch fatigue response of 7075-T651 P/M alloy L and I/M alloy H
- evaluation of a 6 : 1 extrusion ratio
- optimum solution temperature study P/M alloys E and L
- optimum homogenization-evacuation time/temperature/pressure relationship to obtain a 4 ml of H_2/100 gr aluminum partial pressure level and fine dispersion of the Mn and Cr dispersoids
- fracture mechanic and crack growth studies on P/M alloys D, E and L in selected unidirectional hot pressed or hot worked conditions

Phase II

- optical metallography, SEM, and TEM characterization of the various P/M and I/M structures
- microstructure evaluation and its relationship to alloy processing, and properties: effect of oxide on recrystallization, grain size, grain growth, substructure stability, and dislocation density

References

[1] Roberts, S.G.:Powder Fabrication of Aluminum Alloys. WADC-TR-56-481, April 1957. (AD 118 192)

[2] Roberts, S.G.: "An Exploratory Investigation of Prealloyed Powders of Aluminum", Powder Metallurgy. New York: Interscience Publishers (W. Leszynski, Ed.), 1961. page 799-818.

[3] Roberts, S.G.: Reserach Study for Development of Aluminum Base Alloys by Powder Metallurgy Techniques. Dept. of U.S. Army Contract DA-04-200-507-ORD-886.
a. Interim Project Report No. MS PR 59-69. June 18, 1959. (AD 218 563)
b. Summary Project Report No. MS PR 61-69, November 15, 1961. (AD 287 852)

[4] Roberts, S.G.: Vacuum Treatment of Prealloyed Aluminum Powders at Moderate Temperatures. AMMRC CTR 73-33, October 1973. (AD 769 074)

[5] Roberts, S.G.: Degassing Powder Metallurgical Products. U.S. Patent 3, 954, 458. May 4, 1976.

[6] Towner, R.J.: Development of Aluminum Base Alloys. Annual Progress Report 7-62-AP59-S, Frankford Arsenal (U.S. Army), Contract No. DA-36-034-ORD-3559 RD. October 16, 1962. (AD 289 526)

[7] Haarr, A.P.: Development of Aluminum Base Alloys. Annual Progress Report 7-63-AP59-S, Contract No. DA 36-034-ORD-3559 RD. 1963. (AD 423 398)

[8] Lyle, J.P., Jr.: Development of Aluminum Base Alloys - Section I Final Report. Report 66-AP59-S, Contract No. DA-36-034-ORD-3559 RD. September 7, 1966.

[9] Haarr, A.P.: Development of Aluminum Base Alloys - Section II. Final Report No. 13-65-AP 59-S, Contract No. DA-36-034-ORD-3559 RD. December 20, 1965. (AD 479 783)

[10] Haarr, A.P.: Development of Aluminum Base Alloys - Section III. Final Report 13-66-AP59-S, Contract No. DA-36-034-ORD-3559 RD. May 31, 1966. (AD 487 764)

[11] Dudas, J.H. and Dean, W.A.: "The Production of Precision Aluminum P/M Parts". International Journal of Powder Metallurgy, Vol. 5, No. 2, 1969, pp. 21-35.

[12] Lyle, J.P., Jr. and Towner, R.J.: Process for Making High Quality Hot-Worked Products from Aluminum Base Alloy Powders. U.S. Patent 3, 544, 392. December 1, 1970.

[13] Lyle, J.P., Jr. and Towner, R.J.: Aluminum-Copper-Magnesium-Zinc Powder Metallurgy Alloys. U.S. Patent 3, 544, 394. December 1, 1970.

[14] Lyle, J.P., Jr. and Towner, R.J.: Corrosion-Resistant Aluminum-Copper, Magnesium-Zinc Powder Metallurgy Alloys. U.S. Patent 3, 563, 814. February 16, 1971.

[15] Cebulak W.S. and Truax, D.J.: Program to Develop High-Strength Aluminum Powder Metallurgy Products - Phase I - Process Optimization. Contract No. DAAA 25-70-C0358. March 12, 1971. (AD 882 137 L)

[16] Cebulak, W.S. and Truax, D.J.: Program to Develop High-Strength Aluminum Powder Metallurgy Products - Phase II - P/M Alloy Optimization. Contract No. DAAA 25-70-C0358. June 1, 1971. (AD 884 642 L)

[17] Cebulak, W.S. and Lyle, J.P., Jr.: "Fabrication of High-Strength Aluminum Products from Powder". Proceedings of Eighteenth Sagamore Army Materials Research Conference, August 31 - September 3, 1971, Powder Metallurgy for High Strength Applications, pp. 231-54, Burke, J.J. and Weiss, V. (Eds.). Syracuse, New York: Syracuse University Press, 1972.

[18] Buchovecky, K.E. and Rearick, M.R.: "Aluminum P/M Forgings". Metal Progress, Vol. 101, No. 2 (February 1972), pp. 74-78.

[19] Lyle, J.P., Jr. and Towner, R.J.: Aluminum-Copper-Magnesium-Zinc Powder Metallurgy Alloys. U.S. Patent 3, 637, 441. January 25, 1972.

[20] Lyle, J.P., Jr. and Cebulak, W.S.: Properties of High-Strength Aluminum P/M Products. Presented at "The Third Air Force Metal Working Conference, Western Metal and Tool Exposition", March 13-16, 1972. Los Angeles, CA.

[21] Lyle, J.P., Jr.; Cebulak, W.S. and Buchovecky, K.E.: "Properties of High Density Aluminum P/M Products". Progress in Powder Metallurgy - 1972 National P/M Conference Proceedings, April 17-19, Vol. 28, pp. 93-114, Bufferd, A.S. (Ed.). New York: Metal Powder Industries Federation, 1972.

[22] Cebulak, W.S. and Truax, D.J.: Program to Develop High-Strength Aluminum Powder Metallurgy Products - Phase III - Scale Up A. Contract No. DAAA 25-70-C0358. September 29, 1972.

[23] Cebulak, W.S.: Program to Develop High-Strength Aluminum Powder Metallurgy Products - Phase IV A - Vacuum Process. Contract No. DAAA 25-72-C0593

a. First Quarterly Report October 12, 1972.
b. Second " " January 31, 1973.
c. Third " " June 11, 1973.

[24] Cebulak, W.S.: Program to Develop High-Strength Aluminum Powder Metallurgy Mill Products - Phase IVB - Scale-Up to 1545 kg (3400lb) Billet. Contract No. DAAA 25-72-C-0593

a. Fourth Quarterly Report January 14, 1974.
b. Fifth " " March 8, 1974.
c. Sixth " " April 23, 1974. (AD 780 455)
d. Seventh " " December 5, 1974. (AD A-005 661)
e. Final Report, FA-TR-76067 April 25, 1977. (AD 039 862)

AD-A062 981 DEUTSCHE FORSCHUNGS- UND VERSUCHSANSTALT FUER LUFT- U--ETC F/G 11/6
DEVELOPMENT OF IMPROVED HIGH STRENGTH ALUMINUM POWDER METALLURG--ETC(U)
MAY 78 D P VOSS AFOSR-77-3440

UNCLASSIFIED DFVLR-IB-354-77/14 EOARD-TR-78-3 NL

2 OF 2
AD
A062981

END
DATE
FILMED
2-79
DDC

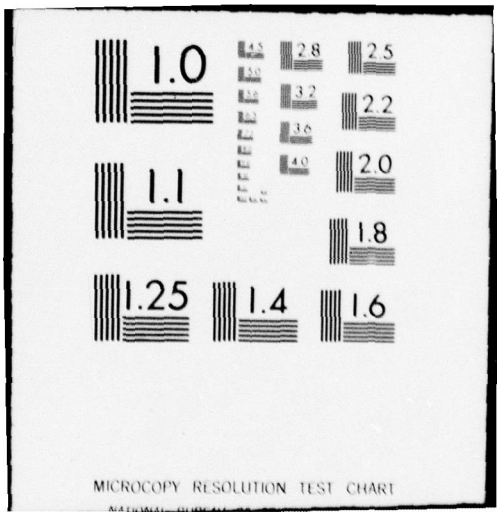
1.0
1.1
1.25
1.4
1.6
1.8
2.0
2.2
2.5
2.8
3.2
3.6
4.0
MICROCOPY RESOLUTION TEST CHART

[25] Lyle, J.P., Jr. and Cebulak, W.S.: "Properties of High-Strength Aluminum P/M Products". Metals Engineering Quarterly, Vol. 14, No. 1 (February 1974), pp. 52-63.

[26] Lyle, J.P., Jr. and Cebulak, W.S.: "Powder Metallurgy Approach for Control of Microstructure and Properties in High Strength Aluminum Alloys". Metallurgical Transactions, Vol. 6A (April 1975), pp. 685-699.

[27] Cebulak, W.S., Johnson, E.W. and Markus, H.: High Strength Aluminum Powder Metallurgy Mill Products. Presented at "P/M Ordnance" Seminar, April 19-20, 1976, Dover, N.J. Proceedings published by Metal Powder Industries Federation, Princeton, N.J. pp. 119-137.

[28] Cebulak, W.S.: Scale-Up of High Strength Aluminum P/M Products to Plant Production Practice. Presented at 5th International Powder Metallurgy Conference, Chicago, Ill., June 27-July 2, 1976. (Sponsored by Metal Powder Industries Federation, Princeton, N.J.)

[29] Botterman, R.C.: Aluminum P/M - A Rapidly Maturing Technology. Presented at 5th International Powder Metallurgy Conference, Chicago, Ill., June 27-July 2, 1976.

[30] Otto, W.L., Jr.: Metallurgical Factors Controlling Structure in High Strength Aluminum P/M Products. AFML-TR-76-60, Contract No. F 33615-74-C-5077. May 1976.

[31] Cebulak, W.S., Johnson, E.W. and Markus, H.:"High Strength Aluminum P/M Products". Metals Engineering Quarterly, Vol. 16, No. 6 (November 1976), pp. 37

[32] Zaleski, F.I.: "High Strength Aluminum Alloys by Powder Metallurgy Extrusion Techniques". Progress in Powder Metallurgy, Vol. 19, 1963, pp. 142-145.

[33] Foerster, G.S.: Aluminum Base Pellet Alloys Containing Copper and Magnesium and Process for Producing the Same. U.S. Patent 3, 265,493. August 9, 1966.

[34] Foerster, G.S.: Process for Preparing High Strength Fabricated Articles from Aluminum Base Alloys Containing Magnesium and Copper. U.S. Patent 3, 291, 654. December 13, 1966.

[35] Fridlyander, I.N., Stepanova, M.G., Setyukov, O.A. and Bryukhovets, A.A.: Powder Alloys of Aluminum with Slightly Soluble Additives. Report No. FTD-HT-23-1350-68, 6 June 1969. (AD 693 511) [Edited translation of Alyuminievye Splavy (USSR), No. 5 (1967), pp. 226-230]

[36] Berman, S.I., Zaleski, V.I., Imanov, Kh.I. and Shelamov, V.A.: "Effect of the Degree of Deformation on the Mechanical Properties of Extruded Semifinished Products from Granules of Aluminum Alloys of the System Al-Zn-Mg-Cu". Soviet Powder Metallurgy and Metal Ceramic, Vol. 84, No. 12 (December 1969), pp. 966-9. (Translated from Poroshkovaya Metallurgiya, Vol. 84, No. 12 (Dec. 1969), pp. 14-18.)

[37] Bower, T.F., Singh, S.N. and Flemings, M.C.: "Development of High Strength Wrought Aluminum Base Alloys". Metallurgical Transactions, Vol 1, No. 1 (January 1970), pp. 191-197.

[38] Wakefield, B.D.: "Aluminum PM Parts: A Good Start". Iron Age, Vol. 205, No. 12 (March 1970), pp. 60-61.

[39] Foerster, G.S.: Aluminum Base Alloy Process and Product. U.S. Patent 3, 539, 405. November 10, 1970.

[40] Jacobson, L.A., Pierce, C.M. and Cook, M.M.: Microstructures of Powder and Conventional Processed 7075 Aluminum Alloy. AFML-TR-71-240. December 1971.

[41] Furrer, P. and Warlimont, H.: "Gefüge und Eigenschaften von Aluminiumlegierungen nach rascher Erstarrung" ("Microstructure and Properties of Aluminum Alloys after Rapid Solidification"). Zeitschrift für Metallkunde, Vol. 62, 1971
a. "Abkühlmethoden, Struktur und Gefügeausbildung", ("Rapid Quenching Techniques, Structural, and Microstructural Features"). No. 1, pp. 12-20.
b. "Übersättigungserscheinungen, Einfluß von Wärmebehandlungen, mechanische Eigenschaften", ("Extension of Solid Solubility, Influence of Thermal Treatments, Mechanical Properties"). No. 2, pp. 100-112.

[42] Sheppard, T. and Chare, P.J.M.: "The Extrusion of Atomized Aluminum Powders". Powder Metallurgy, Vol. 15, No. 29 (1972), pp. 17-41.

[43] Grant, N.J., Pelloux, R.M. and Flemings, M.C.: Structure and Property Control through Rapid Quenching of Liquid Metals. ARPA Contract No. DAHC 15-70-C-0283.
a. Semi-Annual Technical Report 3 January 1, 1972. (AD 739 340)
b. Semi-Annual Technical Report 4 July 31, 1972. (AD 749 679)

[44] Mobley, C.E., Clauer, A.H. and Wilcox, B.A.: "Microstructure and Tensile Properties of 7075 Aluminum Compacted from Melt Spun Ribbon". Journal of the Institute of Metals, Vol. 100, 1972, pp. 142-145.

[45] Dixon, C.F. and Skelly, H.M.: "Properties of Aluminum-Tin Alloys Produced by Powder Metallurgy". Powder Metallurgy, Vol. 16, No. 32 (1973), pp. 366-373 .

[46] Chare, P.J.M. and Sheppard, T.: "Powder Extrusion as a Primary Fabrication Process for Al-Fe Alloys". Powder Metallurgy, Vol. 16, No. 32 (1973), pp. 437-458 .

[47] Rostoker, W., Dudek, R., Freda, C. and Russell, R.: Fast Freezing as a Method for Aluminum Alloy Development. Contract No. F 33615-70-C-1525, AFML-TR-73-36, March 1973. (AD 759 828). [also published: International Journal of Powder Metallurgy, Vol. 9, No. 4 (1973), pp. 139]

[48] Lebo, M. and Grant, N.J.: "Structure and Properties of a Splat Cooled 2024 Aluminum Alloy". Metallurgical Transactions, Vol. 5, No. 7 (July 1974). pp. 1547-1555.

[49] Gurney, F.J., Abson, D.J. and De Pierre, V.: The Influence of Extrusion-Consolidation Variables on the Integrity and Strength of the Product from Prealloyed 7075 Aluminum Powder. AFML-TR-73-252. September 1973. (AD 770 950) [Briefly reviewed in Summary Report on Investigation of Metal Processing Operations. AFML-TR-77-75. April 1977.(AD A042 188)]

[50] Haertlein, J.B. and Sachse,J.F.: "Review of Aluminum Powder Metallurgy". Proceedings of the Annual Meeting of the Metal Powder Assoc., Progress in Powder Metallurgy, Princeton, N.J., 1973, pp. 83-94.

[51] Lawley, A.: "P/M Hot Forming: An Introduction and Overview". New Perspectives in Powder Metallurgy Fundamentals, Methods, and Applications, Vol. 6, 1973, pp. 153-164.

[52] Chare, P.J.M. and Sheppard, T.: "Densification and Properties of Extruded Al-Zn-Mg Atomized Powder". International Journal Powder Metallurgy and Powder Technology, Vol. 10, No. 3 (1974), pp. 203-215.

[53] Stepanova, M.G. and Matveev, B.I.: "P/M Aluminum Alloys". Metal Science Heat Treatment, Vol. 16, No. 5-6 (1974), pp. 492-94.

[54] Gurney, F.J., Abson, D.J. and De Pierre, V.: "The Influence of Extrusion-Consolidation Variables on the Integrity and Strength of the Product from Prealloyed 7075 Aluminum Powder". Powder Metallurgy, Vol. 17, No. 33 (1974), pp. 46-69.

[55] Grosch, J. and Jäniche, H.: "Kaltpreßschweißen von Aluminium-pulver durch Strangpressen". Aluminium , Vol. 50, No. 5 (1974), pp. 343-349. (Translation w/o figures: "Cold Pressure Welding of Aluminum Powder by Extrusion". Aluminium - Supplement in English, pp. 34-48.

[56] Jäniche, H.: Kaltpreßschweißen von Aluminiumpulver durch Strangpressen. Doktor-Ingenieur Dissertation. Berlin: 1975, D 83.

[57] Sheppard, T. "Production of Extruded Material from Metal Powders". Proceedings of the 15th Conference Institute of Machine Tool Design and Research, Birmingham, England, September 18-20, 1974. Halsted Press: 1975, pp. 659-667.

[58] Dowson, A.G. (Ed.): "Properties and Performance of Aluminum P/M Parts". Metal Powder Report, Vol. 31, No. 7 (July 1976), pp. 241-247.

[59] Grosch, J. and Jäniche, J.: Cold Extrusion of Aluminum Powders. Presented at 5th International P/M Conference", Chicago, Ill., June 27, 1976.

[60] Durand, J.P.H.A., Pelloux, R.M. and Grant, N.J.: "Properties of Splat-Quenched 7075 Aluminum Type Alloys". Materials Science and Engineering, Vol. 23, 1967, pp. 247-256.

[61] Abson, D.J., Gurney, F.J. and De Pierre, V.: Microstructure and Mechanical Properties of Product from Extrusion-Consolidated 7075 Al Prealloyed Powder. AFML-TR-76-194. November 1976.

[62] Griffith, W.M. and Cook, M.M.: The Effect of Varying Quench Rates and Heating Rates on the Aging Response of an Aluminum Powder Alloy. AFML-TR-77-67. July 1977.

[63] Birla, N.C., Kulkarni, K.M., Bhattacharyya, S. and Berner, W.: Isothermal P/M Forging of Near Net Aluminum Alloy Component. Presented at 1977 Powder Metallurgy Conference, Detroit, Michigan, May 1977.

[64] Jones, H.: "Development in Aluminum Alloys by Solidification at Higher Cooling Rates". Aluminium, Vol. 54, No. 4 (April 1978), pp. 274-281.

[65] Bhattacharyya, S. and Kulkarni, K.M.: Development of High Strength Aluminum P/M Isothermally Forged Component. Preprint of presentation at "5th European Symposium on Powder Metallurgy", Stockholm, Sweden, 4-8 June 1978.

[66] Dhanvantri, P.R. and Ramakrishnan, P.: Some Aspects of Powder Forging of Aluminum-Copper Alloys. Preprint of presentation at "5th European Symposium on Powder Metallurgy", Stockholm, Sweden, 4-8 June 1978.

[67] Bloch, E.A.: "Dispersion-Strengthened Aluminum Alloys". Metallurgical Reviews, Vol.6, 1961, pp.193-239.

[68] Dromsky, J.A. and Lenel, F.V.: "The Influence of Thermal Treatments upon the Microstructure and Mechanical Properties of Aluminum-Aluminum Oxide Alloys". Transactions of the Metallurgical Society of AIME, Vol.230, October 1964, pp. 1289-1294.

[69] Gualdandi, D. and Jehenson, P.: Products Manufactured From the Composite Material Al-Mg-Al_2O_3-MgO for Nuclear Applications, and Methods of Obtaining the Products and the Material. Great Britian Patent 1,200,969, 5 August 1970.

[70] Military Specification for Heat Treatment of Aluminum Alloys, MIL-H-6088E, 5 February 1971.

[71] Van Horn, K.R. (Ed.). Aluminum. Metals Park, Ohio: ASM, 1967.
a. Vol.1,"Properties, Physical Metallurgy and Phase Diagrams".
b. Vol.2,"Design and Application".
c. Vol.3,"Fabrication and Finishing".

[72] Lyman, T. (Ed.). ASM Metals Handbook, 8th Ed. Metals Park, Ohio: ASM.
a. Vol.4, "Forming", 1969.
b. Vol.5, "Forging and Casting", 1970.

[73] Kroger, P.W.: Method of Making High Strength Aluminum Alloy Forgings and Product Produced Thereby. U.S. Patent 3,791,876. February 12, 1974.

[74] Voss, D.P.: Unpublished data.

[75] Hyatt, M.V.: New Aluminum Aircraft Alloys for the 1980's. Presented at Inter. Meeting on Aluminum Alloys in the Aircraft Industries, Torino, Italy, October 1-2, 1976.

[76] Bardes, B.P. and Flemings, M.C.: "Dendrite Arm Spacing and Solidification Time in a Cast Aluminum-Copper Alloy". Transactions of the American Foundrymen's Society, Vol.74, 1966, pp. 406-412.

[77] Matyja, H., Giessen, B.C. and Grant, N.J.: "The Effect of Cooling Rate on the Dendrite Spacing in Splat-Cooled Aluminum Alloys". Journal of the Institute of Metals, Vol. 96, 1968, pp. 30-32.

[78] Antes, H.W., Lipson, S. and Rosenthal, H.: "Strength and Ductility of 7000-Series Wrought-Aluminum Alloys as Affected by Ingot Structure". Transactions TMS-AIME, Vol. 239, No. 10 (1967), pp. 1634-1642.

[79] Singh, S.N. and Flemings, M.C.: "Solution Kinetics of a Cast and Wrought High Strength Aluminum Alloy". Transactions TMS-AIME, Vol. 245, No. 8 (1969), pp. 1803-1809.

[80] Singh, S.N. and Flemings, M.C.: "Influence of Ingot Structure and Processing on Mechanical Properties and Fracture of a High Strength Wrought Aluminum Alloy". Transactions TMS-AIME Vol. 245, No. 8 (1969), pp. 1811 - 1819.

[81] Antes, H.W. and Markus, H.: "Homogenization Improves Properties of 7000 Series Aluminum Alloys". Metals Engineering Quarterly, Vol. 10, No. 4 (1970), pp. 9-11.

[82] Mulherin, J.H. and Rosenthal, H.: "Influence of Nonequilibrium Second-Phase Particles Formed During Solidification upon the Mechanical Behavior of an Aluminum Alloy". Metallurgical Transactions, Vol. 2, No. 2 (1971), pp. 427-432.

[83] Solmir, J.G.: "Übersicht über die Pulvermetallurgie des Aluminiums". Zeitschrift für Metallkunde, Vol. 52, No. 10 (1961), pp. 645-651.

Appendix A

Diagrams of Mechanical Property Test Specimens

Tensile

Compressive

Notch Fatigue

Notch Tensile

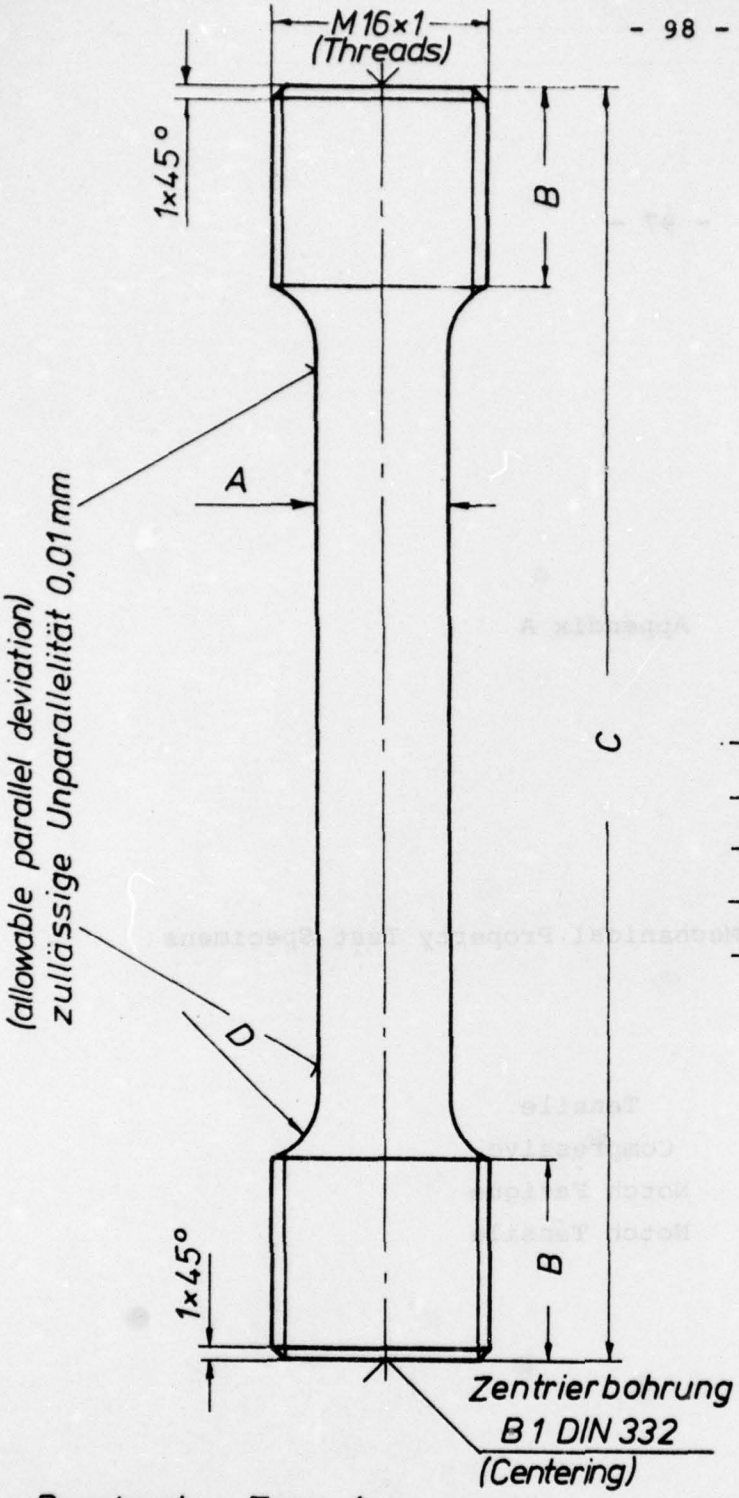

Maß	(dimensions)
A	ϕ 6 $^{-0,05}$
B	10
C	60 $^{-0,1}$
D	R 5

Rundprobe Form A

Teil	Benennung				Werkstoff	Stückzahl	Bemerkung
Änd. Zust.	Änderung	Tag	Name	Zeichnung Nr. 1-3-73	Tensile Test Specimen Rundprobe		
				1973 / Tag / Name			
				gez. 11.1. Brümmer	Form A (All dimensions in mm)		
				gepr.			
				DFVLR INSTITUT FÜR WERKSTOFF-FORSCHUNG	Auftraggeber:		Maßst.: (Scale) 2:1
					Auftrags-Nr.:		
					Ersatz für:	Ersetzt durch:	Urheberrechtlich geschützt

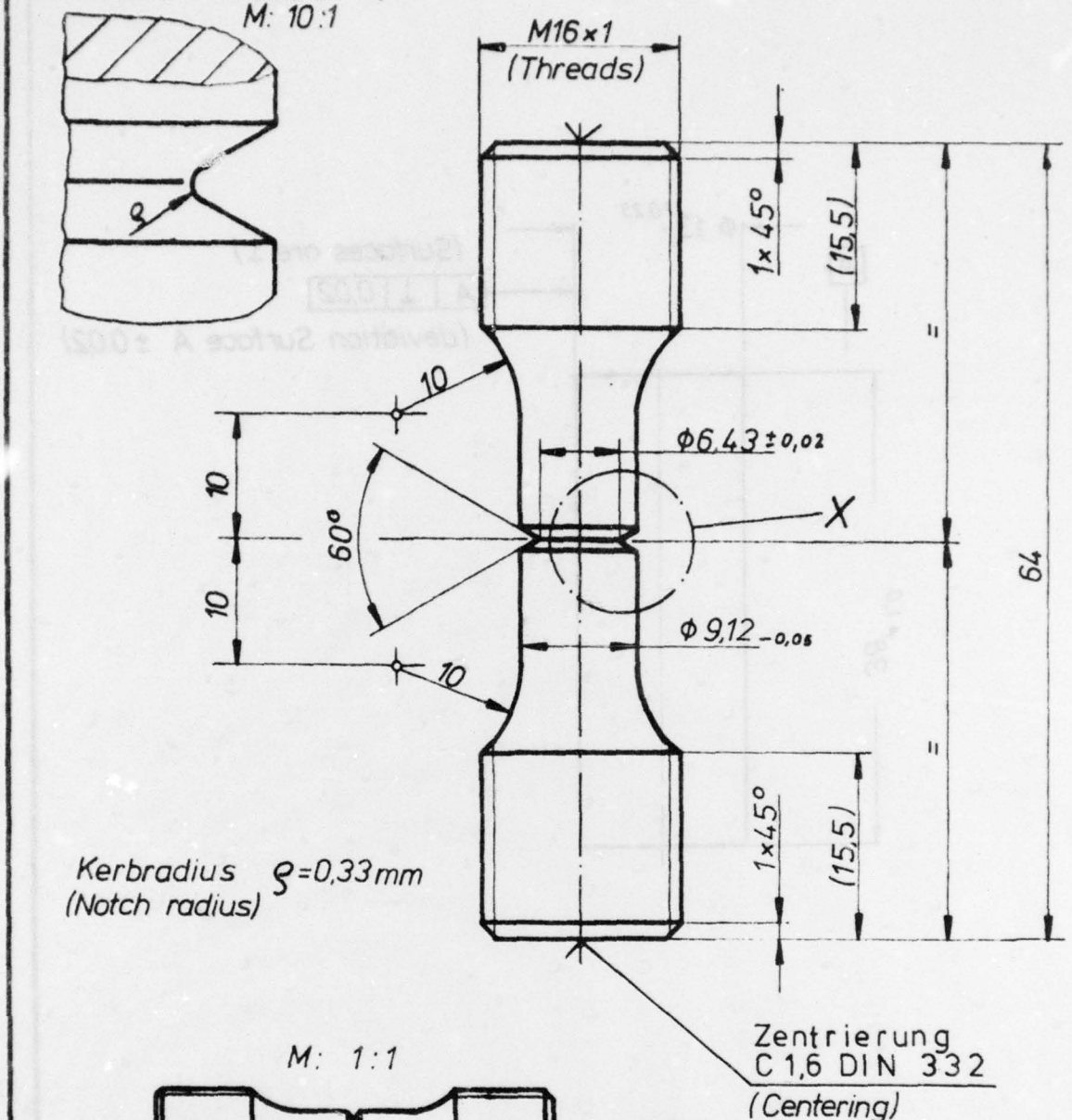

Ausgabe	Änderung	Tag	Name

Freimaßtoleranzen

	1977	Tag	Name
Bearb.		23.11.	Schramm
Gepr.			
Norm.			

Notch Fatique Test Specimen
$K_t = 3$ (Scale)

Kerbermüdungsprobe

Maßstab 2:1 (10:1) (1:1)

(All dimensions in mm)

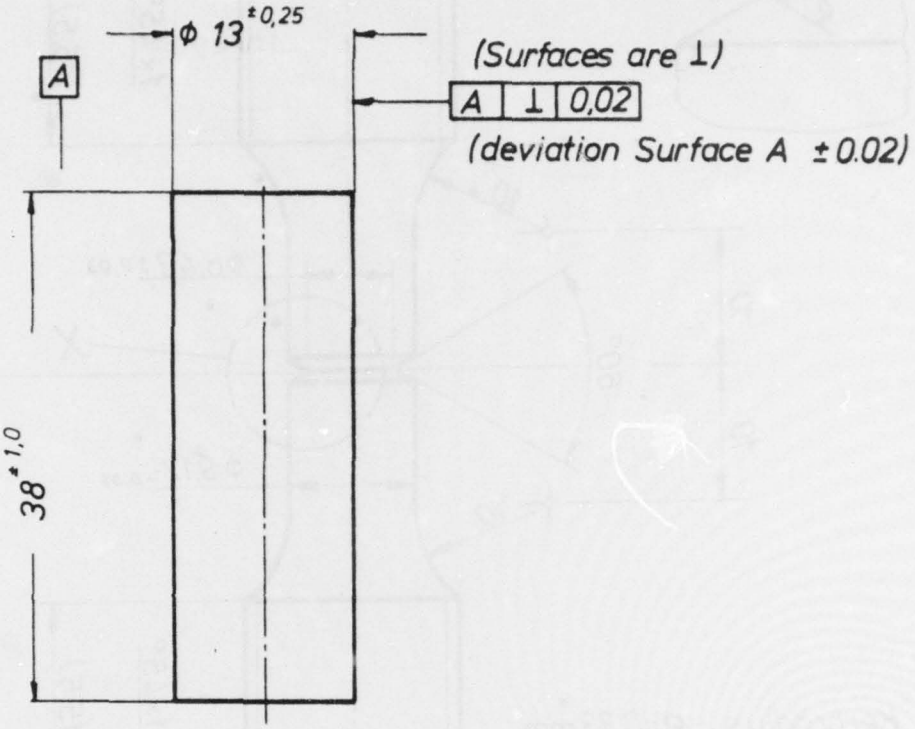

Teil	Benennung				Werkstoff	Stückzahl	Bemerkung
Änd. Zust.	Änderung	Tag	Name	Zeichnung Nr.	Stauchprobe		
				Tag / Name	Compressive Strength Test Specimen as per ASTM		
				gez. 17.05			
				gepr.			
				DFVLR INSTITUT FÜR WERKSTOFF-FORSCHUNG	(All dimensions in mm)		Maßst.: (Scale) 2:1
					Ersatz für:	Ersetzt durch:	Urheberrechtlich geschützt

Einzelheit (Detail) X

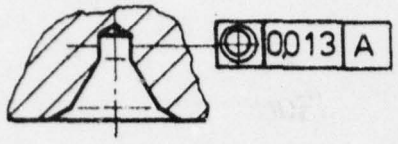

M: 5:1

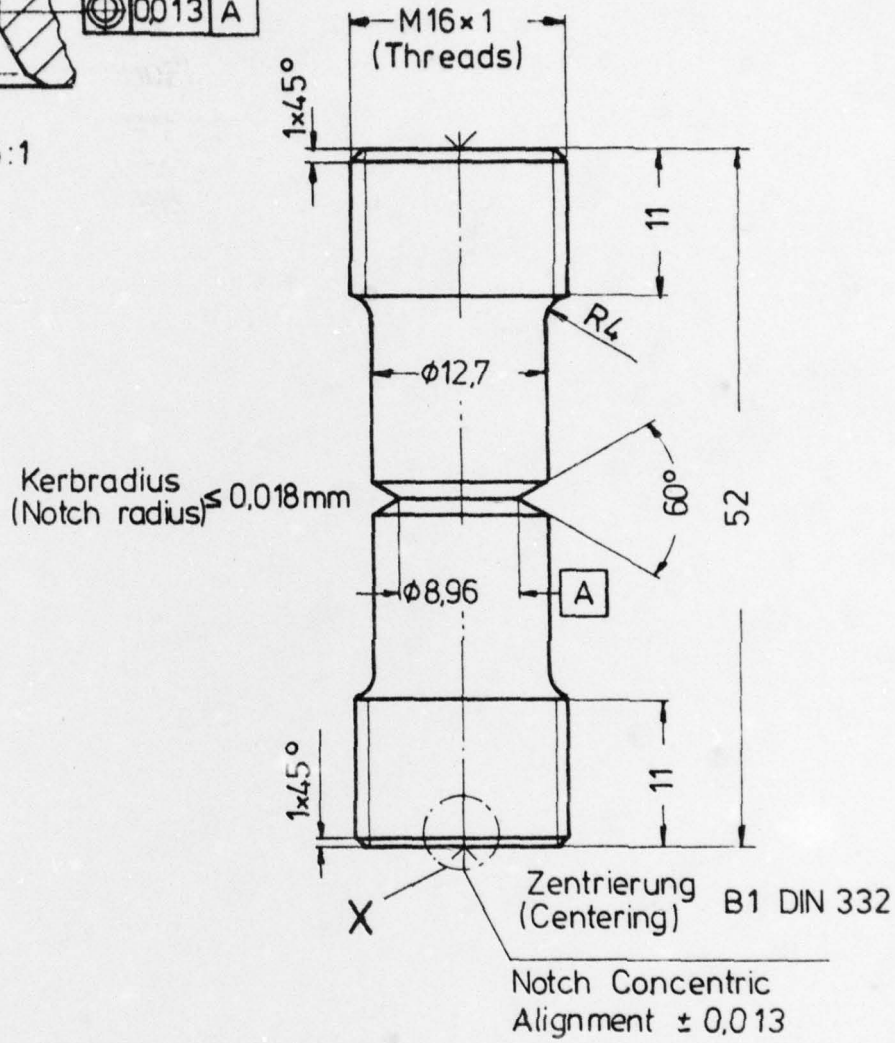

Änd. Zust.	Änderung	Tag	Name

	Tag	Name
gez.		
gepr.		

DFVLR
INSTITUT FÜR WERKSTOFF-FORSCHUNG

Kerbzugprobe

Notch Tensile Test Specimen as per ASTM

(All dimensions in mm)

Ersatz für:	Ersetzt durch:	Urheberrechtlich geschützt

Maßst.: Scale) 2:1 5:1